



UNIVERSITÀ DEGLI STUDI DI PADOVA

Dipartimento di Fisica e Astronomia “Galileo Galilei”

Master Degree in Physics

Final Dissertation

Heavy field Radiative Corrections to the Primordial Power Spectrum during Inflation

Thesis supervisor:

Prof. Marco Peloso

Thesis co-supervisors:

Prof. Laura Covi

Dr. Jinsu Kim

Candidate:

Francesco Costa

Academic Year 2019/2020

Nearly scale-invariant primordial power spectrum is one of the key features of cosmic inflation. The amplitude of the power spectrum as well as its spectral tilt are constrained by modern experiments. To date no sign of deviations from the simplest single-field inflation models has been observed. On the other hand, realistic models of inflation, meaning particle physics-based models, contain multiple fields other than the inflaton. The presence of heavy fields coupled to the inflaton may alter the predictions of the single-field inflation models.

In this thesis we consider the effects of heavy fields on the primordial power spectrum, studying a generic model which contains massive scalar and fermion fields coupled to the inflaton. The spacetime background for the quantum fields during inflation is time-dependent due to the expansion of the Universe and the time translation symmetry is broken. Therefore we expect the radiative corrections to the inflaton power spectrum to be time-dependent.

The natural theoretical framework to formulate such models is the Schwinger-Keldysh also known as the *in-in* formalism. We first introduce the Schwinger-Keldysh formalism. We then compute the one-loop radiative corrections to the inflaton two-point correlation function due to the heavy fields; without specifying the inflaton potential at first, keeping the inflationary scenario general. We perform the computations in a de Sitter spacetime, choosing the initial state at some initial conformal time τ_{in} to be the Bunch-Davies vacuum.

We explicitly single-out, in both the bosonic and fermionic contributions to the one-loop inflaton two-point function, the quadratic and logarithmic divergences, in terms of a cut-off, as expected from the results on the Minkowski background. The analytical analysis is performed using the WKB approximated mode functions. We then compute numerically the same radiative corrections, using the full expressions for the solution of the mode functions. We show that the WKB approximation is a good analytical approximation for massive mode functions and we argue that it is a good tool to capture the UV divergences of massive fields.

Finally we apply our results to the supersymmetric hybrid inflation model. The bosonic and fermionic divergences in the radiative corrections carry opposite sign and we show that they cancel exactly giving rise to a finite total result.

The radiative corrections introduce the presence in the power spectrum of time-dependent features of two type. One arises from the evolution of the background. The other is an oscillatory feature. The scalar and fermion contributions produce a constant shift and this peculiar oscillatory effects on top of the tree-level primordial power spectrum. Future improvements of CMB measurements may refine our current understanding of the primordial power spectrum and lead to a possible detection of these effects.

Introduction	1
1 Standard Cosmological Model	3
1.1 The Homogeneous and Isotropic Universe	3
1.1.1 Friedmann equations	5
1.1.2 Causal structure the Universe	7
1.2 Shortcomings of the Standard Model	8
1.2.1 Horizon problem	9
1.2.2 Flatness problem	9
1.2.3 Unwanted relics	10
1.3 A Single Dynamical Solution	10
1.3.1 Horizon problem	11
1.3.2 Flatness problem	12
1.3.3 Cosmological constant	13
1.4 Slow-Roll Inflation	14
1.4.1 Background dynamics	15
1.4.2 Slow-roll parameters	17
1.4.3 Attractor solution	18
1.5 Cosmological Perturbations	19
1.5.1 Quantum fluctuation	19
1.5.2 Canonical quantization and the vacuum choice	22
1.5.3 Massive scalar field	24
1.5.4 Power spectrum	25
1.6 Perturbations in General Relativity	27
1.7 Fermions in Curved Spacetime	34
1.7.1 The vierbein formalism	34
1.7.2 Dirac equation	37
2 The Schwinger-Keldysh Framework	39
2.1 The Schwinger-Keldysh Formalism	39
2.1.1 Interaction picture in cosmology	40
2.1.2 The expectation values	42
2.1.3 Generating functional for a scalar field	44
2.1.4 Generating functional for a fermion field	46
2.2 The Schwinger-Keldysh Propagators	47
2.2.1 Scalar field	48

2.2.2	Fermion field	51
2.3	The WKB Approximation	54
2.3.1	Scalar field	55
2.3.2	Fermion field	56
3	One-Loop Corrections	59
3.1	The Interacting Lagrangian	60
3.2	Inflaton Two-Point Correlation Function	61
3.2.1	One-loop corrections from a massive scalar	63
3.2.2	One-loop corrections from a massive fermion	68
3.2.3	Numerical calculation	70
3.3	Ultraviolet Behavior	72
3.3.1	Numerical calculation	74
3.4	Analytical Results	75
4	Primordial Power Spectrum	80
4.1	Time Integration	80
4.1.1	Oscillatory behavior	81
4.2	Hybrid Inflation	82
4.2.1	Supersymmetric Hybrid Model	84
4.3	Radiative Corrections to the Primordial Power Spectrum	85
4.3.1	Supersymmetric Hybrid Inflation	86
	Summary and Conclusion	89
	Bibliography	90

Cosmic inflation [1, 2] is a very successful fundamental theory in cosmology. It introduces a primordial epoch of accelerated expansion of the Universe. This paradigm provides a natural dynamical solution to the problems of the Hot Big Bang model related to the initial condition. Moreover the quantum fluctuations of the inflaton furnish the seeds for the cosmological perturbations observed today this relation can explain the temperature anisotropy in the Cosmic Microwave Background and the large scale structure of the Universe.

In the slow-roll scenario for a single-field inflation the spectrum of the primordial perturbations is predicted to be nearly scale invariant and it is consistent with the current observations [3, 4]. However particle physics-based model of inflation include multiple fields which can couple to the inflaton and modify the prediction of the single-field scenario. During the inflationary epoch the peculiar setting in which the fields interact is an expanding Universe: time translation is broken by the inflating background and one expects the cosmological observable to show a time dependence. The natural theoretical framework to address this problem is the Schwinger-Keldysh (or *in-in*) formalism, in particular if we are interested in including quantum effects in the theory [5].

The goal of the thesis is to compute the one-loop radiative corrections to the two-point function of the inflaton due to the interaction with heavy scalar and fermion fields. The initial conditions are chosen at some initial conformal time τ_{in} where the system is expected to be in the Bunch-Davies vacuum. The amputated part of the amplitudes is investigated in the first part of the discussion, in order to understand the type and order of the divergences appearing at one-loop level through the regularization process. The ultraviolet behavior will be singled-out from the regularized amplitude and compared with the result in the Minkowski spacetime. The order of the divergences and the type and number of counter-terms needed to renormalize the amplitude are expected to match those in the Minkowski case [6]. The mode function solution for the heavy field will be treated in the Wentzel–Kramers–Brillouin approximation. Numerical analysis is performed to understand the goodness of the approximation.

The second part of the work is dedicated to study the time dependent features of the primordial power spectrum that arise from the one-loop corrections. We expect the radiative corrections to introduce a twofold time dependence, arising because of the initial conditions and the evolution of the background. We also expect the presence of oscillatory features in the primordial power spectrum due to the radiative corrections, from the analysis of [7].

The general results of the first parts can be adapted straightforwardly to many different inflationary scenarios. In the last part of the thesis we apply them in the framework of supersymmetric hybrid inflation [8]. The bosonic and fermionic contributions to the one-loop corrections are expected to carry opposite sign and of interested is the possibility for the divergences to exactly

cancel. Finally in this setting, a prediction for the Cosmic Microwave Background temperature power spectrum will be formulate, in order to investigate if the imprint of the oscillation expected in the primordial power spectrum can be observed in the temperature power spectrum. The study of the primordial power spectrum and its possible time dependent features can be used to shed light on the physics at a very high energy scale and to discriminate among the large variety of inflationary models.

In Chapter 1 the Hot Big Bang model will be introduced alongside with the fundamentals of the theory of cosmic inflation and the vielbein formalism. In Chapter 2 we introduce the Schwinger-Keldysh formalism and the bosonic and fermionic propagators in the Minkowski and de Sitter spacetime. Chapter 3 is dedicated to both the analytical and the numerical studies of the ultraviolet behavior of the radiative corrections to the inflaton two-point function arising from the interaction with the heavy fields. In Chapter 4 we will discuss the time dependence of the radiative corrections and calculate the primordial power spectrum prediction in the supersymmetric hybrid inflation scenario. The thesis ends with a discussion of the results in the Conclusions.

The standard cosmological model [9–12], often called Hot Big Bang model, is the framework within which we are able to describe the evolution of the Universe interpreting astronomical observations. The past century has seen the triumphs of modern cosmology through three main observational evidences: the expansion of the Universe [13], the existence of the Cosmic Microwave Background (CMB) [14] and the measurement of the relative abundance of light element [15]. Despite the great success before the 1980s there were still open questions in the Standard Model of cosmology.

They should not be considered as inconsistencies but rather problems related to the required initial conditions. In fact the Hot Big Bang model never aimed to explain the primordial phase of the Universe. Alan Guth in the 1980s [1] realized that an initial phase of accelerated expansion of the Universe could provide a simple solution to these problems. From this idea started the development of the inflationary theory [1, 16, 17]. The discussion presented in this chapter is inspired by the work in [5, 7, 10, 18].

1.1 The Homogeneous and Isotropic Universe

The keystone of the standard cosmology is the idea that the Universe has no privileged position nor direction, that translates into two fundamental properties: homogeneity and isotropy. This is known as the cosmological principle and it is important to emphasize that it is not an exact statement, it is an approximation that holds on sufficiently large scales. In fact, it is clear that at small scales the Universe presents inhomogeneities as stars, galaxies and galaxy clusters and anisotropies in their distribution.

It is compelling how, thanks to the great achievements of modern precision cosmology, the *Cosmological Principle* that was once an assumption is now an experimentally tested hypothesis. In fact there are several studies [3, 19, 20] that suggest its validity and that set the *large scale* to be around 100 Mpc, that means scales larger than cluster of galaxies. We remark that this applies only to the portion of the Universe that we can observe.

Nowadays the most convincing theory of gravity is Einstein's General Relativity (GR) in which the fundamental quantity that describes the geometry of spacetime is the metric. Imposing the symmetries given by the cosmological principle to the most generic metric allowed in GR, we obtain

$$ds^2 = -dt^2 + a(t)^2 \left(\frac{dr^2}{1 - \kappa r^2} + r^2 d\theta^2 + r^2 \sin^2 \theta d\phi^2 \right), \quad (1.1)$$

the so-called Friedmann-Lemaître-Robertson-Walker (FLRW) metric which describes a maximally

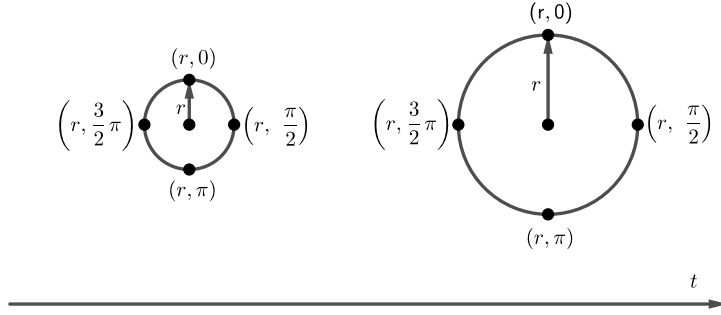


Figure 1.1: During the expansion of the Universe the points keep the same comoving coordinates. Their comoving distance is constant while the physical distance changes according to the value of the scale factor. Figure inspired by [9]

symmetric spacetime. The equation (1.1) uses a special set of coordinates (t, r, θ, ϕ) which are adapted to a comoving observer. A comoving observer is the observer that sees the source of the spacetime geometry homogeneous and isotropic. Since the spatial part is time-independent, beside the factor $a(t)$, it is possible to picture it as a grid that uniformly expand according to the $a(t)$ value. However in this expansion process the points do not change their comoving coordinates as shown in figure 1.1.

While comoving distance between two points remain constant during the elapsing of time t , the physical distance R (given by $R = a(t)r$) evolves, since it is proportional to $a(t)$, the scale factor. The $a(t)$ variable measures the relative expansion of the Universe and it is set to be 1 today. Finally κ is a constant that can assume three possible values accordingly to the class of Universe that we are considering: $\kappa = -1$, $\kappa = 0$, $\kappa = 1$ for an Universe with spatial curvature respectively negative, zero and positive. The Universe we observe today is compatible with $\kappa = 0$ [3], the spatially flat solution. This experimental observation leads to one of the shortcomings of the Hot Big Bang as we will discuss in section 1.2. Thus assuming $\kappa = 0$, the metric reads

$$ds^2 = -dt^2 + a(t)^2 \delta_{ij} dx^i dx^j. \quad (1.2)$$

We can describe the same spacetime using the conformal time τ

$$ds^2 = a(t)^2 (-d\tau^2 + \delta_{ij} dx^i dx^j), \quad (1.3)$$

where we defined τ as

$$d\tau := \frac{dt}{a(t)}. \quad (1.4)$$

Another useful definition is the Hubble parameter

$$H := \frac{\dot{a}(t)}{a(t)}. \quad (1.5)$$

that characterizes the rate of expansion of the Universe, where the dot notation $\dot{A}(t) := \frac{dA}{dt}$ stands for the derivative with respect to the cosmic time.

1.1.1 Friedmann equations

The dynamics of the metric in the presence of matter and energy is described by the Einstein equations [21, 22]

$$G_{\mu\nu} := R_{\mu\nu} - \frac{1}{2}R g_{\mu\nu} = \frac{1}{M_{\text{P}}^2}T_{\mu\nu}, \quad (1.6)$$

where $R_{\mu\nu}$ is the Ricci tensor, R the Ricci scalar and M_{P} the reduced Planck mass. The equation (1.6) describes how the geometry influences the dynamics of the matter and energy and the other way around. The energy momentum tensor in the general relativistic setting is defined as

$$T_{\mu\nu} := -\frac{2}{\sqrt{-g}} \frac{\delta(\sqrt{-g} \mathcal{L}_m)}{\delta g^{\mu\nu}}, \quad (1.7)$$

where g is the determinant of the metric and \mathcal{L}_m the matter content Lagrangian. We assume in the following that the matter content can be treated as a perfect fluid, that is one of the possibilities to have an energy momentum tensor that satisfies the cosmological principle. So $T_{\mu\nu}$ reads [12]

$$T_{\mu\nu} = \left(\rho(t) + P(t) \right) u_\mu u_\nu + P(t) g_{\mu\nu}, \quad (1.8)$$

where u_μ is the four velocity and both ρ , the energy density, and P , the isotropic pressure, depend only on the time because of the homogeneity and isotropy requirement. For a comoving observer the energy-momentum tensor assumes a particularly simple form

$$T_{\mu\nu} = \begin{pmatrix} \rho & 0 & 0 & 0 \\ 0 & P & 0 & 0 \\ 0 & 0 & P & 0 \\ 0 & 0 & 0 & P \end{pmatrix}. \quad (1.9)$$

Another condition on the stress-energy tensor is its covariant conservation

$$\nabla_\nu T^{\mu\nu} = 0, \quad (1.10)$$

derived from the Bianchi identity of the Riemann curvature tensor [23].

With these important facts on the metric and the energy content we can now proceed to study the evolution of the Universe through the Einstein equations. Using the FLRW metric (1.1), the Einstein equations (1.6) and equations (1.10) and (1.9) we obtain the Friedmann equations [9, 24]

$$H^2 = \frac{1}{3M_{\text{P}}^2} - \frac{\kappa}{a^2}, \quad (1.11)$$

$$\frac{\ddot{a}}{a} = -\frac{1}{6M_{\text{P}}^2}(\rho + 3P), \quad (1.12)$$

from which we derive the continuity equation

$$\dot{\rho} + 3H(\rho + P) = 0. \quad (1.13)$$

The Friedmann equations describe the evolution of the Universe in terms of the scale factor evolution. An equation of state for the fluid is needed to close the system of equations. We assume that the relation between the pressure and the energy density has the following form

$$P = \omega\rho, \quad (1.14)$$

with ω is being constant. From the second Friedmann equation (1.12) it is straightforward to obtain the condition for an accelerated expansion

$$\boxed{\omega < -\frac{1}{3}}. \quad (1.15)$$

Inflation, as we will discuss later, requires the presence of an exotic fluid with equation of state that satisfies (1.15). There is a particular case of fluid with this property that is worth examining: $\omega = -1$. This is called the de Sitter (dS) Universe in which the pressure P is exactly $-\rho$ and the scale factor is

$$a(t) \propto e^{Ht}. \quad (1.16)$$

The dS solution describes an exponentially expanding Universe¹. It is worth noticing that the energy density in this solution is constant with time $\rho = \text{const}$; it is also called the cosmological constant solution.

Solving the system of Friedmann equations for a fluid with $\omega \neq -1$ we obtain the general solution

$$a(t) \propto t^{\frac{2}{3(1+\omega)}}, \quad (1.17)$$

There are two particularly interesting cases. The non-relativistic (NR) matter solution, where the pressure is negligible, so $\omega = 0$. The radiation solution, which has the equation of state $P = \rho/3$. These solutions are summarized in Table 1.1.

	NR Matter	Radiation	de Sitter
ω	0	1/3	-1
$a(t)$	$t^{2/3}$	$t^{1/2}$	e^{Ht}

Table 1.1: Solution of the Friedmann equations for a Universe characterized by $\kappa = 0$, spatially flat, and for different types of perfect fluid.

Studying the evolution of the Universe using the Friedmann equations we can then recognize different eras where one of the components dominated the total energy density and the scale factor evolved accordingly. Figure 1.2 summarizes it. In the Λ CDM model [9], according to the latest Planck results [3], the different energy density components are distributed as shown in Table 1.2

Let us introduce a parameter that will be useful in the section 1.2, the density parameter Ω [24]

$$\Omega(t) := \frac{\rho(t)}{\rho_c}, \quad (1.18)$$

where ρ_c , the critical energy density, corresponds to a flat Universe. From the Einstein equations we learned that there is a relation between the geometry and the matter-energy content and this fact

	Radiation	NR Matter	Cosmological Constant
Ω_0	$(9.13821 \pm 0.00035) \cdot 10^{-5}$	0.3111 ± 0.0056	0.6889 ± 0.0056

Table 1.2: Highlights of the experimental constraints on some of the parameter of the Λ CDM model presented by the Planck collaboration [3]. The subscript zero on Ω indicates its value today

¹As we will discuss in the following a de Sitter expansion cannot be a realistic model of inflation.

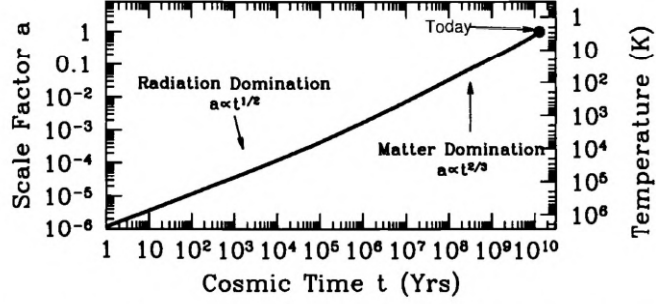


Figure 1.2: The early Universe energy density was dominated by radiation with the scale factor growing as $a(t) \propto t^{1/2}$. Around redshift $z \simeq 1090$ the matter-radiation equality point is reached and it is then dominated by non-relativistic matter with scale factor evolving as $a(t) \propto t^{2/3}$. Figure from [9].

is also reflected here. Indeed measuring ρ we can determine Ω that describe the overall geometry of the Universe, since we can connect it to κ through the Friedmann equations.

The curvature of the spacetime with Ω greater, equal to or less than 1 is respectively negative, zero and positive. From the Friedmann equations we obtain the time dependence of Ω

$$\Omega(t) - 1 = \frac{\kappa}{a^2(t)H^2(t)}. \quad (1.19)$$

Ω varies with time but the overall geometry is fixed.

1.1.2 Causal structure the Universe

To understand the causal structure of the Universe we need to study the propagation of light in a spacetime characterized by the FLRW metric (1.1). The property of isotropy allows us to fix any given θ and ϕ leading to $d\Omega^2 = 0$ and the massless nature of the photons assures that their motion is along null geodesics, $ds^2 = 0$. These conditions lead to

$$0 = ds^2 = dt^2 - a(t)^2 dr^2. \quad (1.20)$$

Therefore the comoving distance traveled by light in an interval between t_i and t_f is

$$r = \int_{t_i}^{t_f} \frac{1}{a(t')} dt'. \quad (1.21)$$

It is now possible to define the radius of a comoving sphere around an observer O that contains all the points that may have interacted with O from zero initial time until a time t as

$$r_p(t) := \int_0^t \frac{1}{a(t')} dt'. \quad (1.22)$$

$r_p(t)$ is a comoving distance, the physical distance is as usual

$$d_p(t) = a(t) r_p(t). \quad (1.23)$$

$d_p(t)$ is called *particle horizon*. The name 'horizon' suggests the meaning of the variable: points that are separated by a distance greater than $d_p(t)$ at time t cannot have been in causal contact in all past history of the Universe. Notice that it is an actual horizon only if it is a finite quantity

that means only if the integral in equation (1.22) converges. From the general solutions for $a(t)$, equation (1.17), it follows that the particle horizon exists only if

$$\boxed{\omega > -\frac{1}{3}}, \quad (1.24)$$

this condition holds both in the radiation and non-relativistic matter solutions. The particle horizon d_p assumes the form

$$d_p(t) = \frac{3(1+\omega)}{3\omega+1}t. \quad (1.25)$$

The condition (1.24) is equivalent to a decelerated expansion $\ddot{a}(t) < 0$, as opposed to the condition (1.15).

It is useful to introduce now the *Hubble radius* d_h that we can later relate to the particle horizon. Let us take an observer O and consider a sphere around it with varying radius. As the radius increases, the receding velocity of a point on the surface of the sphere increases, since the Universe is expanding. The Hubble radius is defined as the distance reached when the receding velocity is equal to the speed of light. Therefore it is defined as follows

$$d_h := \frac{a}{\dot{a}} = \frac{1}{H}. \quad (1.26)$$

Introducing the Hubble time as $\tau_h = H^{-1}$, that is the typical expansion time (approximately the time in which the Universe doubles its size) we can interpret the Hubble radius as the maximum distance that a particle can travel in a τ_h , in fact reintroducing c ,

$$d_h = c\tau_h. \quad (1.27)$$

This is a complementary way to describe causal connection between points of the spacetime. The comoving Hubble radius is

$$r_h := \frac{1}{aH}. \quad (1.28)$$

To emphasize the difference between the Hubble radius and the particle horizon we can rewrite the latter as

$$r_p(a) = \int_0^a \frac{da'}{a'} \cdot \frac{1}{a'H(a')} \quad (1.29)$$

The comoving particle horizon is the logarithmic integral of the comoving Hubble radius. The difference between the two quantities is highlighted by the integral. In fact if particles at a given time t are separated by a distance greater than r_p they have never been able to interact before, hence the integral over all the history of the Universe. While if the distance is larger than r_h they are not in causal contact now (or better, they have not been in contact in the past τ_h) but they could have been in the past. It is possible to have r_p much larger than r_h if the contribution of the Hubble radius from the early times was dominating [9].

1.2 Shortcomings of the Standard Model

The Standard Model of cosmology at first did not aim to explain the first moments of the Universe's history. In fact, as mentioned above, in order to explain the experimental observations it needed a set of fine-tuned initial condition. We are now going to explore these issues of the model.

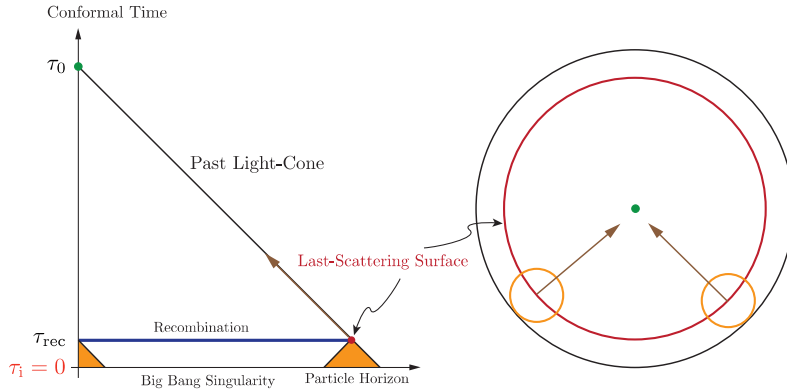


Figure 1.3: Conformal diagram of the history of the Universe in the Standard Model of cosmology. Photons observed today share the same properties even if they could not have been in thermal contact before the last scattering instant, their past light cone do not overlap. Figure from [25].

1.2.1 Horizon problem

The part of the Universe contained inside the sphere of radius r_p is also called observable Universe since it is the section of the spacetime we are able to observe from a theoretical point of view and at present it is increasing in size. The horizon problem lays in the fact that the new scale λ_0 that enters the horizon today, shows the same property of homogeneity and isotropy of the parts of the Universe already known. Up until now this observation cannot be explained in the context of the Hot Big Bang model unless we fix isotropy and homogeneity as initial condition. In fact there has not been causal connection on scale λ_0 before today. It is actually even more problematic since small inhomogeneity of the energy density have been detected [3] and they should also be properly produced by fixing ad-hoc the initial condition.

The CMB is the perfect example to clarify this issue. In fact if we computed the particle horizon at the time of recombination² and the angle in the sky subtended by such distance we obtain $\theta_h \simeq 1.16^\circ$ [25]. So two photons that reach us from an angle larger then θ_h should not have been causally connected in the past and therefore they should not have had the possibility to thermalize. Here lays the discrepancy: the experimental observations show isotropy in the temperature of the CMB photons in the full sky (with fluctuation of the order of $\frac{\Delta T}{T} \simeq 10^{-5}$ [3]). Starting from the conformal metric in equation (1.3), we can compute the light cone for a photon that has null geodesic and travels radially, obtaining

$$d\tau = \pm dr, \quad (1.30)$$

that is the same condition as in the Minkowski spacetime. We then see in figure 1.3 that the majority of the photons from the last scattering surface had not been in causal contact with each other. Their past light cones do not overlap in the past however they arrive at the observer at τ_0 sharing the same properties.

1.2.2 Flatness problem

The latest experimental observations [3] showed that the present Universe is compatible with a spatially flat solution i.e. $\kappa = 0$ and $\Omega = 1$. To understand why this is a problem we recall how the density parameter evolves with time

²The time of recombination, or last scattering, is the time after which Thompson scattering has a negligible scattering rate with respect to the Universe expansion rate. Photons and electrons are no longer in thermal equilibrium and the former can now freely travel toward us today.

$$\Omega(t) - 1 = \frac{\kappa}{a^2(t)H^2(t)} = \kappa r_h^2(t), \quad (1.31)$$

where we connected it with the comoving Hubble radius. Considering only a Universe composed of matter and radiation, r_h is always growing with time and so is the difference between Ω and 1. Therefore the differences between a flat solution and an open or closed one should become more and more relevant during the evolution of the Universe.

Furthermore being $\kappa = 0$ a solution with null probability of realization, since it is one configuration over infinity possibilities; we expect our Universe to have a spatial curvature different from zero. The problem is now evident: we need to fix Ω very close to 1, as initial condition, to explain the observed Universe today.

Quantitatively today we observe [3]

$$|\Omega_0 - 1| = 0.0007 \pm 0.0019 \text{ (68\%)}, \quad (1.32)$$

and assuming the presence of only matter and radiation, the value that we should fix at the Planck scale $E_P = 10^{19}$ GeV³ is given by [24]

$$|\Omega(t_p) - 1| \simeq |\Omega_0 - 1| 10^{-60}, \quad (1.33)$$

$$|\Omega(t_p) - 1| \lesssim 10^{-62}. \quad (1.34)$$

It is clear that this is not an inconsistency of the model but rather a very unnatural and fine-tuned initial condition we need to fix in order to explain the experimental observations within our model.

1.2.3 Unwanted relics

Historically the first problem that arose in the Standard Model was a purely theoretical one. In fact it became clear that the integration of various extensions of the Standard Model (SM) of particle physics, e.g Grand Unified Theories (GUT), in the Hot Big Bang model would lead to the production of a number of topological defects in the early Universe at very high energy.

These cosmological defect are usually the result of spontaneous symmetry breaking (SSB) of the GUT group where the type depends on the symmetry and how it is broken. For example the SSB in the most simple GUT model $SU(5) \rightarrow SU(3) \times SU(2) \times U(1)$ would produce magnetic monopoles. The problem is that being produced at very high energy and without any efficient process that reduces the number of relics we would have today

$$\Omega_0^M \gtrsim 10^{16}, \quad (1.35)$$

that would enormously overclose the Universe [24]. A more detailed discussion can be found in [26].

1.3 A Single Dynamical Solution

Inflation is a dynamical mechanism that can solve the three issues of the Hot Big Bang cosmology at the same time. It consists in a primordial epoch of accelerated expansion. Its simplicity lies in the fact that the constraints to be imposed on this epoch to solve both the horizon problem and the flatness problem are equivalent.

³The Planck scale is, at best, the last scale at which the Quantum Field Theory and GR description of nature we are using still holds.

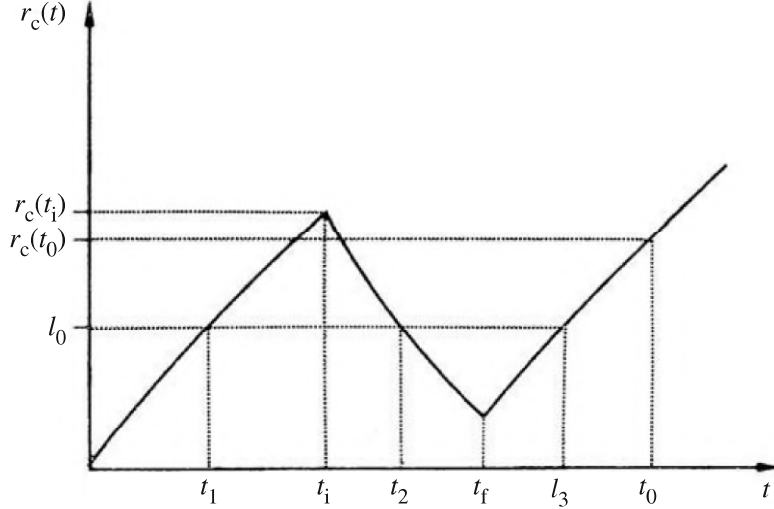


Figure 1.4: The plot describes the evolution of the comoving Hubble radius. It presents the inflationary epoch in the interval $[t_i, t_f]$ where r_h decreases and then in the radiation-matter epoch starts to increase again. Fundamental to solve the problem is that $r_h(t_i) > r_h(t_0)$. The comoving scale l_0 enters the Hubble sphere at t_3 but it was already inside in the past. Figure from [24].

1.3.1 Horizon problem

To solve the horizon problem today there should be a mechanism that allows all the photons of the CMB in the present observable Universe to have been thermalized before the last scattering. This means that the scales that enter the horizon today were actually already inside, at some time t , before the moment of the CMB production and then they have exited. In this way homogeneity and isotropy are naturally explained by primordial thermalization of the photons.

We need an epoch in which the Hubble radius decreases in such a way that the scale that enters today were actually already inside the Hubble sphere in the past. Figure 1.4 shows it explicitly. This condition implies

$$\dot{r}_h < 0 \stackrel{(1.28)}{\implies} \ddot{a} > 0. \quad (1.36)$$

As anticipated before, an epoch of accelerated expansion is necessary to solve the problem. However this is not the only condition. To solve the problem there is a minimum duration we need to require. In fact, as figure 1.4 shows, to solve the horizon problem today we need to demand

$$r_h(t_i) \geq r_h(t_0), \quad (1.37)$$

that is equivalent to ask that all the scales we observe today were already inside the horizon before inflation.

To quantify the duration of inflation it is useful to define the concept of number of e-folds that is

$$N := \ln \left(\frac{a(t_f)}{a(t_i)} \right) = \int_{t_i}^{t_f} dt' H(t'). \quad (1.38)$$

Imposing the requirement (1.37) we obtain $N \gtrsim 60$ [24] that corresponds to a ratio of around 26 order of magnitude between the scale factor at the beginning and at the end of inflation

$$\left(\frac{a(t_f)}{a(t_i)} \right) \gtrsim 10^{26}. \quad (1.39)$$

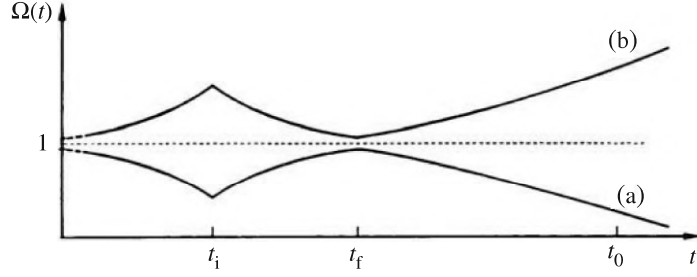


Figure 1.5: Evolution of the density parameter with respect to the cosmic time t . The dotted line at constant $\Omega = 1$ describes a spatially flat Universe. Instead the above and below curves describe respectively an open and a closed Universe. Inflation takes place in the interval $[t_i, t_f]$ and drives Ω towards one. During the matter/radiation dominated Universe, for $t > t_f$, Ω diverges from the flat Universe value $\Omega = 1$. Figure from [24].

1.3.2 Flatness problem

In the case of the flatness problem we need a process that provides naturally the otherwise fine-tuned initial condition, i.e. a primordial process that pushes Ω very close to one. Since

$$\Omega(t) - 1 = \frac{\kappa}{a^2(t)H^2(t)} = \kappa r_h^2(t), \quad (1.40)$$

a decreasing Hubble radius and so an accelerated expansion is needed to solve this issue, as in the previous case.

The effect produced by an inflationary era is to drive the Universe towards a state very close to flatness as shown in figure 1.5. The solution $\Omega = 1$ is an attractor solution during inflation [25]. This is clear when we study

$$\frac{d\Omega(t)}{d \ln a} = (1 + 3w)\Omega(\Omega - 1), \quad (1.41)$$

that is obtained starting from (1.40), taking the time derivative of Ω

$$\frac{d}{dt}\Omega(t) = -\kappa \frac{d}{dt} \left(\frac{1}{\dot{a}^2} \right) = +2\kappa \frac{\ddot{a}}{\dot{a}^3}, \quad (1.42)$$

connecting the a derivative to the t one

$$\frac{d}{d \ln a} = a \frac{d}{da} = \frac{a}{\dot{a}} \frac{d}{dt}, \quad (1.43)$$

using the second Friedmann equation (1.12) and the definition of the density parameter (1.18). During inflation the condition (1.15) is satisfied, therefore equation (1.41) has an attractor solution since the right-hand side is negative and it is almost zero in the neighborhood of $\Omega = 1$.

In order to solve the problem as before we need to fix the minimum amount of lasting time. This is obtained by imposing

$$\Omega(t_i) - 1 < \Omega(t_0) - 1. \quad (1.44)$$

It turns out [24] that the requirement in equation (1.44) implies

$$N \gtrsim 60,$$

that means that with one mechanism and same constraint both flatness and horizon problems can be solved.

1.3.3 Cosmological constant

In the previous discussion we encountered a fluid candidate with negative pressure that can provide an accelerated expansion: the cosmological constant. In fact the scale factor for this solution grows exponentially

$$a(t) \propto e^{Ht} \quad (1.45)$$

with H being constant. This solution, that requires $\omega = -1$, is equivalent to simply adding a constant to the Einstein equation, that is allowed by the theory,

$$G_{\mu\nu} = 8\pi G \left(T_{\mu\nu} - \frac{1}{8\pi G} \Lambda g_{\mu\nu} \right), \quad (1.46)$$

when the constant dominates the energy density. Therefore in a Universe dominated by the cosmological constant

$$P_\Lambda = -\frac{\Lambda}{8\pi G}, \quad (1.47)$$

$$\rho_\Lambda = \frac{\Lambda}{8\pi G}, \quad (1.48)$$

the energy density is positive and constant and the pressure is negative and constant. The scale factor and the Hubble parameter, according to the Friedmann equations are

$$H^2 = \frac{\Lambda}{3}, \quad (1.49)$$

$$a(t) \propto \exp\left(\sqrt{\frac{\Lambda}{3}}t\right). \quad (1.50)$$

However an exact cosmological constant cannot be the solution to the initial conditions problem. In fact we need a dynamical solution, inflation has to reach an end in a finite amount of time and has to produce afterwards the radiation dominated era for which we have experimental evidences.

The modern interpretation of this solution is that energy density ρ_Λ describes the energy density of the ground state of a quantum system, the *vacuum state*. The ground state does not contain any particle species but, due to quantum fluctuation, virtual particles are created and annihilated. Therefore the energy of the vacuum state is non zero.

Quantitatively the energy generated by the fluctuations of a given particle species is obtained by the vacuum expectation value (VEV) of its stress energy tensor

$$\langle 0|T_{\mu\nu}|0\rangle = \langle 0|\rho|0\rangle g_{\mu\nu}. \quad (1.51)$$

Inserting this expression into the Einstein equation we obtain

$$G_{\mu\nu} = 8\pi G \langle \rho \rangle g_{\mu\nu}. \quad (1.52)$$

The important message of equation (1.52) is that if the VEV of a particle species is constant for a certain time interval it behaves exactly as a cosmological constant. It is important to underline that in GR it is not possible to shift the energy of the ground state to zero as we are used to do in Quantum Field Theory (QFT) in the Minkowski spacetime. Any form of energy is in fact source of and subject to gravity.

1.4 Slow-Roll Inflation

In section 1.3 we described the kinematical properties of the process that can solve the shortcomings of the Hot Big Bang model. In section 1.3.3 we suggested how a dynamical field can indeed produce the period of accelerated expansion we are looking for.

The simplest model of inflation we can study is a single scalar field minimally coupled to gravity. The dynamics of the field is governed as usual by the action

$$S_\phi = \int d^4x \sqrt{-g} \mathcal{L}_\phi(\phi, g_{\mu\nu}). \quad (1.53)$$

However to completely describe a scalar field in a curved spacetime we need to consider also the Einstein-Hilbert action [23], the action that produces the Einstein equation (1.6) in vacuum,

$$S_{EH} = \frac{1}{16\pi G} \int d^4x \sqrt{-g} R. \quad (1.54)$$

The Lagrangian for the scalar field is given by [11]

$$\mathcal{L}_\phi = -\frac{1}{2} g^{\mu\nu} \partial_\mu \phi \partial_\nu \phi - V(\phi), \quad (1.55)$$

where in the kinetic term we have the minimal coupling of the scalar field with the metric through. $V(\phi)$ is the potential that contains the mass term, self interaction and eventual effective description of the interaction with other particle that were integrated out. One could also consider the term

$$\mathcal{L}_\phi \supset \frac{1}{2} \xi \phi^2 R, \quad (1.56)$$

in the action, which would imply a direct coupling of the field ϕ with gravity. This type of interaction appears in the so called scalar-tensor theories [27, 28]. Considering only a minimally coupled field, we set $\xi = 0$ in the following discussion.

The stress energy tensor associated to the field follows from the GR definition given in equation (1.7). With some algebra and recalling the matrix property

$$\text{Tr}(\log(g)) = \log(\det(g)) \quad (1.57)$$

it is possible to derive [11]

$$T_{\mu\nu} = \partial_\mu \phi \partial_\nu \phi + g_{\mu\nu} \mathcal{L}_\phi. \quad (1.58)$$

Before moving on to the equation of motion of the field it is useful to think how to tackle and simplify the problem. Both the metric $g_{\mu\nu}$ and ϕ are fields that depend on the spacetime point. However we know that in the zeroth order approximation we expect the Universe to be homogeneous and isotropic. This means that the background metric value is the FLRW metric in (1.1) on top of which we can add some perturbations.

Moreover since we want to use the scalar field to describe inflation and solve the problem of the initial conditions, we expect also the background value of field, ϕ_0 , to be homogeneous and isotropic meaning independent from the spatial coordinates. We therefore split the fields into two contributions:

$$g_{\mu\nu}(x, t) = g_{\mu\nu}^{(0)}(t) + \delta g_{\mu\nu}(x, t), \quad (1.59)$$

$$\phi(x, t) = \phi_0(t) + \delta\phi(x, t), \quad (1.60)$$

with $g_{\mu\nu}^{(0)}(t) = g_{\mu\nu}^{FLRW}(t)$. This is nothing else than a perturbative expansion and so, to be physically sensible, the perturbations need to satisfy the following conditions

$$\langle \delta\phi^2(x, t) \rangle \ll \phi_0^2(t), \quad (1.61)$$

$$\langle \delta g_{\mu\nu} \rangle \ll g_{\mu\nu}^{(0)}. \quad (1.62)$$

During the model building of an inflationary theory we need always to check if these requirements are met; they are not trivial conditions.

The procedure of perturbative splitting can be justified if we consider the experimental measurement of the CMB [3]. In fact the temperature anisotropies are found to be much smaller than its mean value, in particular

$$\frac{\Delta T}{T} \simeq 10^{-5} \quad (1.63)$$

Since the anisotropies of the temperature are directly connected with overdensity and then with perturbations of the field [10], as we will discuss in section 1.5.1, the perturbative splitting in equations (1.60) and (1.59) has a observational basis.

1.4.1 Background dynamics

The dynamics of the background fields should produce the accelerated expansion needed. As stated before, the background fields are homogeneous and isotropic, meaning that the only non null components of the stress-energy tensor of the scalar field are the diagonal ones, considering the comoving reference frame:

$$T_{\mu\nu} = \begin{pmatrix} \rho_\phi & 0 & 0 & 0 \\ 0 & P_\phi & 0 & 0 \\ 0 & 0 & P_\phi & 0 \\ 0 & 0 & 0 & P_\phi \end{pmatrix}. \quad (1.64)$$

It follows then from equation (1.58) that

$$\rho_\phi = \frac{1}{2}\dot{\phi}_0^2 + V(\phi_0), \quad (1.65)$$

$$P_\phi = \frac{1}{2}\dot{\phi}_0^2 - V(\phi_0). \quad (1.66)$$

It is clear now that with a scalar field is possible to have a fluid with negative pressure, that is equivalent to an accelerated expansion: taking a look at equation (1.66), if $V(\phi_0) > \dot{\phi}_0^2$ the pressure assumes negative values. From the equation of state of the fluid (1.14) the fluid parameter is

$$\omega = \frac{\frac{1}{2}\dot{\phi}_0^2 - V(\phi_0)}{\frac{1}{2}\dot{\phi}_0^2 + V(\phi_0)}, \quad (1.67)$$

We can ask the scalar to behave like a cosmological constant for a given time interval, this means asking $\omega \simeq -1$ that translates to the first slow-roll condition

$$\boxed{\dot{\phi}_0^2 \ll V(\phi_0)}. \quad (1.68)$$

The condition in equation (1.68) implies that $P_{\phi_0} \simeq -\rho_{\phi_0}$, a state similar to a cosmological constant. It describes a scalar field whose potential energy dominates over the kinetic part. This means that the field is moving slowly along the potential and thus this can be obtained by an almost flat potential during inflation as shown in figure 1.6. As we will see later we will need a second condition that assures equation (1.68) to be satisfied for $N \approx 60$.

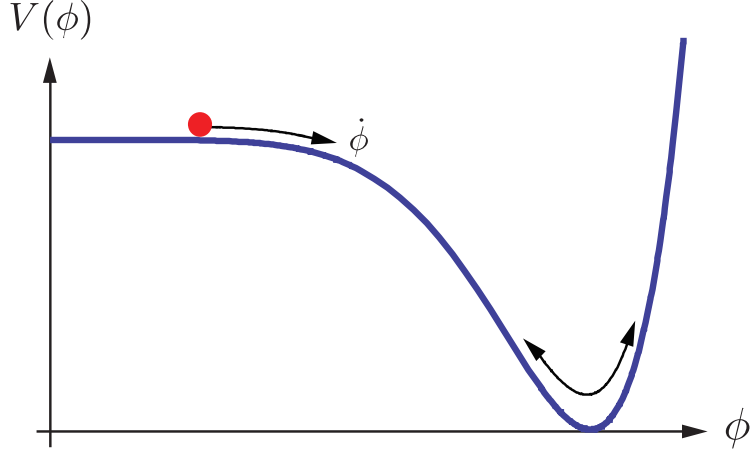


Figure 1.6: The energy density of the scalar field during inflation is dominated by its potential since its kinetic energy is subdominant. ϕ is slowly rolling on a quasi flat potential $V(\phi)$. Inflation ends when the potential starts to present a strong dependence on the field. Figure from [25].

The scalar field is thus mimicking a cosmological constant during this phase but the process remains dynamical. This solution represents a quasi de Sitter expansion, the Hubble parameter is almost constant during inflation and therefore the scale factor has a nearly exponential dependence on time.

$$H^2 = \frac{8\pi G}{3}\rho_{\phi_0} \simeq \frac{8\pi G}{3}V(\phi_0) \simeq \text{const}, \quad (1.69)$$

$$a(t) \propto e^{Ht}. \quad (1.70)$$

We now introduce the equation of motion for the scalar field obtained by extremizing the action in equation (1.53)

$$\square \phi = \frac{\partial V}{\partial \phi}, \quad (1.71)$$

where in GR the d'Alembertian operator assumes the form

$$\square \phi = \frac{1}{\sqrt{-g}}\partial^\mu(\sqrt{-g}g_{\mu\nu}\partial^\nu\phi). \quad (1.72)$$

In a FLRW Universe because of the isotropy of the background field, $\nabla^2\phi/a^2 = 0$ and the equation of motion reads

$$\ddot{\phi}_0 + 3H\dot{\phi}_0 = -\frac{\partial V}{\partial \phi_0}, \quad (1.73)$$

where the only difference with the Klein-Gordon equation in a flat spacetime is the presence of the term $3H\dot{\phi}_0$. This is a friction-like term in classical mechanics and it describes the fact that the scalar field evolves on a background that is expanding. If the expansion was absent ($H = 0$) we recover the solution in the Minkowski spacetime. In all this treatment we are assuming that in the inflationary epoch the scalar field is the dominant contribution to the energy density of the Universe.

1.4.2 Slow-roll parameters

The properties that the scalar field has to satisfy can be summarized by the introduction of model-independent parameters. These parameters will be applied to particular theories to constrain the potential. Considering a quantity $Q(t)$ in an expanding Universe, its evolution can be measured in terms of the scale factor $a(t)$ and parameterized as follows

$$\epsilon_Q := \frac{d \ln Q(t)}{d \ln a(t)} = \frac{\dot{Q}(t)}{HQ(t)}. \quad (1.74)$$

As discussed above the Hubble parameter remains almost constant during a quasi dS inflation, we can thus define the first slow-roll parameter as

$$\epsilon := \frac{d \ln H(t)}{d \ln a(t)} = -\frac{\dot{H}}{H^2}. \quad (1.75)$$

The parameter is closely related to the second derivative of the scale factor, in fact

$$\ddot{a} = \dot{a}H + a\dot{H} = aH^2 \left(1 + \frac{\dot{H}}{H^2} \right) = aH^2(1 - \epsilon) \quad (1.76)$$

Therefore inflation ends when $\epsilon \rightarrow 1$. It can be easily shown that the slow-roll condition in equation (1.68) is equivalent to

$$\boxed{\epsilon \ll 1}. \quad (1.77)$$

The second requirement is connected to the duration of inflation. In fact in order to solve the initial conditions problems we need the first slow-roll condition, that assures $\ddot{a} > 0$, to be satisfied for a time such that the Universe can expand by (around) 60 e-folds⁴. We can parametrize this asking ϵ to evolve slowly, defining

$$\eta := \frac{d \ln \epsilon(t)}{d \ln a(t)} = \frac{\dot{\epsilon}}{H\epsilon}, \quad (1.78)$$

and requiring

$$\boxed{\eta \ll 1}, \quad (1.79)$$

during inflation. This is the second slow-roll condition. The η parameter is also related to the dynamics of the field, in fact the previous condition is equivalent to

$$\ddot{\phi} \ll 3H\dot{\phi}. \quad (1.80)$$

Both η and ϵ are model independent parameters.

The two slow-roll conditions can be translated using the Friedmann equations to conditions that constrain the shape of the potential. We can introduce a new set of parameters tightly connected with the potential as follows

$$\epsilon_V := \frac{1}{16\pi G} \left(\frac{1}{V} \frac{\partial V}{\partial \phi} \right)^2 \quad (1.81)$$

$$\eta_V := \frac{1}{8\pi G} \left(\frac{1}{V} \frac{\partial^2 V}{\partial \phi^2} \right) \quad (1.82)$$

⁴The number of e-folds needed depends on the energy scale of inflation and on the details of reheating process. For details please refer to section 5.1 of [29].

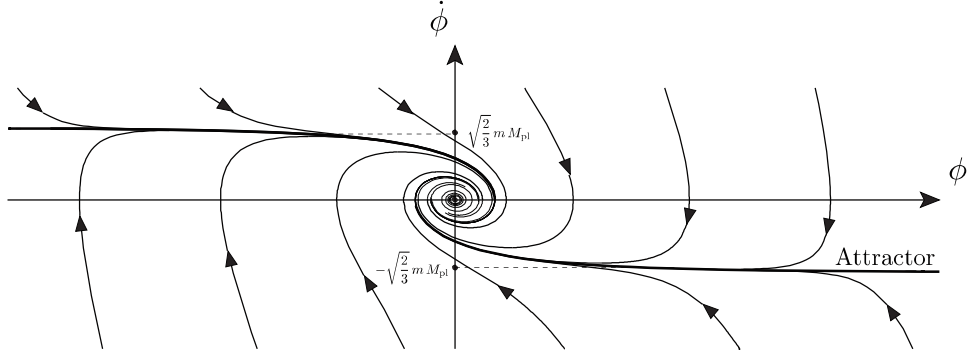


Figure 1.7: Phase space diagram for the inflationary model with potential $V(\phi) = 1/2m^2\phi^2$ [30]. It is clear the presence of an attractor solution in the origin. Figure from [5]

If the conditions in equations (1.77) and (1.79) are satisfied, at first order in the slow-roll parameters,

$$\epsilon_V \simeq \epsilon, \quad (1.83)$$

$$\eta_V \simeq \eta + \epsilon. \quad (1.84)$$

Therefore it is now clear that the slow-roll conditions imply the need for a flat potential.

The experimental bounds on the parameters are given by the Planck experiment [3]

$$\epsilon_V < 0.0097 \quad (95\%CL), \quad (1.85)$$

$$\eta_V = -0.10^{+0.0078}_{-0.0072} \quad (68\%CL). \quad (1.86)$$

1.4.3 Attractor solution

In general scalar models of inflation have attractor solutions [25, 30]. Let us study the most simple example: single field inflation with potential

$$V(\phi) = \frac{1}{2}m^2\phi^2. \quad (1.87)$$

The equation of motion starting from equation (1.73) is

$$\ddot{\phi} + 3H\dot{\phi} + m^2\phi = 0, \quad (1.88)$$

using the equivalence

$$\ddot{\phi} = \dot{\phi} \frac{d}{d\phi} \dot{\phi}, \quad (1.89)$$

we re-write (1.88) as

$$\frac{d\dot{\phi}}{d\phi} + 3H + m^2 \frac{\phi}{\dot{\phi}} = 0. \quad (1.90)$$

Using the first Friedmann equation 1.11 we have

$$H^2 = \frac{1}{6M_P^2} (\dot{\phi}^2 + m^2\phi^2), \quad (1.91)$$

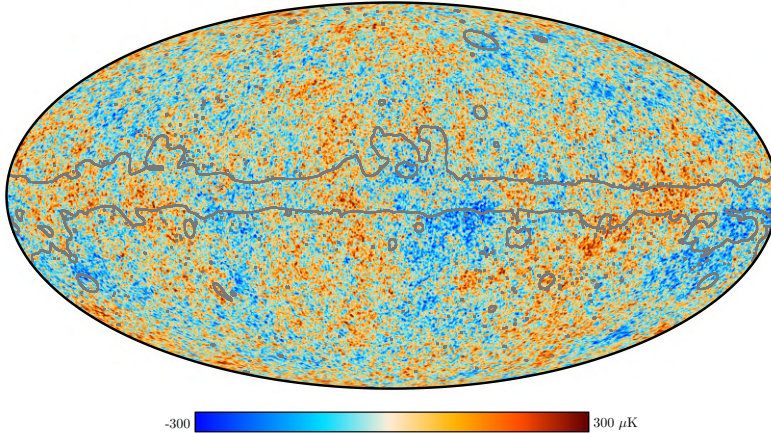


Figure 1.8: The Planck map of the temperature anisotropies of the CMB. Figure from [3].

therefore

$$\frac{d\dot{\phi}}{d\phi} = -\frac{\sqrt{\frac{3}{2}} \frac{1}{M_{\text{Pl}}^2} (\dot{\phi}^2 + m^2 \phi^2)^{1/2} \dot{\phi} + m^2 \phi}{\dot{\phi}}. \quad (1.92)$$

The phase diagram is presented in figure 1.7. The presence of an attractor solution is very important in our treatment as it justifies the use of the Friedmann equation during the inflationary epoch. In fact even if we start from a strongly inhomogeneous and anisotropic Universe every state is rapidly evolving towards the attractor that is a FLRW Universe where the Friedmann equations are valid.

1.5 Cosmological Perturbations

Up until now we discussed the zeroth order properties of the Universe (homogeneity and isotropy) but the measurements from CMB show the presence of temperature fluctuations of the order $\frac{\Delta T}{T} \sim 10^{-5}$ as shown in figure 1.8. This temperature fluctuations can be connected to energy-density perturbation in the early Universe [10, 11].

In this section we will try to understand how to explain the presence of this fluctuations in the context of the Standard Model of cosmology and we will encounter a strong prediction of the inflationary mechanism: the quantum fluctuations of the scalar field are the seed of the cosmological perturbations we observe today. Let us start by studying the dynamics of the perturbation of the scalar field using the decomposition in equation (1.60).

1.5.1 Quantum fluctuation

The complete Klein-Gordon equation for an inhomogenous scalar field $\phi(x, t)$ (1.71)

$$\ddot{\phi}(x, t) + 3H\dot{\phi}(x, t) - \frac{\nabla^2}{a^2}\phi(x, t) = -\frac{\partial V}{\partial \phi}. \quad (1.93)$$

In the following we will consider the evolution of a scalar field perturbation in a fixed de Sitter background spacetime⁵. Using the background equation (1.73) and the decomposition in equation (1.60) we obtain

⁵In this section we will deal with a fixed background metric while we know that a perturbation of ϕ produces a perturbation of the metric. A complete treatment is left for section 1.5

$$\delta\ddot{\phi} + 3H\delta\dot{\phi} - \frac{\nabla^2\delta\phi}{a^2} = -\frac{\partial^2 V}{\partial\phi^2}\delta\phi \quad (1.94)$$

that is the equation of motion for the perturbation $\delta\phi(x, t)$ at linear order. Before moving forward to the complete solution let us have a qualitative view of the perturbations at large scales, meaning at cosmological scales [31]. Cosmological scales λ are super-horizon scales: $\lambda > H^{-1}$.

In this limit the Laplacian term can be neglected: we are filtering the perturbation modes, concentrating only on the one relevant at large scale. We have now a system of equations, the equation of motion for the background and for the perturbation

$$\begin{cases} \ddot{y} + 3H\dot{y} = -\frac{\partial^2 V}{\partial\phi^2}y \\ \delta\ddot{\phi} + 3H\delta\dot{\phi} - \frac{\nabla^2\delta\phi}{a^2} = -\frac{\partial^2 V}{\partial\phi^2}\delta\phi \end{cases} \quad (1.95)$$

where we defined $y := \dot{\phi}$ to underline the similarity between the two equations. We can now show that the two equations are not independent, in fact the Wronskian function is

$$W(y, \delta\phi) = y\delta\phi - y\delta\dot{\phi}, \quad (1.96)$$

knowing that if $W = 0$ the variables y and $\delta\phi$ are linearly dependent and from some trivial computation we obtain

$$\dot{W} = -3HW \implies W \propto e^{-3Ht}, \quad (1.97)$$

$$W \xrightarrow{t > 1/H} 0. \quad (1.98)$$

Therefore $\delta\phi$ and $\dot{\phi}_0$ become linearly dependent very fast, after a transient time $\sim 1/H$. So we can write

$$\delta\phi(x, t) \propto \dot{\phi}_0(t), \quad (1.99)$$

where we note that we lack a term dependent on the spatial part, so

$$\delta\phi(x, t) = -\delta\tau(x)\dot{\phi}_0(t), \quad (1.100)$$

where the minus sign is conventional. We can re-write the decomposition of the scalar field as

$$\phi(x, t) = \phi_0(t) + \delta\phi(x, t) = \phi_0(t) - \delta\tau(x)\dot{\phi}_0(t), \quad (1.101)$$

and therefore

$$\phi(x, t) = \phi_0(t - \delta\tau(x)). \quad (1.102)$$

Equation (1.102) tell us that the fluctuations of the scalar field are such that the field reaches the classical value ϕ_0 at different times depending on the position x in which it is. The field ϕ will have the same history in all parts of the Universe but at slightly different times.

To solve equation (1.94) it is convenient to go to Fourier space since we are considering linear perturbations and the various modes k evolve independently,

$$\delta\phi(x, t) = \frac{1}{(2\pi)^3} \int d^3k e^{ikx} \delta\phi_k. \quad (1.103)$$

Note that in the Fourier expansion we used a plane-wave spatial decomposition that is valid only in a flat spacetime, which is a good approximation for the spatial part of the Universe during inflation. The equation of motion is then

$$\delta\ddot{\phi}_k + 3H\delta\dot{\phi}_k + \frac{1}{a^2}k^2\delta\phi_k = -\frac{\partial^2 V}{\partial\phi^2}\delta\phi_k \quad (1.104)$$

where $\delta\phi_k$ are the Fourier modes.

Let us now solve explicitly the equation of motion for the perturbations. We will first discuss the case where the field ϕ is massless

$$\delta\ddot{\phi}_k + 3H\delta\dot{\phi}_k + \frac{k^2}{a^2}\delta\phi_k = 0. \quad (1.105)$$

This model is useful in two ways: it is a first simple example to work with and is a good approximation for the scalar field during inflation. In fact the second slow-roll condition (1.79) can be re-written as

$$\eta_V = \frac{1}{3} \frac{1}{H^2} \frac{\partial^2 V}{\partial\phi^2}, \quad (1.106)$$

therefore even when the potential contains a massive term $V \supset m_\phi^2\phi^2/2$ the condition $\eta_V \ll 1$ is equivalent to considering an almost massless field $m_\phi \ll H$ (since H fixes the relevant energy scale). Let us study the solution in two different regimes:

Small scale regime

When the scale we are considering is well inside the horizon $\lambda \ll H^{-1}$ (*sub-horizon*) we are in the small scale region. The wavenumber satisfies the relation $k \gg aH$ therefore the friction term $3H\delta\dot{\phi}_k$ can be neglected and we are left with a simple harmonic oscillator equation

$$\delta\ddot{\phi}_k + \frac{k^2}{a^2}\delta\phi_k = 0, \quad (1.107)$$

where the frequency is $f(t) = \frac{k^2}{a(t)^2}$, decreasing with time. In the small scale regime the perturbation are rapidly oscillating.

Large scale regime

Regarding fluctuations at a scale $\lambda \gg H$ (*super-horizon*) meaning $k \ll aH$, the equation (1.105) reduces to

$$\delta\ddot{\phi}_k + 3H\delta\dot{\phi}_k = 0, \quad (1.108)$$

that has a simple exact solution

$$\delta\phi_k = A e^{-3Ht} + B, \quad (1.109)$$

where a and b are constants. Because of the term e^{-3Ht} the first term becomes negligible very fast and the perturbations remain constant. Therefore perturbations at super-horizon scale are said to be frozen at the horizon crossing ($\lambda = H^{-1}$) value

$$\delta\phi_k \simeq B(k). \quad (1.110)$$

The behavior is shown in figure 1.9. It also shows the later regime when the scale re-enters the horizon and the density perturbations start to evolve again and in particular they collapse because of gravitational instability forming the large scale structures we observe today. To have an estimate of B we can match the sub-horizon and the super-horizon solution at the horizon crossing time, considering the absolute value,

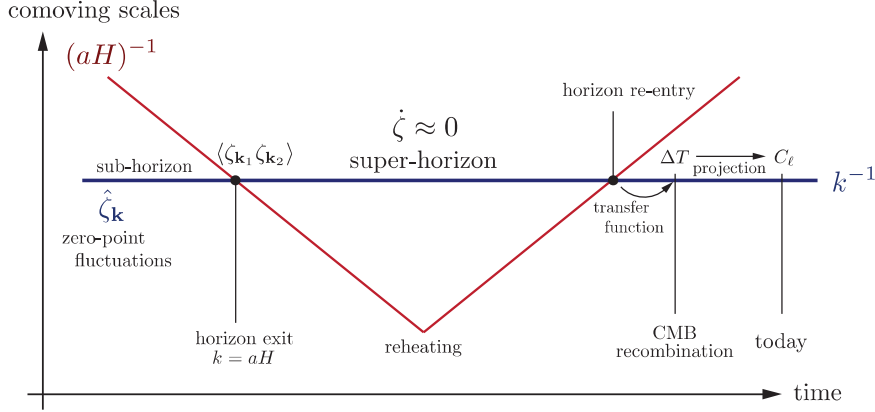


Figure 1.9: The curvature perturbations ζ during and after inflation. Later we will show how the curvature perturbation is proportional to the density perturbation in a given gauge (and so proportional to $\delta\phi$ during inflation) and we will introduce it formally. Inflation is represented by the first part of the red curve, where the Hubble radius is decreasing. During this era the scale λ exits the horizon. The perturbation is then frozen. The comoving scale λ (the blue line) re-enters the horizon at a late time in a FLRW Universe. The perturbation will then evolve and eventually produce the fluctuation signature we can measure today in the CMB. We can therefore connect the measured temperature perturbation of the CMB with the primordial quantum fluctuation. Figure from [25].

$$|B(k)| := \left. \frac{e^{-ik\tau}}{a\sqrt{2k}} \right|_{k=(aH)}, \quad (1.111)$$

that gives

$$|B(k)| = \left. \frac{1}{a\sqrt{2k}} \right|_{k=(aH)} \longrightarrow |\delta\phi_k| = \frac{H}{\sqrt{2k^3}}, \quad (1.112)$$

the value of the perturbation at super-horizon scale.

1.5.2 Canonical quantization and the vacuum choice

In the previous section we studied the behavior in the two limits we can now move to the study of the complete solution of equation (1.105). Since we want to describe this fluctuation as originated by quantum effects we proceed quantizing them, working in conformal time τ . Firstly we introduce a new variable $\widehat{\delta\phi}(x, \tau)$

$$\widehat{\delta\phi}(x, \tau) = a(\tau)\delta\phi(x, \tau). \quad (1.113)$$

We then promote it to an operator introducing the mode expansion

$$\widehat{\delta\phi}(x, \tau) = \frac{1}{(2\pi)^3} \int d^3k \left[u_k(\tau) b_k e^{ik \cdot x} + u_k^*(\tau) b_k^\dagger e^{-ik \cdot x} \right], \quad (1.114)$$

where we have introduced the creation and annihilation operators b_k, b_k^\dagger that are defined as

$$b_k|0\rangle = 0, \quad (1.115)$$

for all values of k and producing excited states as usual

$$|m_{k_1}, n_{k_2}, \dots\rangle = \frac{1}{\sqrt{m!n!\dots}} [(b_{k_1}^+)^m (b_{k_2}^+)^n \dots] |0\rangle, \quad (1.116)$$

where $|0\rangle$ is the vacuum of the theory. Notice that the mode function depends on the conformal time τ since we expanded only the spatial Fourier modes as explained above. Choosing the normalization [25]

$$u_k^{I*}(\tau)u_k(\tau) - u_k^*(\tau)u_k^I(\tau) = i, \quad (1.117)$$

we have the familiar commutation rules

$$\begin{aligned} [b_k, b_{k'}] &= [b_k^\dagger, b_{k'}^\dagger] = 0, \\ [b_k, b_{k'}^\dagger] &= \hbar \delta^{(3)}(k - k'). \end{aligned} \quad (1.118)$$

Even considering a free theory, as in this case, the vacuum $|0\rangle$ is not completely determined by the normalization condition in equation (1.117) (in section 2.3.2 of [25] there is a clear example of the ambiguity of the vacuum).

To fix a unique vacuum we have to introduce a physical insight, that is the equivalence principle. For small scales and small time intervals the spacetime has to be locally approximated by Minkowski. In Minkowski the solution to equation (1.105), since $a = 1$, is simply a plane-wave solution. Therefore we can impose the following condition to our mode functions

$$u_k(\tau) \xrightarrow{k \gg aH} \frac{e^{-i\omega_k \tau}}{\sqrt{2k}} \quad (1.119)$$

that is known as the Bunch-Davies vacuum choice [32]. We are now ready to solve analytically equation (1.105) in de Sitter spacetime, where we recall that the conformal time is

$$\tau = -\frac{1}{aH}, \quad (1.120)$$

so that equation (1.105) expanded in mode function gives

$$u_k''(\tau) + \left(k^2 - \frac{a''}{a}\right) u_k(\tau) = 0, \quad (1.121)$$

where we defined the derivative of a quantity A with respect the conformal time as

$$A' := \frac{dA}{d\tau}. \quad (1.122)$$

The exact solution to equation (1.121) in terms of the field perturbation is

$$\delta\phi_k = \frac{1}{a} \left[A \frac{e^{-ik\tau}}{\sqrt{2k}} \left(1 - \frac{i}{k\tau}\right) + B \frac{e^{ik\tau}}{\sqrt{2k}} \left(1 + \frac{i}{k\tau}\right) \right], \quad (1.123)$$

where A and B are constants to be fixed by the Bunch-Davies vacuum. Asking at early times the survival of only the positive frequency modes ($B = 0$) and using the condition (1.119) we have the physical solution

$$\delta\phi_k = \frac{1}{a} \frac{e^{-ik\tau}}{\sqrt{2k}} \left(1 - \frac{i}{k\tau}\right) \quad (1.124)$$

that reproduces exactly the behaviour in the two regimes studied before.

1.5.3 Massive scalar field

The study of a massive scalar field σ in a de Sitter background is also relevant in our discussion [31]. Proceeding as before we have

$$\widehat{\delta\sigma}(x, \tau) = a(t)\delta\sigma(x, \tau), \quad (1.125)$$

and using the Fourier expansion

$$\widehat{\delta\sigma}(x, \tau) = \frac{1}{(2\pi)^3} \int d^3k \delta\sigma_k(\tau) e^{ik \cdot x}. \quad (1.126)$$

In this case the equation of motion of the mode function (1.121) is modified containing also the mass term as follow

$$\delta\sigma_k'' + \left(k^2 + \frac{1}{\tau^2} \left(\frac{m_\sigma^2}{H^2} - 2 \right) \right) \delta\sigma_k = 0 \quad (1.127)$$

that can be re-written as

$$\delta\sigma_k'' + \left[k^2 - \frac{1}{\tau^2} \left(\nu_\sigma^2 - \frac{1}{4} \right) \right] \delta\sigma_k = 0, \quad (1.128)$$

where we defined the index ν_σ ⁶ as

$$\nu_\sigma^2 = \left(\frac{9}{4} - \frac{m_\sigma^2}{H^2} \right) \quad (1.129)$$

that, at first order in the slow-roll parameters, is

$$\nu_\sigma \simeq \frac{3}{2} - \eta_V \quad (1.130)$$

We are considering a massive field but with a small mass because of the consideration made in section 1.5.1, therefore we consider the index ν_σ to be real. The solution of equation (1.127) is then given by the Hankel functions

$$\delta\sigma_k = \sqrt{-\tau} \left(AH_{\nu_\sigma}^{(1)}(-k\tau) + BH_{\nu_\sigma}^{(2)}(-k\tau) \right). \quad (1.131)$$

and again A and B are to be fixed by the initial conditions. Using the expansion of the Hankel functions we can study the behaviour of the solution at small scales, where we have

$$\begin{aligned} H_{\nu_\sigma}^{(1)}(k \gg aH) &\sim \sqrt{\frac{-2}{k\tau\pi}} e^{i(-k\tau - \frac{\pi}{2}\nu_\sigma - \frac{\pi}{4})}, \\ H_{\nu_\sigma}^{(2)}(k \gg aH) &\sim \sqrt{\frac{-2}{k\tau\pi}} e^{-i(-k\tau - \frac{\pi}{2}\nu_\sigma - \frac{\pi}{4})}. \end{aligned} \quad (1.132)$$

Imposing the Bunch-Davies vacuum, we can fix

$$\begin{aligned} A(k) &= \frac{\sqrt{\pi}}{2} e^{i(\nu_\sigma + \frac{1}{2})\frac{\pi}{2}}, \\ B(k) &= 0, \end{aligned} \quad (1.133)$$

therefore the exact solution is

$$\delta\sigma_k = \frac{\sqrt{\pi}}{2} e^{i(\nu_\sigma + \frac{1}{2})\frac{\pi}{2}} \sqrt{-\tau} H_{\nu_\sigma}^{(1)}(-k\tau). \quad (1.134)$$

Regarding the massless case we saw that, on super-horizon scales, the perturbations are constant and are

$$|\delta\phi_k| = \frac{H}{\sqrt{2k^3}}. \quad (1.135)$$

⁶We are considering a real ν_σ index, assuming $m < 3/2 H$.

In the massive case instead there is a small time dependence in the solution in fact

$$|\delta\sigma_k| \simeq \frac{H}{\sqrt{2k^3}} \left(\frac{k}{aH} \right)^{\frac{3}{2}-\nu_\sigma} \quad (1.136)$$

where we used

$$H_{\nu_\sigma}^{(1)}(k \ll aH) \sim \sqrt{\frac{2}{\pi}} e^{-i\frac{\pi}{2}} 2^{\nu_\sigma-\frac{3}{2}} \left(\frac{\Gamma(\nu_\sigma)}{\Gamma(3/2)} \right) (-k\tau)^{-\nu_\sigma}, \quad (1.137)$$

the expansion of the Hankel function in the super-horizon ($k \ll aH$) regime.

A similar computation [31] can be performed in the case of a quasi de Sitter spacetime where $\epsilon \neq 0$ but still $\epsilon \ll 1$ and the scale factor is, using the conformal time definition (1.4),

$$a(\tau) = -\frac{1}{H(1-\epsilon)\tau}, \quad (1.138)$$

$$\frac{a''}{a} = \frac{2}{\eta^2} \left(1 + \frac{3}{2}\epsilon + \mathcal{O}(\epsilon^2, \eta^2) \right). \quad (1.139)$$

where we stopped the expansion at first order in the slow-roll parameters. The equation of motion is again equation (1.128) but with

$$\nu_\sigma \simeq \frac{3}{2} + \epsilon - \eta_V, \quad (1.140)$$

and we already know the solution. This result will be useful for the discussion in the next section.

1.5.4 Power spectrum

A fundamental tool to study the perturbation of a stochastic field is the power spectrum, we will use it to characterize the statistical properties of the quantum perturbations of the scalar field. The statistical properties of a random field $\delta(t, x)$ are determined by an infinite set of correlation functions, that are nothing else than the ensemble average over the product of δ at different points

$$\begin{aligned} \langle \delta(t, x_1) \delta(t, x_2) \rangle &= \xi(x_1, x_2) \\ \langle \delta(t, x_1) \delta(t, x_2) \delta(t, x_3) \rangle &= \xi(x_1, x_2, x_3) \\ &\vdots \\ \langle \delta(t, x_1) \delta(t, x_2) \dots \delta(t, x_N) \rangle &= \xi(x_1, x_2, \dots, x_N). \end{aligned} \quad (1.141)$$

If and only if the process is Gaussian the two-point function $\xi(x_1, x_2)$ is enough to characterize $\delta(t, x)$ since all the even N correlation functions are combinations of $\xi(x_1, x_2)$ and the odd ones vanish. The concept of power spectrum arises when we consider the field in Fourier space, using the plane-wave expansion

$$\delta(t, x) = \frac{1}{(2\pi)^3} \int d^3k e^{ik \cdot x} \delta_k(t). \quad (1.142)$$

defining the power spectrum as

$$\langle \delta_{k_1}(t) \delta_{k_2}(t) \rangle = (2\pi)^3 \delta^{(3)}(k_1 + k_2) P(k), \quad (1.143)$$

we see that it is nothing else than the Fourier transform of the two-point function

$$\xi(r) = \frac{1}{(2\pi)^3} \int d^3k e^{ik \cdot r} P(k), \quad (1.144)$$

where we are considering that in a homogeneous and isotropic Universe

$$\xi(r) = \xi(|x_1 - x_2|), \quad (1.145)$$

the two-point function depends only on the relative distance. The dimensionless power spectrum can then be introduced as

$$\Delta(k) := \frac{k^3}{2\pi^2} P(k), \quad (1.146)$$

After some calculations we can show that

$$\langle \delta^2(x) \rangle = \int \frac{dk}{k} \Delta_\delta(k) = \int d(\ln k) \Delta_\delta(k), \quad (1.147)$$

which means that the dimensionless power spectrum is the contribution to the variance per (logarithmic) intervals of k . It is useful to introduce another parameter, the spectral index that describes the slope of the power spectrum in a logarithmic scale

$$n(k) - 1 = \frac{d \ln \Delta_\delta}{d \ln k}, \quad (1.148)$$

and we see that in general it depends on the scale k considered. If the spectral index is scale invariant, $n(k) = \text{const}$, the power spectrum has a simple power-law dependence on k

$$\Delta(k) = \Delta(k_0) \left(\frac{k}{k_0} \right)^{n-1}, \quad (1.149)$$

with k_0 being a pivot scale. One particular case is for a scale invariant power spectrum (Harrison-Zel'dovich power spectrum) that means $n(k) = 1$. At each scale λ the perturbations have the same amplitude. We now connect the power spectrum to the Fourier modes of the perturbation and summarize the behavior of the power spectrum for the cases studied in Table 1.3: firstly we use the fact that the perturbation is real

$$\langle \delta\phi_k(t) \delta\phi_{k'}^*(t) \rangle = (2\pi)^3 \delta^{(3)}(k - k') |\delta\phi_k|^2, \quad (1.150)$$

therefore

$$\Delta_{\delta\phi}(k) = \frac{k^3}{2\pi^2} |\delta\phi_k|^2. \quad (1.151)$$

Massless inflaton, de Sitter	$\Delta_{\delta\phi}(k) \simeq \frac{H^2}{4\pi^2}$
Massive inflaton, de Sitter	$\Delta_{\delta\phi}(k) = \left(\frac{H}{2\pi}\right)^2 \left(\frac{k}{aH}\right)^{3-2\nu_\sigma} \simeq \left(\frac{H}{2\pi}\right)^2 \left(\frac{k}{aH}\right)^{-2\eta_V}$
Massive inflaton, quasi-de Sitter	$\Delta_{\delta\phi}(k) = \left(\frac{H}{2\pi}\right)^2 \left(\frac{k}{aH}\right)^{3-2\nu_\sigma} \simeq \left(\frac{H}{2\pi}\right)^2 \left(\frac{k}{aH}\right)^{2\epsilon-2\eta_V}$

Table 1.3: Power spectrum of the inflaton perturbation in three relevant cases, at first order in the slow-roll parameters.

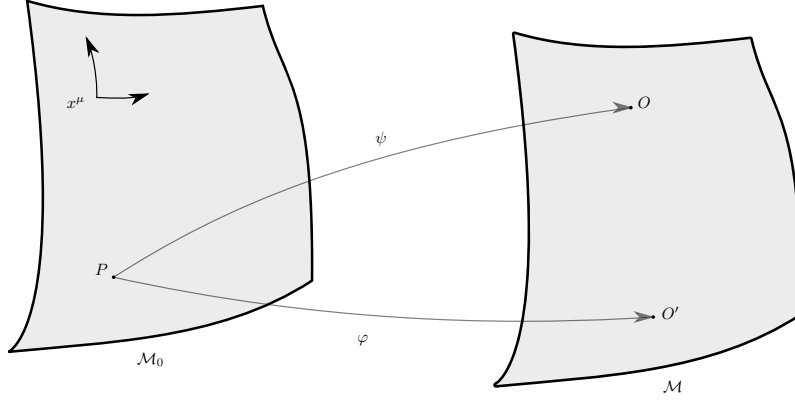


Figure 1.10: Passive approach: the point P in \mathcal{M}_0 is mapped to two different points O, O' depending on the gauge choice. Figure inspired by [33].

1.6 Perturbations in General Relativity

In the previous discussion we actually studied a simplified version of the problem. In fact we studied the evolution of the scalar field perturbations in an unmodified background metric (de Sitter and quasi de Sitter). But we know that the Einstein equations (1.6) tell us that any perturbation of the stress-energy tensor produces a disturbance in the metric side. We therefore need to take that into account to have a complete description. In order to study it we first briefly introduce the perturbation theory in General Relativity.

In the previous sections we argued that the Universe can be described as homogeneous and isotropic at zeroth order and on top of that we can introduce small perturbations as described in equation (1.59). Any tensorial quantity can be split into a homogeneous and a perturbative part

$$T(t, x) = T_0(t) + \delta T(t, x), \quad (1.152)$$

where $T_0(t)$ is the homogeneous and isotropic background value of T in the background spacetime \mathcal{M}_0 that in our case is the FLRW spacetime. T instead lives in a different spacetime, the perturbed one, that we will call \mathcal{M} . Since we know that the perturbations are small ($|\delta T| \ll |T_0|$) we can consider only the linear term in the perturbation expansion. The Einstein equations up to the first order of perturbation read

$$\delta G_{\mu\nu} = 8\pi G \delta T_{\mu\nu}. \quad (1.153)$$

Re-arranging equation (1.152) we have

$$\delta T = T - T_0, \quad (1.154)$$

and we notice that the perturbation δT is not uniquely defined in General Relativity. In fact T and T_0 live in two different spacetimes while to compare tensor we need to evaluate them at the same spacetime point. Therefore we need to introduce a map, a diffeomorphism, that connects the background and the perturbed spacetimes ($\mathcal{M}_0, \mathcal{M}$). The map is defined as

$$\psi : \mathcal{M}_0 \longrightarrow \mathcal{M}, \quad (1.155)$$

$$\psi(P) \longrightarrow O, \quad (1.156)$$

where $P \in \mathcal{M}_0$ and $O \in \mathcal{M}$. It is clear that ψ is not an unique map but in the same way we can define a second map φ as shown in figure 1.10. When choosing a map we are making a gauge

choice. The gauge freedom is twofold, it is a tool to simplify a problem or to have a better physical insight but it is also an issue. In fact the gauge freedom translate to a gauge dependence of the perturbations, which is known as the gauge problem [25, 31]. Let us give an example of this. If we have two maps that connect \mathcal{M}_0 , in which we have T_0 , and \mathcal{M} , in which we have T and T' , the perturbation is different due to the gauge choice, in fact

$$\begin{aligned}\delta T &= T - T_0 \\ \delta T' &= T' - T_0\end{aligned}\tag{1.157}$$

where in general $\delta T \neq \delta T'$. The choice of gauge can hide physical perturbations or can introduce fictitious ones. To avoid ambiguities we need to study gauge-invariant quantities that are combinations of both matter-energy perturbations and metric perturbations. We refer to [31, 34] for a full treatment of the gauge problem and gauge transformation. Here we just indicate the result of a gauge transformation at linear order that is

$$\delta \tilde{T} = \delta T + \mathcal{L}_\xi T_0\tag{1.158}$$

where we defined a gauge transformation as the choice of different map connecting the perturbed manifold to the unperturbed one. \mathcal{L}_ξ is the Lie derivative along the vector ξ .

Perturbation of the metric and the stress energy tensor

In the previous study we discussed the perturbation of the inflaton. We are now ready to discuss also the perturbation of the metric. If we perturb at linear order the FLRW metric we obtain [25, 31]

$$\begin{aligned}g_{00} &= -a^2(\tau)[1 + 2\Psi(x, \tau)], \\ g_{0i} &= g_{i0} = a^2(\tau)\omega_i(x, \tau), \\ g_{ij} &= a^2(\tau)[(1 - 2\Phi(x, \tau))\delta_{ij} + \gamma_{ij}(x, \tau)],\end{aligned}\tag{1.159}$$

where Φ, Ψ are scalar functions, ω_i is a vector and γ_{ij} a traceless tensor $\gamma^i_i = 0$. The decomposition in these three categories of a well-defined object in a manifold \mathcal{M} is very useful since at linear order their dynamics are decoupled. Furthermore we can decompose vectors into solenoidal and longitudinal part (the Helmholtz theorem). Similarly we can decompose also tensors. We then have

$$\omega_i = \partial_i \omega^\parallel + \omega_i^\perp,\tag{1.160}$$

$$\gamma_{ij} = D_{ij}\gamma^\parallel + \partial_i\gamma_j^\perp + \partial_j\gamma_i^\perp + \gamma_{ij}^T,\tag{1.161}$$

with

$$D_{ij} = \partial_i\partial_j - \delta_{ij}\frac{\nabla^2}{3},\tag{1.162}$$

where ω^\parallel and γ^\parallel are scalar function, ω_i^\perp and γ_i^\perp are solenoidal vectors ($\partial^i\omega_i^\perp = 0, \partial^i\gamma_i^\perp = 0$) with two degrees of freedom and γ_{ij}^T is the symmetric, solenoidal, transverse and traceless tensor part, with again two degrees of freedom.

We have the freedom to perform a gauge transformation, meaning adding the Lie derivative of the background metric over a vector ξ^μ

$$\delta \tilde{g}_{\mu\nu} = \delta g_{\mu\nu} + \left(\mathcal{L}_\xi g^{(0)}\right)_{\mu\nu}.\tag{1.163}$$

It is useful to separate this vector in its four degrees of freedom

$$\begin{aligned}\xi^0 &= \alpha, \\ \xi^i &= \partial^i \beta + d^i,\end{aligned}\tag{1.164}$$

with $\partial^i d_i = 0$. Performing the transformation on the metric we obtain [31]

$$\begin{aligned}\tilde{\Psi} &= \Psi + \alpha' + \mathcal{H}\alpha, \\ \tilde{\Phi} &= \Phi - \frac{1}{3}\nabla^2\beta - \mathcal{H}\alpha, \\ \tilde{\omega}^{\parallel} &= \omega^{\parallel} - \alpha + \beta', \\ \tilde{\omega}_i^{\perp} &= \omega_i^{\perp} + d'_i, \\ \tilde{\gamma}^{\parallel} &= \gamma^{\parallel} + 2\beta, \\ \tilde{\gamma}_i^{\perp} &= \gamma_i^{\perp} + d_i, \\ \tilde{\gamma}_{ij}^T &= \gamma_{ij}^T,\end{aligned}\tag{1.165}$$

where $\mathcal{H} = a'/a$ and the prime now stands for the derivative with respect the conformal time. From this calculation we already obtained the first invariant quantity we were searching: γ_{ij}^T . The tensor perturbations of the metric are gauge invariant.

A similar procedure applies to the matter part of the Einstein equations, the stress-energy tensor. Starting from the stress-energy tensor for a fluid [12]

$$T_{\mu\nu} = (\rho + P)u_{\mu}u_{\nu} + Pg_{\mu\nu} + \sigma_{\mu\nu},\tag{1.166}$$

where introduced the anisotropic stress tensor $\sigma_{\mu\nu}$. We can decompose the perturbation with respect the perfect fluid tensor into scalar, vector and tensor parts. We are not interested in the complete treatment since we are going to consider only the departure from the background stress-energy tensor due to scalar energy density perturbation that is [25, 34]

$$T^0_0 = -(\rho_0 + \delta\rho).\tag{1.167}$$

We again use the gauge freedom to perform a gauge transformation of the perturbation

$$\delta\tilde{\rho} = \delta\rho + \alpha\rho'_0,\tag{1.168}$$

that shows that ρ is a scalar under general coordinate transformation but its perturbation is gauge dependent. Moreover we learn that scalars are independent on the coordinates within hypersurfaces of constant conformal time τ .

Scalar perturbation

Having described both metric and matter perturbation we can now search for a scalar gauge invariant quantity as combination of the two in order to characterize effectively the scalar perturbations. We are going to consider only the scalar part of the perturbations. Equation (1.165) reduces then to

$$\begin{aligned}\tilde{\Psi} &= \Psi + \alpha' + \mathcal{H}\alpha, \\ \tilde{\Phi} &= \Phi - \frac{1}{3}\nabla^2\beta - \mathcal{H}\alpha, \\ \tilde{\omega}^{\parallel} &= \omega^{\parallel} - \alpha + \beta', \\ \tilde{\gamma}^{\parallel} &= \gamma^{\parallel} + 2\beta,\end{aligned}\tag{1.169}$$

with the same gauge transformation defined in equation (1.164). Let us introduce the intrinsic spatial curvature on hypersurfaces at constant τ for a Universe with $\kappa = 0$ as assumed in equation (1.2)

$${}^{(3)}R = \frac{4}{a^2} \nabla^2 \hat{\Phi} \quad (1.170)$$

where we have defined

$$\hat{\Phi} := \Phi + \frac{1}{6} \nabla^2 \gamma^{\parallel}. \quad (1.171)$$

Therefore we will refer to $\hat{\Phi}$ as curvature perturbation but notice that it is not a gauge invariant quantity. In fact under a gauge transformation,

$$\tilde{\hat{\Phi}} = \hat{\Phi} - \mathcal{H}\alpha. \quad (1.172)$$

Let us define a special slicing where the energy density perturbation is vanishing $\delta\rho_{\text{uni}} = 0$, called the hypersurface of uniform energy density. We want to move from a general slicing to this particular one, performing a gauge transformation

$$\tilde{\delta\rho} = \delta\rho_{\text{uni}} = \delta\rho + \alpha\rho' = 0, \quad (1.173)$$

and thus we need $\alpha = -\delta\rho/\rho'$. Under the same shift the curvature perturbation $\hat{\Phi}$ transforms as

$$\tilde{\hat{\Phi}} = \hat{\Phi}_{\text{uni}} = \hat{\Phi} - \mathcal{H}\alpha = \hat{\Phi} + \mathcal{H} \frac{\delta\rho}{\rho'}. \quad (1.174)$$

Therefore we can define a gauge invariant quantity

$$-\zeta := \hat{\Phi} + \mathcal{H} \frac{\delta\rho}{\rho'}, \quad (1.175)$$

where ζ is the gauge invariant curvature perturbation of the hypersurfaces with uniform energy density, in a particular gauge it reduces to the gauge dependent curvature perturbation $\hat{\Phi}$

$$\zeta = -\hat{\Phi}_{\delta\rho=0}. \quad (1.176)$$

As shown in [31] ζ has a fundamental property during inflation on super-horizon scales

$$\zeta' = 0 \quad \rightarrow \quad \zeta = \text{const}, \quad (1.177)$$

being also gauge invariant. In any gauge on super-horizon scale, it is constant and allows us to connect the early Universe scalar field perturbations to the density perturbation that produces the temperature anisotropy of the CMB. In fact we have

$$\zeta_{t_H^{(1)}(k)} = \zeta_{t_H^{(2)}(k)}, \quad (1.178)$$

where $t_H^{(1)}(k)$ and $t_H^{(2)}(k)$ are respectively the time at which the mode k exits and re-enters the horizon. Therefore if we consider a mode k that re-enters the horizon during the radiation dominated era we have

$$-\zeta_{t_H^{(2)}(k)} = \frac{1}{4} \frac{\delta\rho}{\rho} \Big|_{t_H^{(2)}(k)} = \frac{\delta T}{T} \Big|_{t_H^{(2)}(k)} = -\zeta_{t_H^{(1)}(k)} = H \frac{\delta\phi}{\dot{\phi}} \Big|_{t_H^{(1)}(k)}. \quad (1.179)$$

where we used the uniform curvature gauge ($\hat{\Phi} = 0$) and we used the fact that in single field inflation on super-horizon scales⁷

$$\zeta = -\hat{\Phi} - \frac{\mathcal{H}}{\phi'} \delta\phi. \quad (1.180)$$

In this way we were able to connect today observable from the CMB spectrum to quantities that describe inflation.

Therefore the complete treatment of the perturbation of the scalar field has to include the metric perturbation and has to be described in terms of gauge invariant quantities. The first-order perturbed Klein-Gordon equation is [31, 35, 36]

$$\delta\phi'' + 2\mathcal{H}\delta\phi' - \nabla^2\delta\phi + a^2\delta\phi\frac{\partial^2V}{\partial\phi^2} + 2\phi\frac{\partial V}{\partial\phi} - \phi'_0\left(\Psi' + 3\Phi' + \nabla^2\omega^{\parallel}\right) = 0. \quad (1.181)$$

Introducing the Sasaki-Mukhanov gauge invariant variable [37]

$$\mathcal{Q} := \delta\phi + \frac{\phi'}{\mathcal{H}}\hat{\Phi} \quad (1.182)$$

and following the previous procedure to quantize the field, the equation of motion for the mode functions simplifies to [31, 36]

$$\mathcal{Q}''_k + \left(k^2 - \frac{a''}{a} + M_\phi^2 a^2\right) \mathcal{Q}_k = 0, \quad (1.183)$$

where M_ϕ is the effective mass of the inflaton field

$$M_\phi^2 = \frac{\partial^2V}{\partial\phi^2} - \frac{8\pi G}{a^3} \left(\frac{a^3}{H}\dot{\phi}^2\right). \quad (1.184)$$

Imposing the slow-roll condition, at first order in the slow-roll parameters we have

$$\frac{M_\phi^2}{H^2} = 3\eta_V - 6\epsilon, \quad (1.185)$$

$$\mathcal{Q}''_k + \left(k^2 - \frac{1}{\tau^2} \left(\nu_\phi^2 - \frac{1}{4}\right)\right) \mathcal{Q}_k = 0. \quad (1.186)$$

where $\nu_\phi \simeq 3/2 + 3\epsilon - \eta_V$ (at first order in the slow-roll parameters). We recognize that the equation (1.186) is of the same form of equation (1.128) that we solved previously. We already know that the solution at super-horizon scale up to the lowest order in the slow-roll parameters is

$$|\mathcal{Q}_k(k)| = \frac{H}{\sqrt{2k^3}} \left(\frac{k}{aH}\right)^{\frac{3}{2}-\nu_\phi}. \quad (1.187)$$

Now we see that ζ and \mathcal{Q} are connected [31]

$$\zeta = -\frac{\mathcal{H}}{\phi'}\mathcal{Q}, \quad (1.188)$$

and we just have to proceed calculating the power spectrum for ζ

$$\Delta_\zeta(k) = \left(\frac{H^2}{2\pi\dot{\phi}}\right)^2 \left(\frac{k}{aH}\right)^{3-2\nu_\phi}. \quad (1.189)$$

⁷On super-horizon scales $-\zeta$ is equal to the comoving curvature perturbation \mathcal{R} defined as [31]

$$\mathcal{R} = \hat{\Phi} + \frac{\mathcal{H}}{\phi'}\delta\phi = \hat{\Phi} + \frac{H}{\dot{\phi}}\delta\phi$$

The spectral index is then given by

$$n_\zeta - 1 = 3 - 2\nu_\phi = -6\epsilon + 2\eta. \quad (1.190)$$

Here we have the first fundamental prediction of the slow-roll single field inflationary model: the power spectrum for a nearly massless scalar field in a quasi de Sitter spacetime is almost scale invariant but $n_\zeta \neq 1$. Since ζ remains constant at super-horizon scale, let us consider a mode k^* that crosses the horizon at t^* , that is when $k = aH$. The power spectrum is then

$$\Delta_\zeta(k) = \left(\frac{H^2}{2\pi\dot{\phi}} \right)^2 \Big|_{t^*(k)} \quad (1.191)$$

where the dependence on the mode is hidden in t^* , since each mode exits the horizon at different time.

Gravitational waves

The second fundamental prediction is the production of a stochastic gravitational wave (GW) background in the early Universe [25, 38]. To show this let us study only the tensor perturbation of the FLRW metric. We know that at the linear level the evolution of each contribution is independent. Therefore adding a tensor to the metric we have

$$ds^2 = a^2(\tau) [-d\tau^2 + (\delta_{ij} + \gamma_{ij}^\perp(x, \tau))dx^i dx^j]. \quad (1.192)$$

Let us indicate $\gamma_{ij}^\perp = h_{ij}$ and recall its properties in Table 1.4

Symmetric	$h_{ij} = h_{ji}$
Traceless	$h_{ii} = 0$
Divergenceless	$D_i h_j^i$

Table 1.4: Properties of the tensor perturbations of the metric

From the perturbed Einstein equations (1.153) for the tensor perturbation, without a source of tensor anisotropy, we obtain the equation of motion for the perturbations

$$\ddot{h}_{ij} + 3H\dot{h}_{ij} - a^{-2}\nabla^2 h_{ij} = 0. \quad (1.193)$$

Note that equation (1.193) is a wave equation in an expanding Universe and that due to the properties given in Table 1.4, h_{ij} is a wave with two degrees of freedom, meaning two polarizations (+, ×). Moving to Fourier space where we have the expansion

$$h_{ij}(t, x) = \frac{1}{(2\pi)^3} \sum_{\lambda=+, \times} \int d^3k e^{ik \cdot x} h_{\lambda, k}(t) \epsilon_{ij}(k), \quad (1.194)$$

the equation of motion reads now

$$\ddot{h}_\lambda + 3\dot{h}_\lambda + \frac{k^2}{a^2} h_\lambda = 0. \quad (1.195)$$

Notice that each polarization evolves exactly as a massless scalar field minimally coupled to gravity. Therefore we already know the solution when we recognize

$$h_\lambda = \sqrt{32\pi G} \phi_\lambda. \quad (1.196)$$

For the power spectrum we have the tensor power spectrum

$$\Delta_{h_{+,\times}}(k) = 32\pi G \Delta_{\phi_{+,\times}}, \quad (1.197)$$

$$\Delta_{h_{+,\times}}(k) = \frac{8H^2}{\pi M_{\text{P}}^2} \left(\frac{k}{aH} \right)^{-2\epsilon}. \quad (1.198)$$

Summing over the polarization we have

$$\Delta_T = \frac{16H^2}{\pi M_{\text{P}}^2} \left(\frac{k}{aH} \right)^{-2\epsilon}. \quad (1.199)$$

Since it is again a power law it is possible to define a tensorial spectral index

$$n_T := \frac{d \ln \Delta_T(k)}{d \ln k}. \quad (1.200)$$

From equation (1.199) we have

$$n_T = -2\epsilon. \quad (1.201)$$

Summarizing the results we have

$$\begin{aligned} \Delta_\zeta(k) &= A_S \left(\frac{k}{k_0} \right)^{n_\zeta - 1}, \\ \Delta_T(k) &= A_T \left(\frac{k}{k_0} \right)^{n_T}, \end{aligned} \quad (1.202)$$

with both the spectral indices and the amplitudes depending on the inflation dynamics, i.e. on the potential $V(\phi)$, hence on the specific inflationary model. Therefore experimental bounds on these parameters will help us to exclude classes of models.

We have four observable variables to take into consideration but they can be reduced to two. In fact let us define the tensor-to-scalar ratio of the amplitudes as

$$r := \frac{A_T}{A_S}. \quad (1.203)$$

In the slow-roll paradigm we have a further relation, that can either be used as a consistency check or to connect two observables. That is

$$r = 16\epsilon \xrightarrow{(1.201)} r = -8n_T, \quad (1.204)$$

leaving with two independent quantities: r and n_ζ .

The experimental measurement of a GW background would be a smoking gun for the inflationary mechanism but if we were able to test the relation in equation (1.204) we would check a relation that connects independent observables and is a general prediction of the single field slow-roll inflation models. The latter measurement is a very tricky one since we do not only have to measure the gravitational wave but also measure its spectrum shape.

Moreover if the relation holds, the scale dependence of the tensor power spectrum is very small. The latest measurement provides an upper bound for the scalar-to-tensor ratio r [3]

$$r_{0.05} < 0.07 \quad 95\% \text{ CL}. \quad (1.205)$$

The measurement of the amplitude of the GW background is very important because it can also fix the inflationary energy scale. In fact the amplitude is

$$A_T = \frac{2}{\pi^2} \frac{H^2}{M_{\text{P}}^2} \quad (1.206)$$

during inflation and we know that

$$H^2 \simeq (3M_{\text{P}})^{-2} V(\phi). \quad (1.207)$$

Therefore

$$A_T = \frac{2}{3\pi^2} \frac{V(\phi)}{M_{\text{P}}^4}. \quad (1.208)$$

From the last equation we can obtain the energy scale

$$E_{\text{inf}} = V^{1/4} \quad (1.209)$$

and thus we can give an estimation using the consistency equation

$$E_{\text{inf}} = V^{1/4} = (1.88 \times 10^{16} \text{ GeV}) \left(\frac{r}{0.10} \right)^{1/4} \quad (1.210)$$

In the next years the attempts to measure the GW background will be crucial to improve our knowledge of the physics of the primordial Universe.

1.7 Fermions in Curved Spacetime

In this section we will briefly present the theory used to deal with spinors in curved spacetime. When studying QFT in a flat Minkowski space we are able to introduce the concept of spinor as a representation of the Poincaré symmetry group. When we deal with GR the symmetry group changes and it is $GL(1,3)$ that do not allow any spinor representation. We need therefore a formalism to include spinors in GR: the *vierbein field theory* [23, 35]. We will follow the treatment given in [39].

This complementary approach to GR was firstly introduced by Einstein in 1928 during his attempt to unify electromagnetism and gravity, and formalized in 1948 [40]. In a modern perspective this is the correct tool to develop a relativistic QFT in curved spacetime.

1.7.1 The vierbein formalism

The idea behind the vierbein formalism is to change the basis of the tangent space T . The natural basis commonly used is the coordinate basis. At a point p the tangent space T_p has a basis

$$\hat{\mathbf{e}}_{(\mu)} = \partial_{(\mu)}, \quad (1.211)$$

such that any 4-vector $A \in T_p$ can be decomposed into its components A^μ

$$A = A^\mu \hat{\mathbf{e}}_{(\mu)} = (A_0, A_1, A_2, A_3). \quad (1.212)$$

In the following the Greek letters will be associated with the components of the vector in the coordinate basis while for the new basis that we will introduce we will use the Latin indices.

The cotangent space T_p^* basis is given by the differential elements

$$\hat{\mathbf{e}}^{(\mu)} = dx^{(\mu)}, \quad (1.213)$$

therefore the dual vectors $B \in T_p^*$ has components

$$B = B_\mu \hat{\mathbf{e}}^{(\mu)} = g_{\mu\nu} B^\nu \mathbf{e}^{(\mu)}. \quad (1.214)$$

Being $\hat{\mathbf{e}}_{(\mu)}$ and $\hat{\mathbf{e}}^{(\mu)}$ basis for dual spaces their tensor product is simply the identity

$$\hat{\mathbf{e}}^{(\mu)} \otimes \hat{\mathbf{e}}_{(\nu)} = \mathbf{1}^\mu{}_\nu. \quad (1.215)$$

At this point we are still free to change the basis that spans the tangent space T_p . We then choose a new set of basis vectors $\hat{\mathbf{e}}_{(a)}$ that have still to be orthonormal. Since the spacetime we want to describe is a Lorentzian manifold, the orthonormality condition reads

$$g(\hat{\mathbf{e}}_{(a)}, \hat{\mathbf{e}}_{(b)}) = \eta_{ab}, \quad (1.216)$$

where $g(\ , \)$ is the metric tensor, the equation (1.216) describes the inner product and η_{ab} is the Minkowski metric. Basis that are independent from the coordinates are usually called non-coordinate basis and the set of basis vectors are called *tetrad* or *vierbeins*. As before we can now express every vector in term of the new basis vectors; therefore also the coordinate basis vectors in equation (1.211)

$$\hat{\mathbf{e}}_{(\mu)} = e_{\mu}^a(x)\hat{\mathbf{e}}_{(a)}, \quad (1.217)$$

where the components $e_{\mu}^a(x)$ form a 4×4 invertible matrix. This set of functions depends on the spacetime point x ; in fact the role of the $e_{\mu}^a(x)$ matrix is to rotate, in each point, the basis from (to) the coordinate basis to (from) the vierbein basis.

We call the inverse transformation matrix $e^{\mu}_a(x)$ and it satisfies

$$e^{\mu}_a(x)e_{\nu}^a(x) = \delta^{\mu}_{\nu}, \quad e_{\mu}^a(x)e^{\mu}_b(x) = \delta^a_b, \quad (1.218)$$

therefore we have the inverse transformation of equation (1.217)

$$\hat{\mathbf{e}}_{(a)} = e^{\mu}_a(x)\hat{\mathbf{e}}_{(\mu)}. \quad (1.219)$$

From equation (1.218) we obtain the following relation

$$g_{\mu\nu}(x)e^{\mu}_a(x)e^{\nu}_b(x) = \eta_{ab}, \quad (1.220)$$

The physical meaning of the last equation is that we are able to use, point by point, a base where the spacetime metric, in that point, is Minkowski via a rotation of the tangent space basis. Furthermore this relation teaches us how to raise and lower the Latin indices: we do that with the flat metric. In fact re-arranging equation (1.220) we have

$$e^{\mu}_a(x) = g^{\mu\nu}\eta_{ab}e_{\nu}^b(x), \quad (1.221)$$

that shows how both Latin and Greek indices are raised and lowered. Similarly we can search a basis for the dual space $\hat{\mathbf{e}}^{(a)}$ knowing that it has to satisfy

$$\hat{\mathbf{e}}^{(a)} \otimes \hat{\mathbf{e}}_{(b)} = \mathbf{1}^a_b \quad (1.222)$$

therefore connecting it to the coordinate basis we have

$$\hat{\mathbf{e}}^{(a)} = e_{\mu}^a(x)\hat{\mathbf{e}}^{(\mu)}(x) \quad (1.223)$$

and the inverse relation

$$\hat{\mathbf{e}}^{(\mu)}(x) = e^{\mu}_a(x)\hat{\mathbf{e}}^{(a)}. \quad (1.224)$$

Note that imposing the compatibility between the choice of basis of the tangent and cotangent basis through the relation (1.222) we have that the *vierbeins matrices* and inverse $e^{\mu}_a(x)$, $e_{\mu}^a(x)$ are the same as those used to rotate the 1-form basis. Vectors (and 1-forms) can be expressed in both basis and when dealing with vectors components (V^{μ} or V^a) we have the transformation relation

$$V^a = e_{\mu}^a(x)V^{\mu} \quad \text{and} \quad V^{\mu} = e^{\mu}_a(x)V^a, \quad (1.225)$$

which is easily generalized to multi-index objects. The vierbein matrix allows us to move back and forth from Greek and Latin indices.

Now that we have learned the basics we note that since we moved to a non-coordinate basis we can change the basis independently from the coordinates but keeping the relation (1.216) satisfied. The transformations that preserve it are the well-known Lorentz transformations

$$\text{LLT} : \quad \hat{e}_{(a)} \rightarrow \hat{e}_{(a')} = \Lambda^a{}_{a'}(x)\hat{e}_{(a)}. \quad (1.226)$$

Note that, contrary to what we were used to, the matrix Λ depends on the spacetime point. We call these transformation Local Lorentz transformation (LLT). This means that we have the freedom to perform a (different) Lorentz transformation at any point. Of course general coordinate transformations are still a symmetry and the most general transformation is given by

$$T^{a'\mu'}{}_{b'\nu'} = \Lambda^{a'}{}_a \frac{\partial x^{\mu'}}{\partial x^\mu} \Lambda^b{}_{b'} \frac{\partial x^\nu}{\partial x^{\nu'}} T^{a\mu}{}_{b\nu}. \quad (1.227)$$

We need to introduce the covariant derivative in this new formalism, and we just need to replace the usual Christoffel connection with the *spin connection* $\omega_\mu{}^a{}_b$. As usual the covariant derivative is then

$$\nabla_\mu X^a{}_b = \partial_\mu X^a{}_b + \omega_\mu{}^a{}_c X^c{}_b - \omega_\mu{}^c{}_b X^a{}_c. \quad (1.228)$$

The transformation law between the two connections is obtained by asking tensors to be independent from the basis in which they are written. Therefore the covariant derivative of a vector X in coordinate basis is

$$\nabla X = (\nabla_\mu X^\nu) dx^\mu \otimes \partial_\nu \quad (1.229)$$

$$= (\partial_\mu X^\nu + \Gamma_{\mu\lambda}^\nu X^\lambda) dx^\mu \otimes \partial_\nu \quad (1.230)$$

and in a mixed basis it is

$$\nabla X = (\nabla_\mu X^a) dx^\mu \otimes \hat{e}_{(a)} \quad (1.231)$$

$$= (\partial_\mu X^a + \omega_\mu{}^a{}_b X^b) dx^\mu \otimes \hat{e}_{(a)}. \quad (1.232)$$

Converting it to the coordinate basis gives

$$\nabla X = (\partial_\mu (e_\nu{}^a X^\nu) + \omega_\mu{}^a{}_b e_\lambda{}^b X^\lambda) dx^\mu \otimes (e^\sigma{}_a \partial_\sigma) \quad (1.233)$$

$$= e^\sigma{}_a (e_\nu{}^a \partial_\mu X^\nu + X^\nu \partial_\mu e_\nu{}^a + \omega_\mu{}^a{}_b e_\lambda{}^b X^\lambda) dx^\mu \otimes \partial_\sigma \quad (1.234)$$

$$= (\partial_\mu X^\nu + e^\nu{}_a \partial_\mu e_\lambda{}^a X^\lambda + e^\nu{}_a e_\lambda{}^b \omega_\mu{}^a{}_b X^\lambda) dx^\mu \otimes \partial_\nu \quad (1.235)$$

So comparing equation (1.232) and (1.235) we find

$$\Gamma_{\mu\lambda}^\nu = e^\nu{}_a \partial_\mu e_\lambda{}^a + e^\nu{}_a e_\lambda{}^b \omega_\mu{}^a{}_b. \quad (1.236)$$

The important relation, called the tetrad postulate, that states that the covariant derivative of the vierbein matrix is null is nothing else than a restatement of (1.236)

$$\nabla_\mu e_\nu{}^a = \partial_\mu e_\nu{}^a - \Gamma_{\mu\nu}^\lambda e_\lambda{}^a + \omega_\mu{}^a{}_b e_\nu{}^b = 0. \quad (1.237)$$

1.7.2 Dirac equation

Let us recall the action of the internal Lorentz transformation $U(\Lambda)$, acting on spinors, on the Dirac gamma matrices in flat spacetime [41]

$$U(\Lambda)^{-1}\gamma^\mu U(\Lambda) = \Lambda^\mu{}_\sigma \gamma^\sigma \quad (1.238)$$

and we remember also that the Dirac equation

$$(i\gamma^\mu \partial_\mu + m)\psi = 0 \quad (1.239)$$

is invariant under Lorentz transformations in a flat spacetime [41]. Recall that the internal Lorentz transformation $U(\Lambda)$ commutes with the external Lorentz transformations Λ acting on 4-vectors. Let us use a more compact notation in the following

$$\Lambda_{\frac{1}{2}} := U(\Lambda) \quad (1.240)$$

$$\Lambda_{-\frac{1}{2}} := U(\Lambda)^{-1}. \quad (1.241)$$

Recalling the action of Λ on the gamma matrices

$$\Lambda^\mu{}_\sigma \gamma^\sigma = \gamma^\nu \Lambda^\mu{}_\nu, \quad (1.242)$$

we obtain an useful identity

$$\Lambda^\mu{}_\lambda e^\lambda{}_a \gamma^a (\Lambda^{-1})^\nu{}_\mu \Lambda_{\frac{1}{2}} = \Lambda_{\frac{1}{2}} \Lambda_{-\frac{1}{2}} (\Lambda^\mu{}_\lambda e^\lambda{}_a \gamma^a) \Lambda_{\frac{1}{2}} (\Lambda^{-1})^\nu{}_\mu \quad (1.243)$$

$$= \Lambda_{\frac{1}{2}} \Lambda^\mu{}_\sigma (\Lambda^\sigma{}_\lambda e^\lambda{}_a \gamma^a) (\Lambda^{-1})^\nu{}_\mu \quad (1.244)$$

$$= \Lambda_{\frac{1}{2}} \Lambda^\nu{}_\lambda e^\lambda{}_a \gamma^a. \quad (1.245)$$

We want the Dirac equation to be invariant under Lorentz transformations also in curved spacetimes. We know that we need to add a term Γ_μ to the derivative in order to construct the covariant derivatives and make the kinetic term invariant. Let us understand how this term has to behave under $U(\Lambda)$ in order to assure invariance:

$$e^\mu{}_a \gamma^a (\partial_\mu + \Gamma_\mu) \psi(x) \xrightarrow{\text{LLT}} \Lambda^\mu{}_\lambda e^\lambda{}_a \gamma^a (\Lambda^{-1})^\nu{}_\mu (\partial_\nu + \Gamma'_\nu) \Lambda_{\frac{1}{2}} \psi(\Lambda^{-1}x) \quad (1.246)$$

$$= \Lambda^\mu{}_\lambda e^\lambda{}_a \gamma^a (\Lambda^{-1})^\nu{}_\mu \Lambda_{\frac{1}{2}} \left(\partial_\nu + \Lambda_{-\frac{1}{2}} \Gamma'_\nu \Lambda_{\frac{1}{2}} \right) \psi(\Lambda^{-1}x) \quad (1.247)$$

$$+ \Lambda^\mu{}_\lambda e^\lambda{}_a \gamma^a (\Lambda^{-1})^\nu{}_\mu \left(\partial_\nu \Lambda_{\frac{1}{2}} \right) \psi(\Lambda^{-1}x) \quad (1.248)$$

$$= \Lambda_{\frac{1}{2}} \Lambda^\nu{}_\lambda e^\lambda{}_a \gamma^a \left[(\partial_\nu + \Gamma_\nu) - \underbrace{\Gamma_\nu + \Lambda_{-\frac{1}{2}} \Gamma'_\nu \Lambda_{\frac{1}{2}} + \Lambda_{-\frac{1}{2}} \partial_\nu \left(\Lambda_{\frac{1}{2}} \right)}_{=0} \right] \psi(\Lambda^{-1}x). \quad (1.249)$$

The transformation rule for Γ_μ can thus be read from the last equation

$$\Gamma'_\nu = \Lambda_{\frac{1}{2}} \Gamma_\nu \Lambda_{-\frac{1}{2}} - \partial_\nu \left(\Lambda_{\frac{1}{2}} \right) \Lambda_{-\frac{1}{2}}. \quad (1.250)$$

Since the usual mass term is still invariant we can write the invariant Dirac equation in a curved spacetime as

$$i\gamma^a e^\mu{}_a(x) \nabla_\mu \psi - m\psi = 0, \quad (1.251)$$

where the covariant derivative is defined as

$$\nabla_\mu = \partial_\mu + \Gamma_\mu, \quad (1.252)$$

with Γ_μ transforming according to (1.250) and we can define from equation (1.251) the spacetime dependent gamma matrices as $\gamma^\mu(x) := \gamma^a e^\mu_a$. The reader will recognize this procedure to be exactly the same as the one used for gauge field theory with the difference that Γ_μ is not a gauge field.

To complete the treatment we provide the expression of Γ_μ [35, 39]:

$$\Gamma_\alpha = \frac{1}{2} e^\beta_k (\nabla_\alpha e_{\beta h}) S^{hk} \quad (1.253)$$

where S^{hk} are the antisymmetric generators of the Lorentz transformations that satisfy the commutation relation

$$[S^{hk}, S^{ij}] = \eta^{hj} S^{ki} + \eta^{ki} S^{hj} - \eta^{hi} S^{kj} - \eta^{kj} S^{hi}, \quad (1.254)$$

and give the infinitesimal transformation of a spinor

$$\Lambda_{\frac{1}{2}} = 1 + \frac{1}{2} \lambda_{ab} S^{ab}. \quad (1.255)$$

The early Universe is a peculiar setting for the study of quantum fields, since the field operators acquire an explicit time dependence due to the spacetime expansion. In this framework inflation takes place: the inflaton field is responsible for the accelerated expansion but it also presents quantum fluctuations. These fluctuations, that are the seeds for the initial density perturbation that will grow into the large scale structure of the Universe, are the main focus of our discussion and hence we need a formalism to treat quantum fields in this new environment. In fact some differences from the particle physics QFT approach (that is also called the *in-out* formalism) appear in the study of the primordial Universe physics: the Poincaré symmetry is explicitly broken by the evolving background metric, in particular by the time dependent scale factor $a(t)$; this leads the quantum fields action and therefore the cosmological observables to have an explicit time dependence. Moreover the information we seek are different. We are not interested in the S matrix element of scattering processes but rather we want to follow the time evolution of expectation values in a fixed initial state [42]. The Schwinger Keldysh (SK) formalism, also known as the *in-in* formalism, is the appropriate formalism to study the evolution of the cosmological observables in this setting, in particular if we are interested in including quantum effects and non Gaussianities. This new formalism was first introduced by Schwinger [43], developed by Keldysh [44] and translated to relativistic field theory by Chou *et al.* [45] and finally extended by Jordan to curved spacetimes [46]. It has been applied for over fifty years to condensed matter and statistical physics but lately it has been a great complementary tool to the standard *in-out* approach in the study of the early Universe cosmology [47–53].

In section 2.1 we will introduce the Schwinger Keldysh formalism in the context of expanding background spacetime metric and derive the structure of the propagators of the free theory in order to then address the general theory perturbatively. In section 2.2 we will derive the explicit form of the propagators for a massive scalar and a massive fermion field first in the Minkowski spacetime and then in the de Sitter spacetime. Finally in section 2.3 the WKB approximation is studied and the approximated propagators are compared with *full* propagators via numerical methods.

2.1 The Schwinger-Keldysh Formalism

Correlation functions are one of the main objects in the study of both particle physics and cosmology. However, there is a fundamental difference. In particle physics the S -matrix

$$S := \lim_{\substack{t \rightarrow +\infty \\ t_0 \rightarrow -\infty}} U_I(t, t_0) \equiv U_I(+\infty, -\infty), \quad (2.1)$$

is the fundamental object needed to study scattering and decay processes (the evolution operator $U_I(t, t_0)$ and the meaning of operators in the interaction picture, denoted by the label I , will be introduced soon). Knowing the S -matrix we are able to compute the S -matrix elements

$$S_{FI} := \langle \psi_I | S | \psi_F \rangle_I, \quad (2.2)$$

the main focus of the study, since $|S_{FI}|^2$ is the transition probability for the state $|\psi_I\rangle$ fixed in the far past ($t \rightarrow -\infty$) to become some state $|\psi_F\rangle$ in the far future ($t \rightarrow +\infty$). In the very early and late times the particles are considered to be infinitely far apart and so non-interacting. The asymptotic states therefore belong to the Fock space of the free theory.

The main interest in cosmology instead is the expectation values of product of fields at a given time. Boundary condition is imposed only at very early times in this case. As discussed in chapter 1, for wavelength deep inside the sub-horizon region we impose the Bunch-Davies vacuum choice (1.119): we ask the mode function solutions to have the same form as in Minkowski space according to the equivalence principle.

2.1.1 Interaction picture in cosmology

Both in cosmology and in particle physics it is customary to introduce the interaction picture to address the computations. Let us introduce the interaction picture in a context where the background is time dependent. Consider the Hamiltonian $\mathcal{H}[\phi(x, t), \pi(x, t)]$ for the quantum theory we want to describe, where the fields ϕ_i and the conjugate momenta π_i obey the equal time commutation relations

$$[\phi_i(x, t), \pi_j(y, t)] = i\delta_{ij}\delta^3(x - y), \quad (2.3)$$

$$[\phi_i(x, t), \phi_j(y, t)] = 0, \quad (2.4)$$

$$[\pi_i(x, t), \pi_j(y, t)] = 0, \quad (2.5)$$

and the Heisenberg equations of motion

$$\dot{\phi}_i = i[\mathcal{H}, \phi_i], \quad \dot{\pi}_i = i[\mathcal{H}, \pi_i], \quad (2.6)$$

where the indices i, j denote different fields and spin components. In order to introduce the perturbation theory we separate the field into background and perturbation parts as we did in equation (1.60) for the inflaton field ϕ . The background $(\phi_{0,i}, \pi_{0,i})$ is defined to be the homogeneous and isotropic part of the fields (ϕ_0 for the inflaton and $g_{\mu\nu}^{FLRW}$ for the metric), leading to the definition of the perturbation as

$$\phi_i(x, t) = \phi_{0,i}(t) + \delta\phi_i(x, t), \quad \pi_i(x, t) = \pi_{0,i}(t) + \delta\pi_i(x, t). \quad (2.7)$$

Since the background is a complex-valued function the commutators of the perturbation are again

$$[\delta\phi_i(x, t), \delta\pi_j(y, t)] = i\delta_{ij}\delta^3(x - y) \quad (2.8)$$

$$[\delta\phi_i(x, t), \delta\phi_j(y, t)] = 0 \quad (2.9)$$

$$[\delta\pi_i(x, t), \delta\pi_j(y, t)] = 0. \quad (2.10)$$

It is useful to expand the Hamiltonian around the background, leading to

$$\mathcal{H}[\phi, \pi] = \mathcal{H}[\phi_0, \pi_0] + \tilde{\mathcal{H}}[\delta\phi, \delta\pi; t], \quad (2.11)$$

where $\tilde{\mathcal{H}}[\delta\phi, \delta\pi; t]$ is the Hamiltonian for the perturbation that depends on the background; it is second and higher order in $\delta\phi$ and $\delta\pi$ since the terms linear in the perturbation are vanishing due

to the background equation of motion. $\tilde{\mathcal{H}}[\delta\phi, \delta\pi; t]$ governs the time dependence of the fluctuation, as shown in [47],

$$\delta\dot{\phi} = i \left[\tilde{\mathcal{H}}[\delta\phi, \delta\pi; t], \delta\phi \right], \quad \delta\dot{\pi} = i \left[\tilde{\mathcal{H}}[\delta\phi, \delta\pi; t], \delta\pi \right]. \quad (2.12)$$

As usual we can define the evolution operator $U(t, t_0)$

$$\begin{cases} \frac{d}{dt}U(t, t_0) = -i\tilde{H}[\delta\phi(t), \delta\pi(t); t]U(t, t_0), \\ U(t_0, t_0) = 1, \end{cases} \quad (2.13)$$

such that the fluctuations at time t are connected to the same operator at time t_0

$$\begin{aligned} \delta\phi_i(t) &= U^{-1}(t, t_0) \delta\phi_i(t_0) U(t, t_0) \\ \delta\pi_i(t) &= U^{-1}(t, t_0) \delta\pi_i(t_0) U(t, t_0). \end{aligned} \quad (2.14)$$

To solve problems that go beyond a quadratic Hamiltonian $\tilde{\mathcal{H}}[\delta\phi, \delta\pi; t]$ in the perturbations we often need to use the perturbation theory. Therefore we decompose \mathcal{H} into a free part, H_0 , quadratic in the fluctuation and an interacting part, H_{int} ,

$$\tilde{\mathcal{H}}[\delta\phi, \delta\pi; t] = H_0[\delta\phi, \delta\pi; t] + H_{int}[\delta\phi, \delta\pi; t], \quad (2.15)$$

This separation allows to introduce the interaction picture, defining the interaction picture operators $\delta\phi_i^I$ and $\delta\pi_i^I$ whose evolution is determined only by the H_0 part of the Hamiltonian¹

$$\delta\dot{\phi}_i^I = i [H_0[\delta\phi^I, \delta\pi^I; t], \delta\phi_i^I], \quad \delta\dot{\pi}_i^I = i [H_0[\delta\phi^I, \delta\pi^I; t], \delta\pi_i^I], \quad (2.16)$$

with the following initial conditions

$$\delta\phi_i^I(t_0) = \delta\phi_i(t_0), \quad \delta\pi_i^I(t_0) = \delta\pi_i(t_0), \quad (2.17)$$

in order to completely define the interaction picture. Since H_0 is quadratic, the interaction picture operators are free fields. Once again we can describe the evolution using a (free) unitary evolution operator $U_0(t, t_0)$ defined by

$$\begin{cases} \frac{d}{dt}U_0(t, t_0) = -iH_0[\delta\phi(t_0), \delta\pi(t_0); t]U_0(t, t_0), \\ U_0(t_0, t_0) = 1, \end{cases}, \quad (2.18)$$

so that the operators are related to the operators in the Heisenberg picture at early time t_0

$$\begin{aligned} \delta\phi_i^I(t) &= U_0^{-1}(t, t_0) \delta\phi_i(t_0) U_0(t, t_0), \\ \delta\pi_i^I(t) &= U_0^{-1}(t, t_0) \delta\pi_i(t_0) U_0(t, t_0). \end{aligned} \quad (2.19)$$

Defining $F(t, t_0)$ as

$$F(t, t_0) := U_0^{-1}(t, t_0) U(t, t_0), \quad (2.20)$$

from equations (2.13) and (2.18) we have

$$\begin{cases} \frac{d}{dt}F(t, t_0) = -iH_{int}^I[\delta\phi(t_0), \delta\pi(t_0); t]F(t, t_0), \\ F(t_0, t_0) = 1, \end{cases} \quad (2.21)$$

where H_{int}^I is the interaction part of the Hamiltonian in the interaction picture. The system (2.21) has the well-known solution

¹The free part of the Hamiltonian is equivalent in the Heisenberg and in the interaction picture [47].

$$F(t, t_0) = T \exp \left(-i \int_{t_0}^t dt H_{int}^I(t) \right), \quad (2.22)$$

where T is the time ordered product applied to the power series expansion of the exponential. At this point using equations (2.14) and (2.19) we can express the solution for the fluctuation in the Heisenberg picture in terms of the free fields of the interaction picture as

$$\begin{aligned} Q(t) &= F^{-1}(t, t_0) Q^I(t) F(t, t_0) \\ &= \left[\tilde{T} \exp \left(i \int_{t_0}^t dt H_{int}^I(t) \right) \right] Q^I(t) \left[T \exp \left(-i \int_{t_0}^t dt H_{int}^I(t) \right) \right], \end{aligned} \quad (2.23)$$

where $Q(t)$ is any product of the fields and \tilde{T} the anti-time ordered product.

2.1.2 The expectation values

The time evolution operator $F(t, t_0)$ can be used, in the interaction picture, to relate states at different times. In particular, let us consider the vacuum state

$$|\Omega(t)\rangle = F(t, t_0) |\Omega(t_0)\rangle. \quad (2.24)$$

We refer to $|\Omega(t)\rangle$ as the ground state, the vacuum, of the interacting theory and to $|0\rangle$ as the early time (Bunch-Davies) vacuum of the free theory. We are discussing the different vacua because in cosmology the expectation value we want to compute is of the type

$$\langle Q(t) \rangle = \langle in | Q(t) | in \rangle \quad (2.25)$$

where the in state $|in\rangle := |\Omega(t_i)\rangle \equiv |\Omega\rangle$ is the vacuum of the interacting theory at some very early time t_i and $t > t_i$ is a late time (e.g. the time of the horizon crossing). We can relate, using the evolution operator $F(t, t_0)$, the interacting vacuum state to the free one. Let us expand $|0\rangle$ into eigenstates of the full theory

$$|0\rangle = |\Omega\rangle \langle \Omega | 0 \rangle + \sum_n |n\rangle \langle n | 0 \rangle, \quad (2.26)$$

where $|n\rangle$ are the excited states. Therefore

$$e^{-iH(t-t_i)} |0\rangle = e^{-iH(t-t_i)} |\Omega\rangle \langle \Omega | 0 \rangle + \sum_n e^{-iE_n(t-t_i)} |n\rangle \langle n | 0 \rangle. \quad (2.27)$$

Adding a small imaginary part to the time

$$t_i \rightarrow \tilde{t}_i(1 - i\epsilon), \quad (2.28)$$

near $t_i \rightarrow -\infty$ we are able to project away the excited states since the $i\epsilon$ factor introduces a term $e^{-iE_n(t-t_i)} \rightarrow e^{-\infty \cdot \epsilon E_n(\dots)} \rightarrow 0$. Recognizing the evolution operator $F(t, t_0)$ and since $|\Omega\rangle$ is the only state that survives we are left with

$$F(t, \tilde{t}_i) |\Omega\rangle = \frac{F(t, \tilde{t}_i) |0\rangle}{\langle \Omega | 0 \rangle}. \quad (2.29)$$

The $i\epsilon$ prescription physically means to turn off the interaction in the far past therefore projecting the state $|in\rangle$ onto the free vacuum $|0\rangle$. Combining (2.23) and (2.29) the expectation value of an operator Q is given by

$$\langle \Omega | Q(t) | \Omega \rangle = \frac{\langle 0 | \left[\tilde{T} e^{i \int_{\tilde{t}_i}^t dt' H_{int}^I(t')} \right] Q^I(t) \left[T e^{-i \int_{\tilde{t}_i}^t dt'' H_{int}^I(t'')} \right] | 0 \rangle}{|\langle 0 | \Omega \rangle|^2}, \quad (2.30)$$

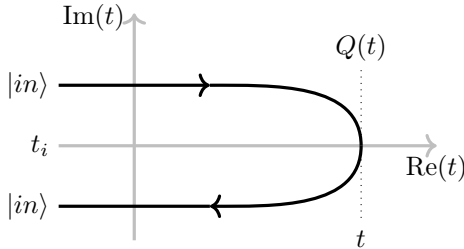


Figure 2.1: The in-in contour \mathcal{C} . We denoted by \mathcal{C}_+ (\mathcal{C}_-) the forward (backward) branch. Figure inspired by [5].

where setting $|\langle \Omega|0\rangle|^2 \rightarrow 1$ we obtain the *in-in* master formula

$$\langle Q(t) \rangle = \left\langle 0 \left| \tilde{T} e^{i \int_{t_i}^t dt' H_{\text{int}}^I(t')} Q^I(t) T e^{-i \int_{t_i}^t dt'' H_{\text{int}}^I(t'')} \right| 0 \right\rangle. \quad (2.31)$$

where the contour \mathcal{C} specified by the above $i\epsilon$ prescription is called the *in-in* contour or Keldysh contour that goes from $t_i(1 + i\epsilon)$ to t where the correlation function is evaluated and back to $t_i(1 - i\epsilon)$ as shown in figure 2.1. This formalism is also referred to as the close-time-path formalism (CTP) because of the shape of the time contour. To proceed and compute the correlation functions perturbatively we expand the exponentials, obtaining at first order [5]

$$\langle Q(t) \rangle = -i \int_{t_i}^t dt' \langle 0 | [Q^I(t), H_{\text{int}}^I(t')] | 0 \rangle, \quad (2.32)$$

where the $i\epsilon$ prescription is to be understood and t_i has to be a sufficiently early time such that the fluctuation wavelength are deep under the horizon and the fluctuations are supposed to behave as free fields and we fix the Bunch-Davies vacuum. Similarly to the case of particle physics transition amplitudes we can introduce the Feynman diagrams for the correlation functions that we will discuss in the following.

The same expectation values can be obtained using the path integral formalism. An advantage of the path integral formalism over the operator formalism is that we can derive the Feynman rules directly from the Lagrangian rather than from the Hamiltonian, and it can produce results beyond perturbation theory. In the *in-out* path integral formulation of QFT the starting point is the generating functional $Z[J]$ which is the vacuum to vacuum transition amplitude in presence of a source and it allows to calculate correlators. As discussed before, in cosmological setting, boundary conditions are imposed only at very early times without making any assumption on the system in the far future. In order to calculate expectation values in the *in* vacuum under these conditions Schwinger [43] introduced a different generating functional

$$Z[J_+, J_-] := \sum_{\lambda} \langle in | \lambda \rangle_{J_-} \langle \lambda | in \rangle_{J_+}, \quad (2.33)$$

where we leave the *in* vacuum evolve independently under two different sources J_+ , J_- and compare it with a common state $|\lambda\rangle$ in the future and we sum over the complete set of $|\lambda\rangle$. Taking the complete and orthonormal set of states $|\lambda\rangle$ to be eigenstates of the field we are considering (in the Heisenberg picture) at some late time t

$$\Phi(x, t) |\lambda\rangle = \lambda |\lambda\rangle, \quad (2.34)$$

we can introduce a path integral representation of $Z[J_-, J_+]$. In the path integral representation equation (2.33) can be interpreted as the sum of all the paths that go forward in time from the *in* vacuum $|in\rangle$ to a state $|\lambda\rangle$ under the action of a source J_+ , where the state $|\lambda\rangle$ is defined on the hypersurfaces at time t , and the back to the *in* vacuum in the presence of J_- .

2.1.3 Generating functional for a scalar field

Let us start considering a massive scalar field ϕ with an action $S[\phi]$. For the moment we turn off all the interactions and study the free theory to then proceed in the next chapter with the perturbation theory [46, 48] We can now introduce the generating functional in equation (2.33) for a scalar field in the path integral representation [46, 47, 52–54]

$$Z[J_+, J_-] = \int \mathcal{D}\phi_+ \mathcal{D}\phi_- \exp \{i(S[\phi_+] + J_+ \phi_+ - S[\phi_-] - J_- \phi_-)\}, \quad (2.35)$$

with the shorthand notation

$$J\phi = \int_{t_i}^t dt' \int d^3x J(x)\phi(x). \quad (2.36)$$

where J_+ (J_-) is the source of ϕ_+ (ϕ_-) with vacuum boundary condition in the far past for both ϕ_+ and ϕ_- and the integral is over all the field configurations that coincide at t , that is, on the hypersurface Σ at time t

$$\phi_+(t) = \phi_-(t). \quad (2.37)$$

Equation (2.35) provides us the tool to calculate expectation values starting from a generating functional with the time integration contour depicted in figure 2.1. Moreover since the path integral description of the theory in the Schwinger-Keldysh formalism in equation (2.35) is equivalent in form to the *in-out* formalism, for a theory of two independent scalar fields, we are already able to deal with an interacting theory in the perturbative regime, proceeding diagrammatically as usual, keeping in mind the peculiar boundary conditions.

In order to proceed to use the perturbation theory we need first to study the propagators of the free theory. The generating functional is now over two fields and two sources and it is convenient to treat them as elements of vectors in some internal space

$$\Phi := \begin{pmatrix} \phi_+ \\ \phi_- \end{pmatrix} \quad \& \quad \mathbf{J} := \begin{pmatrix} J_+ \\ -J_- \end{pmatrix}. \quad (2.38)$$

We can therefore re-write equation (2.35) in the matrix form

$$Z[\mathbf{J}] = \int \mathcal{D}\phi^+ \mathcal{D}\phi^- \exp \left\{ i \int d^4x (\Phi^T \mathcal{L}_\phi \Phi + \mathbf{J}^T \Phi) \right\}, \quad (2.39)$$

where we have defined the matrix Lagrangian as

$$\mathcal{L}_\phi := \begin{pmatrix} \mathcal{L}[\phi_+] & 0 \\ 0 & -\mathcal{L}[\phi_-] \end{pmatrix}. \quad (2.40)$$

The path integral is Gaussian, therefore we have

$$Z[\mathbf{J}] = Z[\mathbf{J} = \mathbf{0}_2] \exp \left\{ i \int d^4x \int d^4y \mathbf{J}^T(x) \mathcal{G}(x^\mu, y^\mu) \mathbf{J}(y) \right\}, \quad (2.41)$$

where the propagators matrix $\mathcal{G}(x^\mu, y^\mu)$ is defined by

$$\mathcal{L}_\phi \mathcal{G}(x^\mu, y^\mu) := \delta^{(4)}(x^\mu, y^\mu) \mathbf{1}_2, \quad (2.42)$$

and we name the various elements of the matrix as follows

$$\mathcal{G}(x^\mu, y^\mu) := \begin{pmatrix} G^{++}(x^\mu, y^\mu) & G^{+-}(x^\mu, y^\mu) \\ G^{-+}(x^\mu, y^\mu) & G^{--}(x^\mu, y^\mu) \end{pmatrix}. \quad (2.43)$$

The four propagators are obtained through the standard procedure of functional derivation of the generating functional with respect to the source

$$G^{++}(x^\mu, y^\mu) = i \left(\frac{\delta}{i\delta J_+(x^\mu)} \right) \left(\frac{\delta}{i\delta J_+(y^\mu)} \right) e^{iW[J_+, J_-]} \Big|_{J_+ = J_- = 0} \quad (2.44)$$

$$= i \int \mathcal{D}\phi_+ \mathcal{D}\phi_- e^{i(S[\phi_+] - S[\phi_-])} \phi_+(x^\mu) \phi_+(y^\mu) \quad (2.45)$$

$$= i \sum_\lambda \langle 0|\lambda\rangle \langle \lambda|T\phi(x^\mu)\phi(y^\mu)|0\rangle \quad (2.46)$$

$$= i \langle 0|T\phi(x^\mu)\phi(y^\mu)|0\rangle = \langle 0|T_C\phi_+(x^\mu)\phi_+(y^\mu)|0\rangle, \quad (2.47)$$

where T is the usual time ordering operator. Similarly for the remaining propagators

$$G^{+-}(x^\mu, y^\mu) = i \langle 0|\phi(y^\mu)\phi(x^\mu)|0\rangle = i \langle 0|T_C\phi_+(x^\mu)\phi_-(y^\mu)|0\rangle, \quad (2.48)$$

$$G^{-+}(x^\mu, y^\mu) = i \langle 0|\phi(x^\mu)\phi(y^\mu)|0\rangle = i \langle 0|T_C\phi_-(x^\mu)\phi_+(y^\mu)|0\rangle, \quad (2.49)$$

$$G^{--}(x^\mu, y^\mu) = i \langle 0|\tilde{T}\phi(x^\mu)\phi(y^\mu)|0\rangle = i \langle 0|T_C\phi_-(x^\mu)\phi_-(y^\mu)|0\rangle, \quad (2.50)$$

where T_C is the time ordering along the path \mathcal{C} defined following the convention in figure 2.1, meaning that the points in the backward branch \mathcal{C}_- are always later in time than the one in the forwards branch \mathcal{C}_+ . The implications are evident in equations (2.48) and (2.49). $G^{++}(x^\mu, y^\mu)$ and $G^{--}(x^\mu, y^\mu)$ are the Feynman and anti-Feynman propagators respectively; this comes from the boundary condition that we have set. Notice that the propagators have some useful relations connecting them

$$G^{+-}(x^\mu, y^\mu) = G^{-+}(y^\mu, x^\mu), \quad (2.51)$$

$$G^{+-}(x^\mu, y^\mu)^* = -G^{-+}(x^\mu, y^\mu). \quad (2.52)$$

that are easily obtained from their definitions. Moreover we can show that the four propagators are not independent: thanks to the time ordering property we can express G^{++} and G^{--} in term of G^{+-} and G^{-+} using the Heaviside $\theta(t_1, t_2)$ function

$$G^{++}(x^\mu, y^\mu) = \theta(x_0 - y_0)G^{-+}(x^\mu, y^\mu) + \theta(y_0 - x_0)G^{+-}(x^\mu, y^\mu), \quad (2.53)$$

$$G^{--}(x^\mu, y^\mu) = \theta(x_0 - y_0)G^{+-}(x^\mu, y^\mu) + \theta(y_0 - x_0)G^{-+}(x^\mu, y^\mu), \quad (2.54)$$

Therefore it follows that

$$G^{++}(x^\mu, y^\mu) + G^{--}(x^\mu, y^\mu) = G^{+-}(x^\mu, y^\mu) + G^{-+}(x^\mu, y^\mu). \quad (2.55)$$

This suggests us that we can move to a more convenient basis where one of the components of the propagator matrix is zero. This is the so-called Keldysh basis. Rotating the field into the new basis we have

$$\phi^{(1)} = \frac{1}{2}(\phi_+ + \phi_-) \quad \& \quad \phi^{(2)} = (\phi_+ - \phi_-), \quad (2.56)$$

rotating the propagators matrix

$$\mathcal{G}'(x^\mu, y^\mu) := \begin{pmatrix} G^{11}(x^\mu, y^\mu) & G^{12}(x^\mu, y^\mu) \\ G^{21}(x^\mu, y^\mu) & G^{22}(x^\mu, y^\mu) \end{pmatrix} := \begin{pmatrix} iF(x^\mu, y^\mu) & G^R(x^\mu, y^\mu) \\ G^A(x^\mu, y^\mu) & 0 \end{pmatrix}. \quad (2.57)$$

The advantage of the new basis is that the correlator $\langle 0|T\phi^{(2)}\phi^{(2)}|0\rangle$ is always vanishing and therefore when drawing the Feynman diagrams we know that they will not contain any “ 22 ” internal leg. The relation with the previous basis is given by

$$F_\phi(x^\mu, y^\mu) = -\frac{i}{2} [G^{-+}(x^\mu, y^\mu) + G^{+-}(x^\mu, y^\mu)] \quad (2.58)$$

$$G_\phi^R(x^\mu, y^\mu) = \theta(x_0 - y_0) [G^{-+}(x^\mu, y^\mu) - G^{+-}(x^\mu, y^\mu)] \quad (2.59)$$

$$G_\phi^A(x^\mu, y^\mu) = G_\phi^R(y^\mu, x^\mu) \quad (2.60)$$

We recognize F as the Hadamard (or Keldysh) propagator and G^R and G^A as the retarded and the advanced propagators. Let us notice moreover that equal time G^R and G^A are also automatically zero because of the Heaviside function. Finally the three propagators are connected to the Feynman propagator G^F by the relation

$$G^F(y^\mu, x^\mu) = \frac{1}{2} [G^R(y^\mu, x^\mu) + G^A(y^\mu, x^\mu)] + iF(y^\mu, x^\mu). \quad (2.61)$$

2.1.4 Generating functional for a fermion field

The discussion for a fermion field is similar to the previous one therefore we will present it briefly. We need to be careful and remember that the fields and the sources in the generating functional in this case are Grassmann variables. Therefore the order in which they show up in the integral is important. We will use the fermion case to express the previous results in a different and complementary form that can be useful for a deeper understanding.

As we learned from the scalar case the computational technique in the Schwinger Keldysh formalism is to double the fields and the sources, in order to write the generating functional for *in-in* correlators Z . The fields ψ_+ , $\bar{\psi}_+$ and the sources η_+ , $\bar{\eta}_+$ live in the \mathcal{C}_+ branch, ψ_- , $\bar{\psi}_-$ and the sources η_- , $\bar{\eta}_-$ in the \mathcal{C}_- branch. The boundary conditions are: $\psi_+(t) = \psi_-(t)$ and $\bar{\psi}_+(t) = \bar{\psi}_-(t)$ on the hypersurface Σ at time t and we impose as the initial state the Bunch-Davies vacuum at t_i , deep inside the horizon. The path integral representation of the generating functional is

$$Z[\eta] = \int \mathcal{D}\bar{\psi}_- \mathcal{D}\psi_- \mathcal{D}\bar{\psi}_+ \mathcal{D}\psi_+ \exp\left(i \int_{t_i}^t dt' \int d^3x \mathcal{L}[\psi_-, \bar{\psi}_-] + \bar{\eta}_- \psi_- + \bar{\psi}_- \eta_-\right) \quad (2.62)$$

$$\times \exp\left(-i \int_{t_i}^t dt' \int d^3x \mathcal{L}[\psi_+, \bar{\psi}_+] + \bar{\eta}_+ \psi_+ + \bar{\psi}_+ \eta_+\right),$$

where $Z[\eta] = Z[\bar{\eta}_-, \bar{\eta}_-, \bar{\eta}_+, \eta_+]$ or equivalently

$$Z[\eta] = \int \mathcal{D}\bar{\psi} \mathcal{D}\psi \exp\left(i \int_{\mathcal{C}} dt' \int d^3x \mathcal{L}[\psi, \bar{\psi}] - \eta\psi + \bar{\psi}\eta\right). \quad (2.63)$$

Using a vector notation

$$\Psi := \begin{pmatrix} \psi_+ \\ \psi_- \end{pmatrix} \quad \& \quad \eta := \begin{pmatrix} \eta_+ \\ -\eta_- \end{pmatrix}, \quad (2.64)$$

$$\bar{\Psi} := (\bar{\psi}_+ \quad \bar{\psi}_-) \quad \& \quad \bar{\eta} := (\bar{\eta}_+ \quad -\bar{\eta}_-), \quad (2.65)$$

leads to

$$Z[\eta] = \int \mathcal{D}\bar{\psi}_- \mathcal{D}\psi_- \mathcal{D}\bar{\psi}_+ \mathcal{D}\psi_+ \exp\left\{i \int d^4x (\bar{\psi}_+ \quad \bar{\psi}_-) \begin{pmatrix} (i\not{\partial} + m) & 0 \\ 0 & -(i\not{\partial} + m) \end{pmatrix} \begin{pmatrix} \psi_+ \\ \psi_- \end{pmatrix}\right\} \quad (2.66)$$

$$\times \exp\left\{(\bar{\eta}_+ \quad -\bar{\eta}_-) \begin{pmatrix} \psi_+ \\ \psi_- \end{pmatrix} + (\bar{\psi}_+ \quad \bar{\psi}_-) \begin{pmatrix} \eta_+ \\ -\eta_- \end{pmatrix}\right\}.$$

Again the integral is quadratic in the fields and we proceed defining the propagators matrix

$$\begin{pmatrix} (i\cancel{\partial} + m) & 0 \\ 0 & -(i\cancel{\partial} + m) \end{pmatrix} \begin{pmatrix} S^{++}(x^\mu, y^\mu) & S^{+-}(x^\mu, y^\mu) \\ S^{-+}(x^\mu, y^\mu) & S^{--}(x^\mu, y^\mu) \end{pmatrix} := \delta^4(x^\mu, y^\mu) \begin{pmatrix} 1 & 0 \\ 0 & 1 \end{pmatrix} \quad (2.67)$$

and the generating functional is re-written in explicit form for the fermion indices as

$$Z[\eta] = Z[\eta = 0] \exp \left\{ i \int d^4x d^4y \left(\bar{\eta}_+^a(x^\mu) \quad -\bar{\eta}_-^a(x^\mu) \right) \begin{pmatrix} S^{++}(x^\mu, y^\mu)_{ab} & S^{+-}(x^\mu, y^\mu)_{ab} \\ S^{-+}(x^\mu, y^\mu)_{ab} & S^{--}(x^\mu, y^\mu)_{ab} \end{pmatrix} \begin{pmatrix} \eta_+^b(y) \\ -\eta_-^b(y) \end{pmatrix} \right\}.$$

The propagators are obtained by the functional derivative with respect to the sources

$$\begin{aligned} & \langle 0 | \left(\tilde{T} \psi^{a_1}(x_1^\mu) \dots \psi^{a_k}(x_k^\mu) \bar{\psi}^{a_{k+1}}(x_{k+1}^\mu) \dots \psi^{a_n}(x_n^\mu) T \psi^{a_{n+1}}(x_{n+1}^\mu) \dots \psi^{a_j}(x_j^\mu) \bar{\psi}^{a_{j+1}} \dots \bar{\psi}^{a_{n+m}}(x_{n+m}^\mu) \right) | 0 \rangle \\ &= \frac{1}{Z[\eta = 0]} \left(i^k \frac{\delta^k}{\delta \bar{\eta}_-^{a_1}(x_1^\mu) \dots \delta \bar{\eta}_-^{a_k}(x_k^\mu)} \right) \left(\frac{1}{i^{n-k}} \frac{\delta^{n-k}}{\delta \eta_-^{a_{k+1}}(x_{k+1}^\mu) \dots \delta \eta_-^{a_n}(x_n^\mu)} \right) \\ & \quad \cdot \left(\frac{1}{i^j} \frac{\delta^j}{\delta \bar{\eta}_+^{a_{n+1}}(x_{n+1}^\mu) \dots \delta \bar{\eta}_+^{a_j}(x_j^\mu)} \right) \left(i^{m-j} \frac{\delta^{m-j}}{\delta \eta_+^{a_{j+1}}(x_{j+1}^\mu) \dots \delta \eta_+^{a_m}(x_m^\mu)} \right) Z[\eta] \Big|_{\eta=0}. \end{aligned}$$

Summarizing the results in matrix form we have

$$\begin{pmatrix} S^{++}(x^\mu, y^\mu)_{ab} & S^{+-}(x^\mu, y^\mu)_{ab} \\ S^{-+}(x^\mu, y^\mu)_{ab} & S^{--}(x^\mu, y^\mu)_{ab} \end{pmatrix} = i \begin{pmatrix} \langle T \psi^a(x^\mu) \bar{\psi}^b(y^\mu) \rangle & -\langle \bar{\psi}^b(y^\mu) \psi^a(x^\mu) \rangle \\ \langle \psi^a(x^\mu) \bar{\psi}^b(y^\mu) \rangle & \langle \tilde{T} \psi^a(x^\mu) \bar{\psi}^b(y^\mu) \rangle \end{pmatrix}. \quad (2.68)$$

Given the identity provided by the definition of time ordering and anti-time ordering operators

$$\langle T \psi^a(x^\mu) \bar{\psi}^b(y^\mu) \rangle + \langle \tilde{T} \psi^a(x^\mu) \bar{\psi}^b(y^\mu) \rangle = -\langle \bar{\psi}^b(y^\mu) \psi^a(x^\mu) \rangle + \langle T \psi^a(x^\mu) \bar{\psi}^b(y^\mu) \rangle, \quad (2.69)$$

we have the correspondent equation to (2.55) for the fermions

$$S_{ab}^{++} + S_{ab}^{--} = S_{ab}^{+-} + S_{ab}^{-+}. \quad (2.70)$$

We then rotate the fields and the propagators into the Keldysh basis with the same matrix used for the scalar obtaining

$$\begin{aligned} \mathbf{S}'(x^\mu, y^\mu) &:= \begin{pmatrix} iF_\psi(x^\mu, y^\mu) & G_\psi^R(x^\mu, y^\mu) \\ G_\psi^A(x^\mu, y^\mu) & 0 \end{pmatrix} \\ &= \begin{pmatrix} \frac{1}{2} \left(S^{+-}(x^\mu, y^\mu) + S^{-+}(x^\mu, y^\mu) \right) & \theta(x_0 - y_0) \left(S^{-+}(x^\mu, y^\mu) - S^{+-}(x^\mu, y^\mu) \right) \\ \theta(y_0 - x_0) \left(S^{+-}(x^\mu, y^\mu) - S^{-+}(x^\mu, y^\mu) \right) & 0 \end{pmatrix}. \end{aligned} \quad (2.71)$$

2.2 The Schwinger-Keldysh Propagators

In this section we will present the scalar and fermion Schwinger-Keldysh propagators in momentum space for two different background spacetimes: Minkowski and de Sitter. The choice of the Minkowski spacetime as background is a good way to warm-up to then approach the de Sitter computations and it will be useful as a check of the future results in the limit $a(t) = 1$ (when the flat FLRW metric is equal to the Minkowski one).

To ease the comparison we Fourier-transform only the spatial coordinates (the spatial part of the fields in dS can still be expanded through plane waves since is spatially flat spacetime). Following the convention for the Fourier transform

$$\phi(x, t) = \int \frac{d^3 p}{(2\pi)^3} \tilde{\phi}(p, t) e^{ip \cdot x}, \quad (2.72)$$

$$\tilde{\phi}(p, t) = \int d^3 x \phi(x, t) e^{-ip \cdot x}, \quad (2.73)$$

we define the expansion of the field in mode functions for a massless, φ , and a massive, σ , scalar field and for a massive fermion field, ψ , respectively as

$$\varphi(x, \tau) = \frac{1}{a(\tau)} \int \frac{d^3 k}{(2\pi)^3} [b(k)u(k, \tau)e^{ik \cdot x} + b^\dagger(k)u^*(k, \tau)e^{-ik \cdot x}], \quad (2.74)$$

$$\sigma(x, \tau) = \frac{1}{a(\tau)} \int \frac{d^3 k}{(2\pi)^3} [c(k)v(k, \tau)e^{ik \cdot x} + c^\dagger(k)v^*(k, \tau)e^{-ik \cdot x}], \quad (2.75)$$

$$\psi(x, \tau) = \frac{1}{a^{3/2}(\tau)} \int \frac{d^3 k}{(2\pi)^3} \sum_{\lambda=\pm 1} [d_\lambda(k)u_\lambda(k, \tau)e^{ik \cdot x} + f_\lambda^\dagger(k)v_\lambda^*(k, \tau)e^{-ik \cdot x}], \quad (2.76)$$

where k is the conformal momentum. The mode functions are the complete set of solutions to the free equations of motion for the fields that we recall here

$$\square \varphi(x, \tau) = 0, \quad (2.77)$$

$$(\square + M_s) \sigma(x, \tau) = 0, \quad (2.78)$$

$$(i\nabla - M_f) \psi(x, \tau) = 0, \quad (2.79)$$

where the covariant derivative and the d'Alembert operator in a curved spacetime are defined in chapter 1 and we defined $\nabla := \nabla^\mu \gamma_\mu(x^\mu)$ with the spacetime dependent $\gamma_\mu(x^\mu)$ matrices defined in equation (1.251).

2.2.1 Scalar field

We are going to derive the relation between the Schwinger-Keldysh propagators and the mode functions and then present their expressions in both the Minkowski and de Sitter background. Using equations (2.48) and (2.74) we have

$$\begin{aligned} G_\varphi^{-+}(x^\mu, y^\mu) &= i \langle \varphi(x^\mu) \varphi(y^\mu) \rangle \\ &= \frac{i}{a(\tau_1) a(\tau_2)} \int \frac{d^3 k}{(2\pi)^3} \int \frac{d^3 p}{(2\pi)^3} \langle (b(k)u(k, \tau_1)e^{ik \cdot x} + b^\dagger(k)u^*(k, \tau_1)e^{-ik \cdot x}) \\ &\quad \times (b(p)u(p, \tau_2)e^{ip \cdot y} + b^\dagger(p)u^*(p, \tau_2)e^{-ip \cdot y}) \rangle \\ &= \frac{i}{a(\tau_1) a(\tau_2)} \int \frac{d^3 k}{(2\pi)^3} \int \frac{d^3 p}{(2\pi)^3} \underbrace{\langle b(k)b^\dagger(p) \rangle}_{=(2\pi)^3 \delta^{(3)}(k-p)} u(k, \tau_1) u^*(p, \tau_2) e^{-ik \cdot x} e^{-ip \cdot y} \\ &= \frac{i}{a(\tau_1) a(\tau_2)} \int \frac{d^3 k}{(2\pi)^3} u(k, \tau_1) u^*(k, \tau_2) e^{-ik \cdot (x-y)}. \end{aligned} \quad (2.80)$$

Therefore the Fourier transform is

$$\tilde{G}_{\varphi}^{-+}(k, \tau_1, \tau_2) = \frac{i}{a(\tau_1)a(\tau_2)} u(k, \tau_1)u^*(k, \tau_2), \quad (2.81)$$

where in the following we will omit the tilde in \tilde{G} since it will be clear when we are dealing with Fourier-transformed quantities by their dependence on the momentum k . The computation is similar for the other propagators, leading to

$$G_{\varphi}^{+-}(k, \tau_1, \tau_2) = \frac{i}{a(\tau_1)a(\tau_2)} u(k, \tau_2)u^*(k, \tau_1), \quad (2.82)$$

$$G_{\sigma}^{-+}(k, \tau_1, \tau_2) = \frac{i}{a(\tau_1)a(\tau_2)} v(k, \tau_1)v^*(k, \tau_2), \quad (2.83)$$

$$G_{\sigma}^{+-}(k, \tau_1, \tau_2) = \frac{i}{a(\tau_1)a(\tau_2)} v(k, \tau_2)v^*(k, \tau_1). \quad (2.84)$$

From the G^{+-} and G^{-+} propagators it is straightforward to construct the propagators in the Keldysh basis as discussed above in equations (2.58), (2.59) and (2.60) so we can proceed now to discuss the various mode function solutions.

Minkowski background

We choose as the initial state for the Minkowski background case the vacuum state of the free theory, the mode function solution is [41]

$$u_{\text{M}}(k, \tau) = \frac{1}{2\omega_k} e^{-i\omega_k \tau}, \quad (2.85)$$

where $\omega_k = \sqrt{k^2 + M_s^2}$ is the time independent frequency and we will see that it is the limit of the WKB mode function for $\omega_k(t) \rightarrow \omega_k$. Thanks to the equations (2.81) and (2.82) the Fourier transformed Schwinger-Keldysh propagators are

$$G_{\varphi/\sigma}^{+-}(k, \tau_1, \tau_2) = \frac{i}{2\omega_k} e^{i\omega_k(\tau_1 - \tau_2)}, \quad (2.86)$$

$$G_{\varphi/\sigma}^{-+}(k, \tau_1, \tau_2) = \frac{i}{2\omega_k} e^{i\omega_k(\tau_2 - \tau_1)}. \quad (2.87)$$

Rotating into the Keldysh basis using equations (2.58), (2.59) and (2.60)

$$F_{\varphi/\sigma}(k, \tau_1, \tau_2) = \frac{1}{2\omega_k} \cos(\omega_k(\tau_1 - \tau_2)), \quad (2.88)$$

$$G_{\varphi/\sigma}^R(k, \tau_1, \tau_2) = \theta(\tau_1 - \tau_2) \frac{1}{2\omega_k} \sin(\omega_k(\tau_1 - \tau_2)), \quad (2.89)$$

$$G_{\varphi/\sigma}^A(k, \tau_1, \tau_2) = G^R(k, \tau_2, \tau_1). \quad (2.90)$$

With the Minkowski space as background the computation are simple and we can study massive and massless case together distinguishing them via ω_k .

De Sitter background

The natural choice of initial state in the de Sitter background is the Bunch-Davies vacuum [32]. As discussed in section 1.5.2 this choice of vacuum fixes the mode functions, when they are deep inside the horizon, to be equal to the positive energy modes of the field in the Minkowski spacetime.

In this case we separate the solution in various limits that will be later useful. The mode function solution for a massless scalar field, already derived in equation (1.124)², is

$$u(k, \tau) = a(\tau) \frac{H}{\sqrt{2k^3}} (1 + ik\tau) e^{-ik\tau}, \quad (2.91)$$

leading to the following propagators

$$G_\varphi^{+-}(k, \tau_1, \tau_2) = i \frac{H^2}{2k^3} (1 + ik\tau_2)(1 + ik\tau_1) e^{ik(\tau_1 - \tau_2)}, \quad (2.92)$$

$$G_\varphi^{-+}(k, \tau_1, \tau_2) = i \frac{H^2}{2k^3} (1 + ik\tau_2)(1 + ik\tau_1) e^{-ik(\tau_1 - \tau_2)}, \quad (2.93)$$

that reads in the Keldysh basis

$$F_\varphi(k, \tau_1, \tau_2) = \frac{H}{2k^3} \left((1 + k^2 \tau_1 \tau_2) \cos(k(\tau_1 - \tau_2)) + k(\tau_1 - \tau_2) \sin(k(\tau_1 - \tau_2)) \right), \quad (2.94)$$

$$G_\varphi^R(k, \tau_1, \tau_2) = \theta(\tau_1 - \tau_2) \frac{H}{2k^3} \left((1 + k^2 \tau_1 \tau_2) \sin(k(\tau_1 - \tau_2)) - k(\tau_1 - \tau_2) \cos(k(\tau_1 - \tau_2)) \right). \quad (2.95)$$

The expansion for $|k\tau| \ll 1$ is interesting since we will perform our computation in the sub-horizon regime [55]

$$F_\varphi(k, \tau_1, \tau_2) = \frac{H^2}{2k^3} \left(1 + \mathcal{O}(k^2 \tau_i^2) \right), \quad (2.96)$$

$$G_\varphi^R(k, \tau_1, \tau_2) = \theta(\tau_1 - \tau_2) \frac{H}{3k^3} \left(k^3 (\tau_1^3 - \tau_2^3) + \mathcal{O}(k^5 \tau_i^5) \right). \quad (2.97)$$

It is also interesting to study the equal time behaviour of the Hadamard propagator since it is the tree-level (TL) contribution to the inflaton two-point function as we will discuss in the next chapter

$$F_\varphi(k, \tau, \tau) = \frac{H^2}{2k^3} (1 + k^2 \tau^2). \quad (2.98)$$

Moving now to the complete solution for a massive field in the de Sitter spacetime, that we will also call *full* solution in the following, we can express it either in momentum space in terms of the Hankel functions [32, 55] or in position space in terms of the Hypergeometric functions [32, 56]

$$v(k, \tau) = -ie^{-\frac{\pi}{2}\nu + i\frac{\pi}{4}} \frac{\sqrt{\pi}}{2a(\tau)} H(-\tau)^{3/2} H_\nu^{(1)}(-k\tau), \quad (2.99)$$

where $\nu = \sqrt{M_s^2/H^2 - 9/4}$, meaning that the order of the Hankel function is purely imaginary for large mass $M_s^2/H^2 > 9/4$,

$$G_\sigma^{-+}(x, y, \tau_1, \tau_2) = \frac{1}{4\pi^2} H^2 \Gamma(3/2 - \nu) \Gamma(2/2 + \nu) {}_2F_1(3/2 - \nu, 3/2 + \nu, 2, 1 - r/4), \quad (2.100)$$

$$r = \frac{(-(\tau_1 - \tau_2)^2 + |x - y|^2)}{\tau_1 \tau_2},$$

where the dependence is only on the modulus of the difference between x and y and the Hypergeometric function is defined for $|\delta| < 1$ by

²To make the connection explicit notice that $\delta\phi(k, \tau) = u(k, \tau)/a$.

$${}_2F_1(\alpha, \beta, \gamma, \delta) = \sum_{n=0}^{\infty} \frac{\alpha_n \beta_n \delta^n}{\gamma_n n!}. \quad (2.101)$$

From equations (2.99) and (2.100) we can construct the Hadamard propagators with both descriptions: in the first case directly from the mode function as we did in the massless case while for the second case noticing that F is just given by the imaginary part of G^{+-} obtained from equation (2.52) and its definition (2.58)

$$F_{\sigma}(x, y, \tau_1, \tau_2) = \text{Im}(G^{+-}(x, y, \tau_1, \tau_2)). \quad (2.102)$$

The Fourier transform after some trivial computation is given by the following expression [7]

$$F_{\sigma}(k, \tau_1, \tau_2) = 4\pi \int_0^{\infty} d\tilde{x} \tilde{x}^2 \frac{\sin(k\tilde{x})}{k\tilde{x}} F(\tilde{x}, 0, \tau_1, \tau_2). \quad (2.103)$$

We can then perform via numerical methods the Fourier transform of the propagator using the software Mathematica [57]. In figure 2.2 we compare the two expressions for the *full* equal time Hadamard massive propagator constructed with numerical methods and we present in the same figure the massless propagators as well. We observe as expected that the massless propagator diverges for infrared momenta while the massive propagator is well-behaved.

The expressions with the Hypergeometric functions and the Hankel functions are related by the Fourier transformation and in figure 2.2 they produce the same result as expected so we can choose the one that has the best numerical stability for further computations. In the following we will always compare the numerical and the analytical results to check the goodness of the approximation we are going to make since it is the *full* massive propagator that describes the exact free dynamics of a massive scalar field in the de Sitter background.

2.2.2 Fermion field

Let us proceed with the same analysis for the fermion field. In the following we will use the Dirac representation of the gamma matrices and we write the four-spinor as [41]

$$u_{\lambda}(k, \tau) = \begin{pmatrix} \eta(k, \tau)\xi_{\lambda} \\ \chi(k, \tau)(\sigma \cdot \hat{k})\xi_{\lambda} \end{pmatrix}, \quad (2.104)$$

where $\eta(k, \tau)$ and $\chi(k, \tau)$ are the mode functions and the two-spinor ξ_{λ} has the following properties

$$\xi_{\lambda}^{\dagger}\xi_{\lambda'} = \delta_{\lambda\lambda'}, \quad (2.105)$$

$$(\sigma \cdot \hat{k})\xi_{\lambda} = \lambda\xi_{\lambda}, \quad (2.106)$$

where \hat{k} is the unit vector in the k direction. Knowing that [58]

$$v_{\lambda}(k, \tau) = u_{\lambda}^C(k, \tau) = i\gamma^2 u_{\lambda}^*(k, \tau), \quad (2.107)$$

we can explicitly write v_{λ} as

$$v_{\lambda}(k, \tau) = \begin{pmatrix} \chi^*(k, \tau)(\sigma \cdot \hat{k})\zeta_{\lambda} \\ \eta^*(k, \tau)\zeta_{\lambda} \end{pmatrix}, \quad (2.108)$$

where

$$\zeta_{\lambda} = -i\sigma^2 \xi_{\lambda}^*, \quad (2.109)$$

Equal-time Hadamard propagator

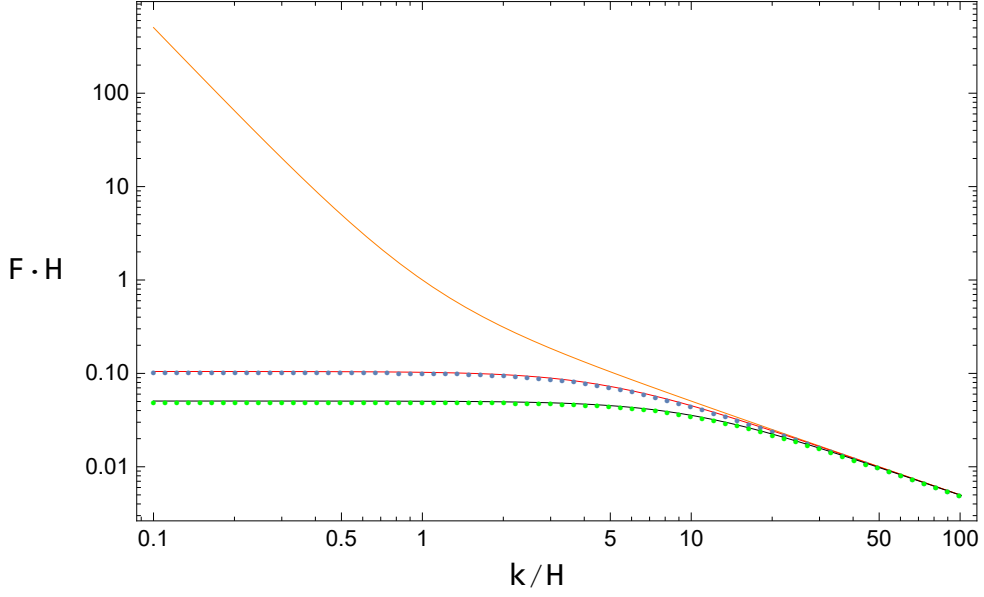


Figure 2.2: Equal-time Hadamard propagator for different mass and for the massless case (orange curve). For $M_s/H = 5$ (blue and red) and $M_s/H = 10$ (green and black) the dotted points and the solid lines are respectively the propagator derived from the hypergeometric and from the Hankel functions.

and the σ matrices are the well known Pauli matrices [41]. We are now ready to proceed and extract the expression for the Schwinger-Keldysh propagators, using (2.68) and (2.76)

$$\begin{aligned}
 S^{-+}(k, \tau_1, \tau_2) &= i \langle \psi(x) \psi(y) \rangle \\
 &= \frac{i}{a^{3/2}(\tau_1) a^{3/2}(\tau_2)} \int \frac{d^3 k}{(2\pi)^3} \int \frac{d^3 p}{(2\pi)^3} \sum_{\lambda, \lambda_1} \left\langle \left(d_\lambda(k) u_{\lambda_1}(k, \tau_1) e^{ik \cdot x} + f_{\lambda_1}(k) u_{\lambda_1}(k, \tau_1) e^{-ik \cdot x} \right) \right. \\
 &\quad \left. \times \left(f_{\lambda_2}(p) \bar{u}_{\lambda_2}(p, \tau_2) e^{ip \cdot y} + d_{\lambda_2}^\dagger \bar{u}_{\lambda_2}(p, \tau_2) e^{-ip \cdot y} \right) \right\rangle \\
 &= \frac{i}{a^{3/2}(\tau_1) a^{3/2}(\tau_2)} \int \frac{d^3 k}{(2\pi)^3} \int \frac{d^3 p}{(2\pi)^3} \sum_{\lambda, \lambda'} \underbrace{\langle d_{\lambda_1}(k) d_{\lambda_2}^\dagger(p) \rangle}_{=(2\pi)^3 \delta^{(3)}(k-p) \delta_{\lambda, \lambda_1}} u_{\lambda_1}(k, \tau_1) \bar{u}_{\lambda_2}(p, \tau_2) e^{ik \cdot x - ip \cdot y} \\
 &= \frac{i}{a^{3/2}(\tau_1) a^{3/2}(\tau_2)} \int \frac{d^3 k}{(2\pi)^3} \left(\sum_{\lambda} u_{\lambda_1}(k, \tau_1) \bar{u}_{\lambda_1}(p, \tau_2) \right) e^{ik \cdot (x^\mu, y^\mu)}, \tag{2.110}
 \end{aligned}$$

Therefore the Fourier transform is

$$S^{-+}(k, \tau_1, \tau_2) = \frac{i}{a^{3/2}(\tau_1) a^{3/2}(\tau_2)} \sum_{\lambda} u_{\lambda}(k, \tau_1) \bar{u}_{\lambda}(p, \tau_2). \tag{2.111}$$

Similarly for the other propagator

$$S^{+-}(k, \tau_1, \tau_2) = -\frac{i}{a^{3/2}(\tau_1) a^{3/2}(\tau_2)} \sum_{\lambda} v_{\lambda}(-k, \tau_1) \bar{v}_{\lambda}(-k, \tau_2), \tag{2.112}$$

where the spin sum is

$$\sum_{\lambda} u_{\lambda}(k, \tau_1) \bar{u}_{\lambda}(p, \tau_2) = \begin{pmatrix} \eta(\tau_1) \eta^*(\tau_2) \mathbb{1}_2 & -\eta(\tau_1) \xi^*(\tau_2) (\sigma \cdot \hat{k}) \\ \xi(\tau_1) \eta^*(\tau_2) (\sigma \cdot \hat{k}) & -\xi(\tau_1) \xi^*(\tau_2) \mathbb{1}_2 \end{pmatrix}, \quad (2.113)$$

$$\sum_{\lambda} v_{\lambda}(-k, \tau_1) \bar{v}_{\lambda}(-k, \tau_2) = \begin{pmatrix} \xi(\tau_1) \xi^*(\tau_2) \mathbb{1}_2 & \eta(\tau_2) \xi^*(\tau_1) (\sigma \cdot \hat{k}) \\ -\xi(\tau_2) \eta^*(\tau_1) (\sigma \cdot \hat{k}) & \eta(\tau_2) \eta^*(\tau_1) \mathbb{1}_2 \end{pmatrix}. \quad (2.114)$$

From equation (2.71) we can construct the Hadamard, the retarded and the advanced propagators

$$iF_{\psi}(x^{\mu}, y^{\mu}) = \frac{1}{2} \left(S^{+-}(x^{\mu}, y^{\mu}) + S^{-+}(x^{\mu}, y^{\mu}) \right) \quad (2.115)$$

$$G_{\psi}^R(x^{\mu}, y^{\mu}) = \theta(x_0 - y_0) \left(S^{-+}(x^{\mu}, y^{\mu}) - S^{+-}(x^{\mu}, y^{\mu}) \right) \quad (2.116)$$

$$G_{\psi}^A(x^{\mu}, y^{\mu}) = \theta(y_0 - x_0) \left(S^{+-}(x^{\mu}, y^{\mu}) - S^{-+}(x^{\mu}, y^{\mu}) \right) \quad (2.117)$$

Minkowski background

We keep the same initial state choice as for the scalar and we have the mode function solution [41]

$$\eta_M(k, \tau) = \sqrt{\frac{\omega_k + M_f}{2\omega_k}} e^{-i\omega_k \tau}, \quad (2.118)$$

$$\chi_M(k, \tau) = \sqrt{\frac{\omega_k - M_f}{2\omega_k}} e^{-i\omega_k \tau}, \quad (2.119)$$

$$\omega_k = \sqrt{k^2 + M_f^2}, \quad (2.120)$$

with again a time independent frequency. Therefore with a Minkowski background the propagators are

$$S^{+-}(k, \tau_1, \tau_2) = -\frac{i}{2\omega_k} e^{i\omega_k(\tau_1 - \tau_2)} \begin{pmatrix} (\omega_k + M_f) \mathbb{1}_2 & \sigma \cdot k \\ -\sigma \cdot k & (\omega_k + M_f) \mathbb{1}_2 \end{pmatrix} \quad (2.121)$$

$$= -\frac{i}{2\omega_k} e^{i\omega_k(\tau_1 - \tau_2)} (\not{k} - M_f), \quad (2.122)$$

where $\not{k} = \gamma_{\mu} k^{\mu}$, $k^0 = \omega_k$, $k^{\mu} = (k^0, k)$ and we use the definitions of the γ s in terms of the Pauli matrices [41]. The S^{-+} propagator is

$$S^{-+}(k, \tau_1, \tau_2) = \frac{i}{2\omega_k} e^{-i\omega_k(\tau_1 - \tau_2)} (\bar{\not{k}} + M_f). \quad (2.123)$$

where $\bar{k}^{\mu} := x(k^0, -k)$; than rotating into the Keldysh basis using equations (2.71)

$$F_{\psi}(k, \tau_1, \tau_2) = \frac{1}{\omega_k} \left((M_f \mathbb{1}_4 - k \cdot \gamma) \cos(\omega(\tau_1 - \tau_2)) - i\omega_k \gamma^0 \sin(\omega_k(\tau_1 - \tau_2)) \right), \quad (2.124)$$

$$G_{\psi}^R(k, \tau_1, \tau_2) = \theta(\tau_1 - \tau_2) \frac{(\omega_k \gamma^0 \cos(\omega_k(\tau_1 - \tau_2)) - i(M_f \mathbb{1}_4 - k \cdot \gamma) \sin(\omega_k(\tau_1 - \tau_2)))}{\omega_k}. \quad (2.125)$$

The propagators discussed here will be used to check the form of the propagators in the de Sitter background and later together with the scalar ones we will use them to compute the amputated diagrams as a warm-up and again to compare the results with the ones in the de Sitter background. In fact we expect from the diagrams the presence of the same divergences since the ultraviolet behavior in de Sitter and in Minkowski should be identical [6].

De Sitter background

In the fermion case we are not interested in the massless limit but only in the *full* form of the propagator since we will need it to perform numerical computation. Given the Dirac equation in the de Sitter spacetime (1.251) and the mode expansion for the fermion (2.76), the fermion mode functions have to satisfy the following differential equations [59]

$$\left(H^2 \tau^2 \frac{\partial^2}{\partial \tau^2} - H^2 \tau \frac{\partial}{\partial \tau} + i M_f H + k^2 H^2 \tau^2 + M_f^2 \right) \eta(k, \tau) = 0, \quad (2.126)$$

$$\left(H^2 \tau^2 \frac{\partial^2}{\partial \tau^2} - H^2 \tau \frac{\partial}{\partial \tau} - i M_f H + k^2 H^2 \tau^2 + M_f^2 \right) \chi(k, \tau) = 0 \quad (2.127)$$

The mode function solution up to a constant phase factor are [59]

$$\eta(k, \tau) = \left(i \frac{\sqrt{\pi(-k\tau)}}{2} H_{\nu}^{(1)}(-k\tau) \right) \exp \left[\frac{\pi}{2} \left(\frac{M_f}{H} \right) \right], \quad (2.128)$$

$$\chi(k, \tau) = \left(\frac{\sqrt{\pi(-k\tau)}}{2} H_{\nu-1}^{(1)}(-k\tau) \right) \exp \left[\frac{\pi}{2} \left(\frac{M_f}{H} \right) \right], \quad (2.129)$$

$$\nu = \frac{1}{2} - i \frac{M_f}{H}. \quad (2.130)$$

Equation (2.128) and (2.129) for small scale limit $-k\tau \ll 1$ reproduce the Minkowski solution therefore they determine a vacuum, analogous to the Bunch-Davies vacuum, for the fermion field (spin $s = 1/2$). The complete expression presented here will be used in the next section to provide a numerical check of the WKB approximated propagators and UV behavior.

2.3 The WKB Approximation

The Wentzel-Kramers-Brillouin (WKB or WKBJ honoring the mathematician Jeffreys) approximation known also as Liouville-Green method was first introduced in the context of semi-classical study of quantum mechanics. The WKB approximation has been used in the context of QFT in curved spacetime [60, 61] in order to define the correct Fock space of the theory.

In fact as introduced in the first chapter, a QFT in a curved background does not have an absolute definition of vacuum and particles. If we consider the creation and annihilation operators to satisfy the usual commutation relations [41], defining the vacuum state by

$$\hat{b}_k |0\rangle = 0, \quad (2.131)$$

for every k , the vacuum choice is actually a choice of the mode function. The adiabatic vacuum corresponds to the choice of the WKB-approximated mode function as (approximate) set of solutions.

The prototype equation to which we can apply the WKB approximation is

$$\frac{d^2 x}{dt^2} + \omega^2(t)x = 0, \quad (2.132)$$

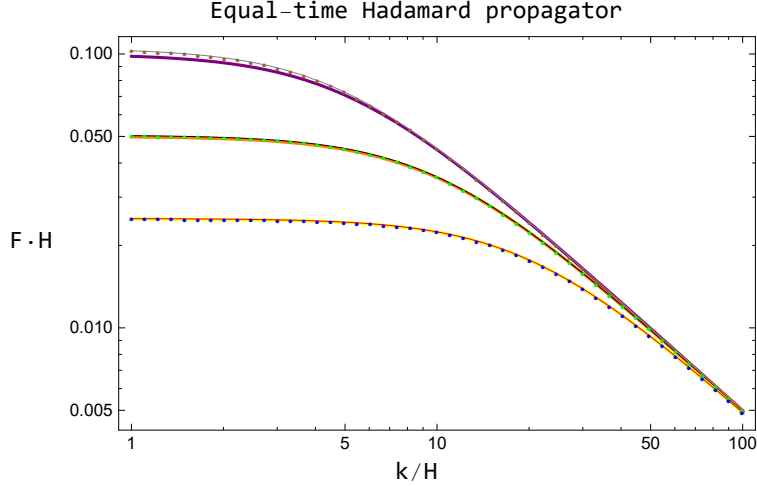


Figure 2.3: The yellow, orange and purple solid lines are the WKB approximated equal-time Hadamard propagators respectively for $M_s/H = 20, 10, 5$. The dotted points and the thin solid lines are the *full* propagators, respectively constructed from the Hypergeometric and Hankel function for the same set of mass to Hubble parameter ratio.

where $\omega(t) > 0$ is always positive and is time dependent (recall that in Minkowski it was constant). This differential equation is exactly the kind of equation that the mode functions have to solve in order to satisfy the Klein-Gordon in a de Sitter background, see equations (1.71).

The frequency $\omega(t)$ is assumed to be slowly changing; its characteristic variation timescale is called T where T^{-1} is called the adiabatic parameter and it is the order parameter of the expansion (for $T \rightarrow \infty$). This condition can be expressed as

$$\left| \frac{d\omega}{dt} \right| \ll \omega^2, \quad (2.133)$$

holding for all times t . Equation (2.133) is the adiabaticity condition. The WKB ansatz is

$$x_{WKB}(t) = \frac{\text{const}}{\sqrt{\omega(t)}} \exp\left(\pm i \int_{t_{in}}^t dt' \omega(t')\right) \quad (2.134)$$

2.3.1 Scalar field

The ansatz in (2.134) is a good approximate solution of the free Klein-Gordon equation for a massive field when (2.133) is satisfied which corresponds to in the $M_s/H \gg 1$ regime [55, 61]. The mode function approximate solution is

$$v(k, \tau) = \frac{1}{\sqrt{2\omega(\tau)}} \exp\left(\pm i \int_{\tau_{in}}^{\tau} d\tau' \omega(\tau')\right), \quad (2.135)$$

$$\omega_k(\tau) = \sqrt{k^2 + M_s^2 a^2(\tau)} \quad (2.136)$$

where the constant was fixed by the requirement that it has to reproduce the Minkowski solution in the limit $\omega_k(t) \rightarrow \omega_k$. This choice of mode functions defines the adiabatic vacuum.

We can easily obtain the expression for the propagators in the Keldysh basis

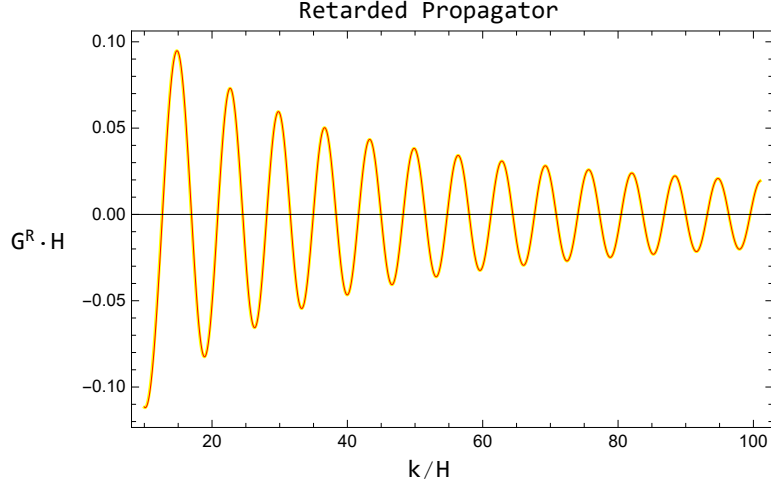


Figure 2.4: The retarded propagator is presented in the figure. The red thin line and the yellow line are the propagators respectively constructed from the *full* and the WKB approximated mode function for $M_s/H = 20$.

$$\begin{aligned}
 F_\sigma(k, \tau_1, \tau_2) &= \frac{\cos \left[\int_{\tau_1}^{\tau_2} d\tau \sqrt{k^2 + m_s^2 a^2(\tau)} \right]}{2a(\tau_1) a(\tau_2) [k^2 + m_s^2 a^2(\tau_1)]^{1/4} [k^2 + m_s^2 a^2(\tau_2)]^{1/4}}, \\
 G_\sigma^R(k, \tau_1, \tau_2) &= - \frac{\theta(\tau_1 - \tau_2) \sin \left[\int_{\tau_1}^{\tau_2} d\tau \sqrt{k^2 + m_s^2 a^2(\tau)} \right]}{a(\tau_1) a(\tau_2) [k^2 + m_s^2 a^2(\tau_1)]^{1/4} [k^2 + m_s^2 a^2(\tau_2)]^{1/4}}.
 \end{aligned} \tag{2.137}$$

In figures 2.3, 2.4 and 2.5 we compare the behaviour of the WKB and *full* propagators in various mass limit. As it is shown there is a very good agreement therefore the WKB mode function is a good sensible approximation of the *full* mode function.

The computations with the use of the mode function described in terms of the Hankel functions are faster and easier since they do not involve the numerical Fourier transform as in the case of the Hypergeometric one. Therefore we will use only the Hankel function expression in the following since we already verified the equivalence of the two.

2.3.2 Fermion field

Equation (2.134) cannot satisfy the normalization condition for a four spinor and therefore is not a possible candidate for the approximated mode function, nor it is its generalized form as shown in [56]. The correct way to obtain the WKB-like expansion is to start from the fact that it should generalize the Minkowski mode functions, equations (2.118) and (2.119), and reproduce them for time independent frequency. Therefore the zeroth order is

$$\begin{aligned}
 \eta^{(0)}(k, \tau) &= \sqrt{\frac{\omega(\tau) + M_f}{2\omega(\tau)}} e^{-i \int_{\tau_{in}}^{\tau} d\tau' \omega(\tau')}, \\
 \chi^{(0)}(k, \tau) &= \sqrt{\frac{\omega(\tau) - M_f}{2\omega(\tau)}} e^{-i \int_{\tau_{in}}^{\tau} d\tau' \omega(\tau')},
 \end{aligned} \tag{2.138}$$

where $\omega = \sqrt{k^2 + M_f^2 a^2(\tau)}$. This is the correct way to proceed and obtain the further adiabatic orders as shown in [59].

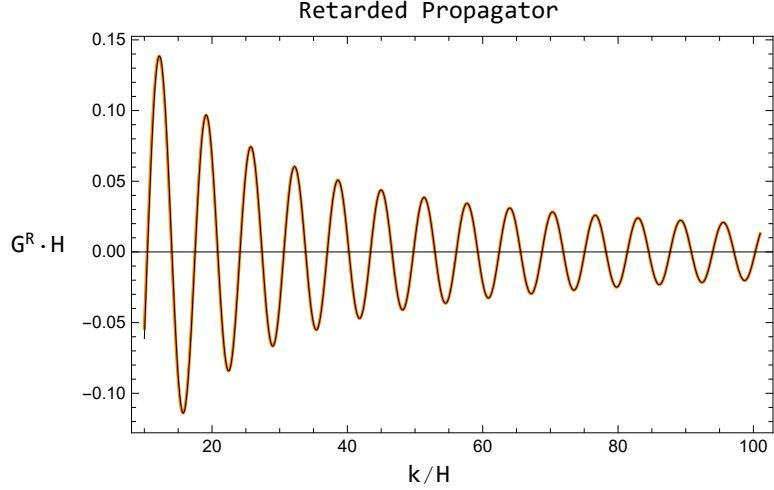


Figure 2.5: The retarded propagator is presented in the figure. The black thin line and the orange line are the propagators respectively constructed from the *full* and the WKB approximated mode function for $M_s/H = 10$.

Since the Schwinger-Keldysh propagators are obtained by combinations of S^{+-} and S^{-+} we just need to check if the WKB-like expression for these propagators are correctly describing the exact behavior; we do this by checking every elements of these matrices. In figure 2.6 and 2.7 we compare two of the matrix elements of the *full* propagators and the WKB-like ones: $\eta(k, \tau)\eta^*(k, \tau)$ and $\chi(k, \tau)\chi^*(k, \tau)$ (at equal conformal time). We observe a good agreement meaning that the WKB mode functions are a good approximation of the complete expression in the large mass limit. The other elements of the propagators matrices produce similar results.

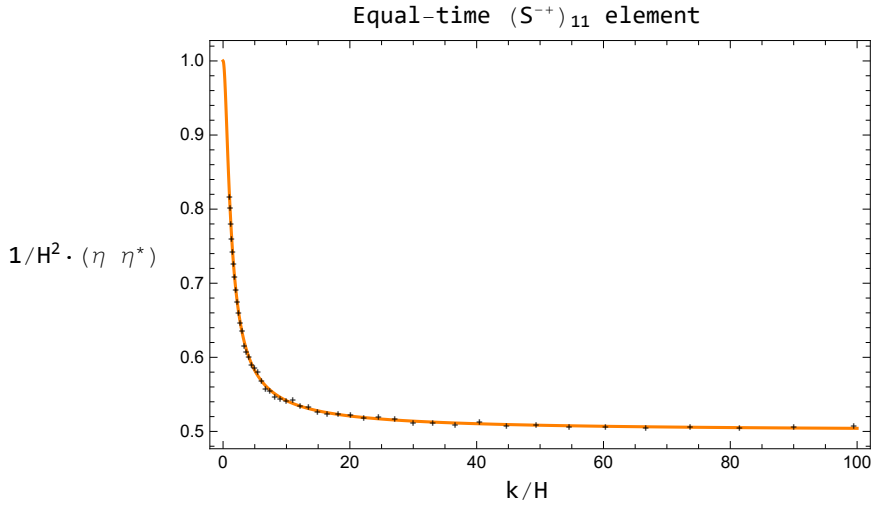


Figure 2.6: Comparison of the (11) element of the fermion propagator S^{-+} , evaluated at equal conformal time. The orange curves is the adiabatic approximated expressions while the full numerical solution is shown in the black cross (+) points. The mass is $M_f = 10H$.

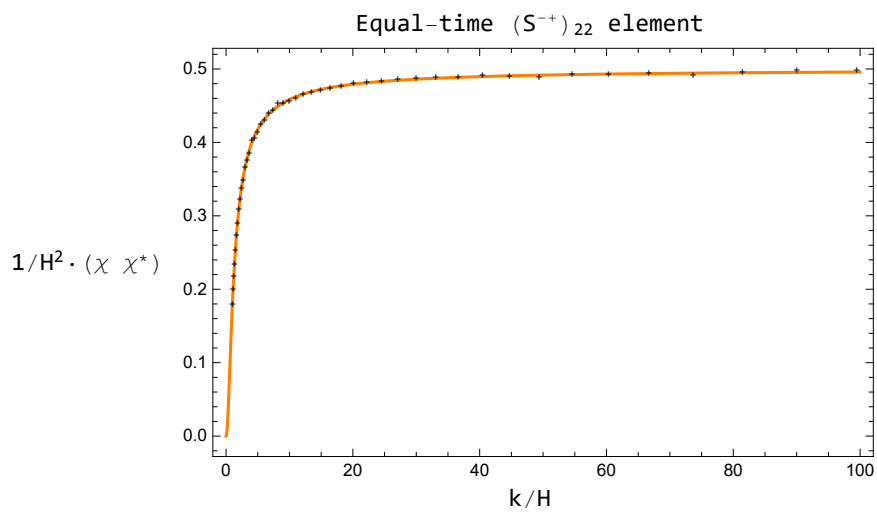


Figure 2.7: Comparison of the (22) element of the fermion propagator S^{-+} , evaluated at equal conformal time. The orange curves is the adiabatic approximated expressions while the full numerical solution is shown in the black cross (+) points. The mass is $M_f = 10H$.

In this chapter we study the one-loop contributions to the inflaton two-point correlation function coming from its interactions with massive scalar and massive fermion fields. We will introduce the Lagrangian density of our model without specifying the inflationary potential so as to keep the discussion on a general ground. We will then discuss the ultraviolet behavior of the two-point function in the Minkowski and de Sitter backgrounds with the use of the formalism developed in chapter 2. The aim of this chapter is to study how the quantum corrections to the cosmological power spectrum modify the tree level result; in particular we will be interested in applying the results into the supersymmetric hybrid model of inflation hence the choice of studying the presence of fermion and scalar fields. But we want to stress that the results obtained here are completely general and are easily applied to a different phenomenological models that include massive fermions and scalar during inflation and are not necessarily supersymmetric.

In section 3.1 we will introduce the chosen model of interactions between the inflaton and the heavy fields and the Feynman rules of the theory. Then the one-loop contribution to the two-point function of the inflaton field will be discussed in section 3.2 and compared with the numerical result. Finally in section 3.3 and section 3.4 the analytical results for the ultraviolet behavior of the various contributions are presented and compared with the numerical computation.

The results of this chapter can be considered the natural continuation of previous works. For the scalar case, our diagram (d) was computed in [7], of which we reproduce the results, and diagrams (a) , (b) and (c) for a massless scalar in [52]. Regarding the fermion contributions we refer to the work in [62, 63], as a comparison of our computation, where they have dealt with massless fermions (or with negligible mass) and for the massive case to [64].

The idea is to start from here in order to provide a complete treatment of fermion and scalar contributions where the ultraviolet behavior is also explicitly presented and singled out. The result has been reported for diagram (d) in [7]. The analytical computation in the *in-in* formalism in Minkowski spacetime of diagram (d) reproduces the one in [7], other diagrams are not found in the literature to our knowledge.

We stress the presence of the complementary formalism of effective field theory [65–67] that can be used to address this type of problems and a bridge between the two could be of interest for future work.

3.1 The Interacting Lagrangian

The action we consider is

$$S = \int d^4x \sqrt{-g} \left[\frac{M_{\text{P}}^2}{2} R - \frac{1}{2} g^{\mu\nu} \partial_\mu \phi \partial_\nu \phi - \frac{1}{2} g^{\mu\nu} \partial_\mu \Sigma \partial_\nu \Sigma + \bar{\chi} i \gamma^\mu \nabla_\mu \chi - V(\phi, \Sigma, \chi) \right], \quad (3.1)$$

and describes a model that consists of a nearly massless scalar field, the inflaton ϕ , a massive scalar field Σ and a massive fermion field χ . The potential $V(\phi, \Sigma, \chi)$ includes the inflaton potential and all the possible interactions between the fields. Its most generic renormalizable form, with Z_2 symmetry for the field Σ , is

$$V(\phi, \Sigma, \chi) = V_{\text{inf}}(\phi) + \frac{1}{2} M_\Sigma^2 \Sigma^2 + \frac{1}{4!} \lambda_\Sigma \Sigma^4 + \frac{1}{2} \mu_{\phi\Sigma} \phi \Sigma^2 + \frac{1}{4} \lambda_{\phi\Sigma} \phi^2 \Sigma^2 + Y \phi \bar{\chi} \chi, \quad (3.2)$$

where V_{inf} is the inflaton potential constrained by the slow-roll conditions, equations (1.77) and (1.79). In this chapter we will not specify the explicit form of this potential, meaning the particular inflationary model, in order to keep the discussion as general as possible. The results will be then applied to a specific model in chapter 4: the supersymmetric hybrid model of inflation.

Assuming the vacuum expectation values of the heavy fields vanish, the fluctuation of the fields around their backgrounds are

$$\phi = \phi_0 + \varphi, \quad \Sigma = 0 + \sigma, \quad \chi = 0 + \psi, \quad (3.3)$$

where $\varphi \equiv \delta\phi$ is the inflaton fluctuation around the value $\phi_0 \equiv \langle \phi \rangle$. The potential now reads

$$V(\phi_0, \varphi, \sigma, \psi) = V_{\text{inf}}(\phi) + \frac{1}{2} M_s^2 \sigma^2 + \frac{\lambda_\Sigma}{4!} \sigma^4 + \mu \varphi \sigma^2 + \lambda \varphi^2 \sigma^2 + M_f \bar{\psi} \psi + Y \varphi \bar{\psi} \psi, \quad (3.4)$$

where we introduced a new set of parameters defined as

$$M_s^2 := m_\Sigma^2 + \mu_{\phi_0\Sigma} \phi_0 + \frac{1}{2} \lambda_{\phi_0\Sigma} \phi_0^2, \quad \mu := \frac{1}{2} \mu_{\phi_0\Sigma} + \frac{1}{2} \lambda_{\phi_0\Sigma} \phi_0, \quad \lambda := \frac{1}{4} \lambda_{\phi_0\Sigma}, \quad M_f := Y \phi_0. \quad (3.5)$$

Note that the dependence of the background field ϕ_0 in M_s , M_f , μ and λ lead them to be slowly-varying rather than exactly constant. Note also that due to the Yukawa-like interaction between the inflaton and the fermion, the latter one gains a mass in the final description of the potential.

In order to calculate the one-loop corrections to the two-point function of the inflaton we will use the Schwinger and Keldysh formalism, doubling the fields into $+$ and $-$ components, rotating the set of fields into the Keldysh basis, as discussed in chapter 2, and then extracting the Feynman rules from the resulting Lagrangian density.

Once we have the Feynman rules we can proceed as usual drawing all the possible topologically inequivalent Feynman diagrams at one-loop. We have four sets of fields (φ_+, φ_-) , (σ_+, σ_-) , (ψ_+, ψ_-) and $(\bar{\psi}_+, \bar{\psi}_-)$ and we construct the Lagrangian density as

$$\mathcal{L}[\varphi, \sigma, \psi, \bar{\psi}]/\sqrt{-g} = \mathcal{L}[\varphi^+, \sigma^+, \psi^+, \bar{\psi}^+]/\sqrt{-g} - \mathcal{L}[\varphi^-, \sigma^-, \psi^-, \bar{\psi}^-]/\sqrt{-g}. \quad (3.6)$$

Rotating into the Keldysh basis through the relations

$$\begin{aligned} 2\varphi_{(1)} &= \varphi^+ + \varphi^-, & \varphi_{(2)} &= \varphi^+ - \varphi^-, & 2\sigma_{(1)} &= \sigma^+ + \sigma^-, & \sigma_{(2)} &= \sigma^+ - \sigma^-, \\ 2\psi_{(1)} &= \psi^+ + \psi^-, & \psi_{(2)} &= \psi^+ - \psi^-, & 2\bar{\psi}_{(1)} &= \bar{\psi}^+ + \bar{\psi}^-, & \bar{\psi}_{(2)} &= \bar{\psi}^+ - \bar{\psi}^-, \end{aligned}$$

the Lagrangian density reads




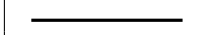
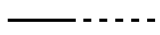
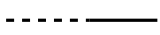



Diagram	Expression	Diagram	Expression	Diagram	Expression
	$F_\varphi(k, \tau_1, \tau_2)$		$-iG_\varphi^R(k, \tau_1, \tau_2)$		$-iG_\varphi^A(k, \tau_1, \tau_2)$
	$F_\sigma(k, \tau_1, \tau_2)$		$-iG_\sigma^R(k, \tau_1, \tau_2)$		$-iG_\sigma^A(k, \tau_1, \tau_2)$
	$F_\psi(k, \tau_1, \tau_2)$		$-iG_\psi^R(k, \tau_1, \tau_2)$		$-iG_\psi^A(k, \tau_1, \tau_2)$

Table 3.1: Feynman rules for the propagators in the Keldysh basis.

$$\begin{aligned}
\mathcal{L} = \sqrt{-g} \left[\right. & \partial_\mu \varphi_{(1)} \partial^\mu \varphi_{(2)} + \partial_\mu \sigma_{(1)} \partial^\mu \sigma_{(2)} - M^2 \sigma_{(1)} \sigma_{(2)} - \mu \varphi_{(2)} \sigma_{(1)}^2 - 2\mu \varphi_{(1)} \sigma_{(1)} \sigma_{(2)} & (3.7) \\
& - \frac{\mu}{4} \varphi_{(2)} \sigma_{(2)}^2 - 2\lambda \varphi_{(1)}^2 \sigma_{(1)} \sigma_{(2)} - 2\lambda \varphi_{(1)} \varphi_{(2)} \sigma_{(1)}^2 - \frac{\lambda}{2} \varphi_{(1)} \varphi_{(2)} \sigma_{(2)}^2 - \frac{\lambda}{2} \varphi_{(2)}^2 \sigma_{(1)} \sigma_{(2)} \\
& - m \left(\bar{\psi}_{(1)} \psi_{(2)} + \bar{\psi}_{(2)} \psi_{(1)} \right) - Y \varphi_{(1)} \bar{\psi}_{(1)} \psi_{(2)} - Y \varphi_{(1)} \bar{\psi}_{(2)} \psi_{(1)} \\
& \left. - Y \varphi_{(2)} \bar{\psi}_{(1)} \psi_{(1)} - \frac{1}{4} Y \varphi_{(2)} \bar{\psi}_{(2)} \psi_{(2)} \right],
\end{aligned}$$

where we ignored the σ self interaction that is not relevant in our discussion. We can now associate a Feynman representation to each propagator in the Keldysh basis, Table 3.1, where thin line represents the inflaton fluctuation, the thick line the massive scalar and the fermion is represented with an arrowed line.

In Keldysh basis the (1) and (2) components of the field set are represented respectively by a solid and a dashed lines; recall that we defined iF and G^R respectively as G^{11} and G^{12} of the propagators matrix in the Keldysh basis; see equation (2.57). From the Lagrangian density we extract the Feynman rules for the interaction vertices summarized in Table 3.2. Observe that each vertex contains a factor a^4 coming from the term $\sqrt{-g}$, needed to assure the invariance of the action measure under general coordinate transformation.

Note that the Feynman rules in the Minkowski spacetime are those in Table 3.2 but with $a \rightarrow 1$. Moreover we do not specify counterterms at this stage: we will see in the following that in general it would be needed to produce a finite one-loop amplitude. We will indeed present the explicit dependence of the two-point function on a cut-off Λ , used to regularize the integrals. Note however that in the supersymmetric theory we expect the cancellation of the divergences as long as supersymmetry is exact.

3.2 Inflaton Two-Point Correlation Function

Before moving to the analysis of one-loop diagrams we note that the tree level contribution to the two-point inflaton correlation function comes only from the Keldysh propagator

$$\begin{array}{c} \tau \\ \hline \tau \end{array} \quad F_\varphi(k, \tau, \tau), \quad (3.8)$$

since the equal time contribution from the retarded $G^R(k, \tau, \tau)$ and advanced propagator $G^A(k, \tau, \tau)$ is vanishing. This is an useful property and it helps us see that a certain class of one-loop diagrams is identically zero: the amputated diagrams with no external dashed line. An example of such diagram is

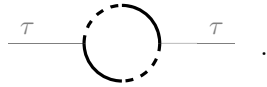


Diagram	Expression	Diagram	Expression
	$-ia^4(\tau_1)\mu$		$-ia^4(\tau_1)2\mu$
	$-ia^4(\tau_1)\frac{\mu}{4}$		$-ia^4(\tau_1)\delta_{m_\phi}^2$
	$-ia^4(\tau_1)\frac{\lambda}{2}$		$-ia^4(\tau_1)2\lambda$
	$-ia^4(\tau_1)2\lambda$		$-ia^4(\tau_1)\frac{\lambda}{2}$
	$-ia^4(\tau_1)Y$		$-ia^4(\tau_1)Y$
	$-ia^4(\tau_1)Y$		$-ia^4(\tau_1)\frac{Y}{4}$

Table 3.2: Feynman rules for the vertices in the Keldysh basis.

The reason is that diagrams of this type always contain a closed loop of two $G^{R/A}$ propagators and this is vanishing because of the presence of the two step functions

$$G^R(k, \tau_1, \tau_2)G^R(k, \tau_2, \tau_1) \sim \theta(\tau_1 - \tau_2)\theta(\tau_2 - \tau_1) = 0. \quad (3.9)$$

We can compare the result obtained for the two-point function of the inflation given in chapter 1 in Table 1.3 with the one we can extract from the tree level computation of $F(k, \tau, \tau)$ in chapter 2, equation (2.98) in the Schwinger-Keldysh formalism. The solution of the equation of motion for a massless scalar field in de Sitter, equation (1.124), is

$$\delta\phi_k = \frac{1}{a} \frac{e^{-ik\tau}}{\sqrt{2k}} \left(1 - \frac{i}{k\tau}\right), \quad (3.10)$$

therefore we have

$$|\delta\phi_k|^2 = \frac{H^2}{2k^3} (1 + k^2\tau^2), \quad (3.11)$$

which is equivalent to what we obtained for the tree level equal time Hadamard propagator, equation (2.98)

$$F_\varphi^{\text{tree}}(k, \tau, \tau) = \frac{H^2}{2k^3} (1 + k^2\tau^2). \quad (3.12)$$

We here showed that we obtained the same result with both formalisms and we can therefore give the expression for the tree level power spectrum of a massless scalar field on super horizon scale ($|k\tau| \ll 1$), calculated from the Schwinger-Keldysh formalism as

$$\Delta_\varphi^{\text{tree}}(k) = \frac{k^3}{2\pi^2} F_\varphi^{\text{tree}}(k, \tau, \tau) \simeq \frac{H^2}{4\pi^2}, \quad (3.13)$$

equivalent to the one presented in Table 1.3.

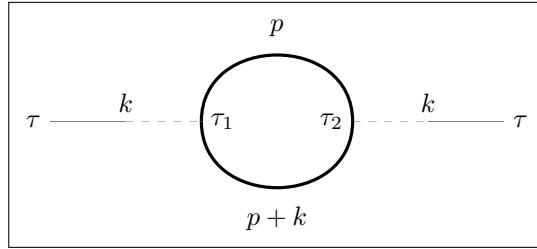
3.2.1 One-loop corrections from a massive scalar

At one-loop level the heavy scalar contributions to the two-point function come from the diagrams shown in figure 3.2. We need to consider also the mirrored diagrams, that we will denote in the following with $'$; in figure 3.1 we give an explicit example. The one-loop correction due to the inflaton quartic self-interaction has been studied previously in [52, 55] and the interaction with an heavy field of the type $\phi^2\Sigma$ and $\phi^3\Sigma$ in [68, 69]. These interactions are not presented in our study since we imposed a Z_2 symmetry. In other words we focus on the contributions purely coming from the heavy fields.

We shall to evaluate the one-loop diagrams using the Feynman rules in Table 3.2 both in the Minkowski and de Sitter background spacetimes aiming to extract the ultraviolet (UV) behavior in the next sections.

Minkowski background

Let us evaluate step by step the Feynman amplitude corresponding to the diagram (a)



The amplitude associate to the diagram (a) is

$$\begin{aligned}
 A_{\text{scalar}}^{(a)} = & \underbrace{\int_{\tau_i}^{\tau} d\tau_1 \int_{\tau_i}^{\tau} d\tau_2 (-iG_{\varphi}^R(k, \tau, \tau_1)) (-iG_{\varphi}^R(k, \tau, \tau_2))}_{\text{External legs contribution}} \\
 & \times V_1 V_2 \frac{1}{2} \underbrace{\int \frac{d^3 p}{(2\pi)^3} F_{\sigma}(p, \tau_1, \tau_2) F_{\sigma}(p+k, \tau_1, \tau_2)}_{\text{Amputated amplitude } A_{\text{amp}}^{(a)}}, \quad (3.14)
 \end{aligned}$$

where $V_1 = V_2 = -i\mu$ are the contribution coming from the vertices and $1/2$ is the symmetry factor associated to the diagram. In this chapter we will dedicate our attention to the amputated amplitude, $A_{\text{amp}}^{(a)}$, since we are interested in extracting the UV behavior of the corrections.

The amputated amplitude neglecting the external momentum, i.e. $|\mathbf{k} + \mathbf{p}| \approx |\mathbf{p}| \equiv p^1$ is:

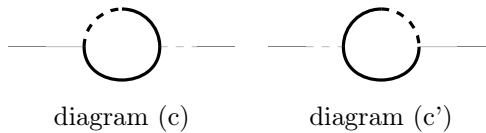


Figure 3.1: Example of diagram (c) and its mirrored version (c')

¹The meaning and the goodness of the approximation will be addressed in the next section when studying the de Sitter case.

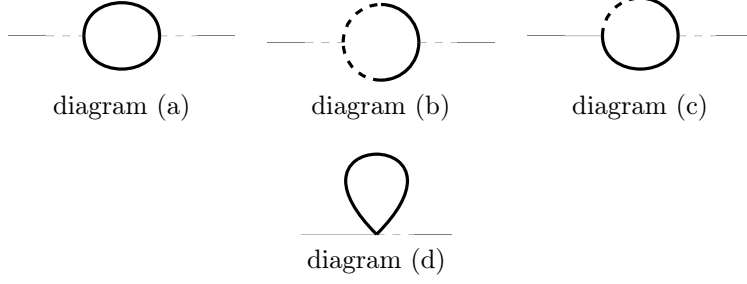


Figure 3.2: One-loop Feynman corrections to the inflaton two-point function due to the interaction with a massive scalar field.

$$A_{\text{amp, scalar}}^{(a)} = -\frac{\mu^2}{2} \int \frac{d^3 p}{(2\pi)^3} F_\sigma(p, \tau_1, \tau_2) F_\sigma(p, \tau_1, \tau_2). \quad (3.15)$$

To perform the internal momentum integration, we split the momentum into a small momentum $p < p_c$ and a large momentum parts $p > p_c$. Here $p_c := M_s$. Therefore we have

$$A_{\text{amp, scalar}}^{(a)} = -\frac{\mu^2}{4\pi^2} \left\{ \int_0^{p_c} dp p^2 [F_\sigma(p, \tau_1, \tau_2)]^2 + \int_{p_c}^{p_{UV}} dp p^2 [F_\sigma(p, \tau_1, \tau_2)]^2 \right\}, \quad (3.16)$$

where we imposed an explicit UV cutoff $p_{UV} := \Lambda$ as a regulator of the otherwise divergent integral. The choice of a cutoff in momentum as a regulator instead of other possible prescriptions (e.g. dimensional regularization) was done for two main reasons. It is a very physical realization of the regularization processes, meaning the process of *cutting out* our ignorance of the physics at very high energy scale [70]. Moreover it is very convenient for both analytical and numerical calculation and it does not have disadvantages since we do not have to deal with a gauge invariant theory.

Diagram (a): Explicitly performing the integrations in (3.16), we obtain

$$\begin{aligned} A_{\text{amp, scalar}}^{(a)} &= -\frac{\mu^2}{4\pi^2} \left\{ \int_0^{M_s} dp p^2 \frac{1}{M_s^2} \cos^2 [M_s(\tau_1 - \tau_2)] + \int_{M_s}^{\Lambda} dp p^2 \frac{1}{4p^2} \cos^2 [p(\tau_1 - \tau_2)] \right\} \\ &= -\frac{\mu^2}{192\pi^2} \left\{ 4M_s \cos^2 [M_s(\tau_1 - \tau_2)] + 6(\Lambda - M_s) \right. \\ &\quad \left. + \frac{3}{\tau_1 - \tau_2} \left(\sin[2\Lambda(\tau_1 - \tau_2)] - \sin[2M_s(\tau_1 - \tau_2)] \right) \right\}. \end{aligned} \quad (3.17)$$

Diagram (b): Following the same steps and using the same conventions in naming the variables we evaluate the amputated diagram (b)

$$\begin{aligned} A_{\text{amp, scalar}}^{(b)} &= +\frac{\mu^2}{16\pi^2} \theta(\tau_2 - \tau_1) \left\{ \frac{M_s}{3} \sin^2 [M_s(\tau_1 - \tau_2)] + \frac{1}{2} (\Lambda - M_s) \right. \\ &\quad \left. - \frac{1}{4(\tau_1 - \tau_2)} \left(\sin[2\Lambda(\tau_1 - \tau_2)] - \sin[2M_s(\tau_1 - \tau_2)] \right) \right\}. \end{aligned} \quad (3.18)$$

Diagram (b'): Its mirror diagram (b'), i.e. the diagram with the exchange $\tau_1 \leftrightarrow \tau_2$ is

$$A_{\text{amp, scalar}}^{(b')} = + \frac{\mu^2}{16\pi^2} \theta(\tau_1 - \tau_2) \left\{ \frac{M_s}{3} \sin^2[M_s(\tau_2 - \tau_1)] + \frac{1}{2}(\Lambda - M_s) - \frac{1}{4(\tau_1 - \tau_2)} \left(\sin[2\Lambda(\tau_1 - \tau_2)] - \sin[2M_s(\tau_1 - \tau_2)] \right) \right\}. \quad (3.19)$$

Diagram (a + b + b'): We note that the non-local linear divergences are cancelled in the sum of the three previous amplitudes. In section 3.3 we will address the issue of the divergences. The result of the sum is

$$A_{\text{amp, scalar}}^{(a+b+b')} = - \frac{\mu^2 M_s}{48\pi^2} \left\{ \cos[2M_s(\tau_2 - \tau_1)] - \frac{\mu^2}{32\pi^2(\tau_1 - \tau_2)} \left(\sin[2\Lambda(\tau_1 - \tau_2)] - \sin[2M_s(\tau_1 - \tau_2)] \right) \right\}. \quad (3.20)$$

Diagram (c) and (c'): The result of the integration for diagram (c) and (c') is

$$A_{\text{amp, scalar}}^{(c)} = + \frac{\mu^2}{\pi^2} \theta(\tau_2 - \tau_1) \left\{ i \frac{M_s}{12} \sin[2M_s(\tau_2 - \tau_1)] - \frac{i}{8(\tau_1 - \tau_2)} \left(\cos[2\Lambda(\tau_1 - \tau_2)] - \cos[2M_s(\tau_1 - \tau_2)] \right) \right\} \quad (3.21)$$

and

$$A_{\text{amp, scalar}}^{(c')}(\tau_2 - \tau_1) = A_{\text{amp, scalar}}^{(c)}(\tau_1 - \tau_2), \quad (3.22)$$

Diagram (d): The amputated amplitude of the tadpole-like diagram (d) can be evaluated without using any of the above approximations, obtaining

$$\begin{aligned} A_{\text{amp, scalar}}^{(d)} &= \int \frac{d^3p}{(2\pi)^3} V_1 F_\sigma(p, \tau_1, \tau_2) \\ &= - \frac{i\lambda}{2\pi^2} \int_0^\Lambda dp \frac{1}{2\sqrt{p^2 + M_s^2}} \\ &= - \frac{i\lambda}{4\pi^2} \left\{ \Lambda^2 - M_s^2 \ln \left(\frac{2\Lambda}{M_s} \right) \right\}. \end{aligned} \quad (3.23)$$

The results obtained in Minkowski will be useful to check the consistency of the ones we will obtain in the next sections when moving to the de Sitter background. The result of the UV behavior of diagram (d) can be directly compared and are in agreement with previous literature [7] and with analogous computations in *in-out* formalism [71]. Regarding the amplitudes of the diagram (c + c') further manipulations are needed to extract the ultraviolet behavior as discussed in the next sections.

De Sitter background

We are going to perform the same computations in a background of cosmological interest: de Sitter spacetime. We use diagram (a) as an example to calculate the amputated amplitude. There are some differences with the Minkowski case: the vertex factors acquire a time dependence through $a^4(\tau_j)$, $j = 1, 2$, coming from the Feynman rules in Table 3.2.

The momentum p_c and the UV cutoff p_{UV} are also time dependent, in fact we have

$$\omega(\tau_\beta) = \sqrt{p^2 + M_s^2 a^2(\tau_\beta)} = \sqrt{p^2 + p_c^2} \simeq \begin{cases} p & p \gg p_c \\ p_c & p \ll p_c \end{cases} \quad (3.24)$$

where we defined $p_c := M_s a(\tau_\beta) = -M_s/(H\tau_\beta)$ as the momentum scale we use to split the integral into large momentum $p > p_c$ and small momentum $p < p_c$ part; τ_β is the latest time that occurs in the loop, i.e., $|\tau_\beta| = \min\{|\tau_1|, |\tau_2|\}$. We choose again a cutoff to regularize the integral in momentum space $p_{UV} := \Lambda a(\tau_\beta)$ with $a_\beta := a(\tau_\beta)$.

In order for Λ to be a physical cutoff we need to multiply it by the scale factor since we are imposing a cutoff to an integral on comoving momenta. The cutoff Λ regularizes integrals in k_{phys} , while Λa_β regularize integrals in $k = k_{\text{phys}} a_\beta$. The choice of τ_β to be the latest time means choosing the largest physical cutoff between Λa_β with $\beta = 1, 2$ [65].

As discussed in the previous chapter to perform the analytical computation we will use the WKB approximated propagators that in the two momentum limits take the following form

$$F_\sigma(p < p_c, \tau_1, \tau_2) \approx \frac{1}{2M_s a_1^{3/2} a_2^{3/2}} \cos \left[\frac{M_s}{H} \ln \frac{\tau_1}{\tau_2} \right], \quad (3.25)$$

$$F_\sigma(p > p_c, \tau_1, \tau_2) \approx \frac{4p^2 - M_s^2(a_1^2 + a_2^2)}{8p^3 a_1 a_2} \cos [p(\tau_1 - \tau_2)] \quad (3.26)$$

$$- \frac{M_s^2(\tau_1 - \tau_2)}{4a_1 a_2 H^2 \tau_1 \tau_2 p^2} \sin [p(\tau_1 - \tau_2)],$$

$$G_\sigma^R(p < p_c, \tau_1, \tau_2) \approx - \frac{\theta(\tau_1 - \tau_2)}{M_s a_1^{3/2} a_2^{3/2}} \sin \left[\frac{M_s}{H} \ln \frac{\tau_1}{\tau_2} \right], \quad (3.27)$$

$$G_\sigma^R(p > p_c, \tau_1, \tau_2) \approx \theta(\tau_1 - \tau_2) \left\{ \frac{4p^2 - M_s^2(a_1^2 + a_2^2)}{4a_1 a_2 p^3} \sin [p(\tau_1 - \tau_2)] \quad (3.28)$$

$$+ \frac{M_s^2(\tau_1 - \tau_2)}{2a_1 a_2 H^2 \tau_1 \tau_2 p^2} \cos [p(\tau_1 - \tau_2)] \right\},$$

The amputated amplitude for diagram (a), neglecting the external momentum, i.e. $|\mathbf{k} + \mathbf{p}| \approx |\mathbf{p}| \equiv p$, is given by

$$A_{\text{amp, scalar}}^{(a)} = \frac{\mu^2 a^4(\tau_1) a^4(\tau_2)}{2} \int \frac{d^3 p}{(2\pi)^3} F_\sigma(p, \tau_1, \tau_2) F_\sigma(p, \tau_1, \tau_2), \quad (3.29)$$

and splitting the integral in momentum space gives

$$A_{\text{amp, scalar}}^{(a)} = \frac{\mu^2 a_1^4 a_2^4}{4\pi^2} \left\{ \int_0^{p_c} dp p^2 [F_\sigma(p, \tau_1, \tau_2)]^2 + \int_{p_c}^{p_{UV}} dp p^2 [F_\sigma(p, \tau_1, \tau_2)]^2 \right\}. \quad (3.30)$$

We neglected the external momentum k in the loop integration. Primarily we are interested in the UV behavior of the amplitudes; since the integral over large momenta is dominating, we can say that $|\mathbf{k} + \mathbf{p}_{UV}| \approx |\mathbf{p}_{UV}| \equiv p$ is a good approximation.

After subtracting the divergences through renormalization, we should in principle consider k and its effects in particular in the small momenta integral. In this case the reference scale is p_c so our approximation would be sensible if $|\mathbf{k} + \mathbf{p}_c| \approx |\mathbf{p}_c|$. We are considering modes that are inside the comoving Hubble radius during inflation and therefore there exists a maximum value of k_m that is its value at horizon exit at the end of inflation $k_m = a(t_f)H$. Therefore as long as p_c is larger than k_m we can still consider $k < p_c$. And since $p_c = aM$ and we are considering massive field $M \gg H$ we can use $|\mathbf{k} + \mathbf{p}| \approx |\mathbf{p}| \equiv p$ as zero order approximation.

Diagram (a): Using equations (3.25) and (3.26) we have

$$\begin{aligned}
A_{\text{amp, scalar}}^{(a)} = & -\frac{\mu^2 a_1 a_2 a_\beta^2 p_c}{48\pi^2} \cos^2 \left[\frac{p_c}{H a_\beta} \ln \frac{\tau_1}{\tau_2} \right] - \frac{\mu^2 a_1^2 a_2^2 (p_c - p_{UV})(a_1^2 p_c + a_2^2 p_c - 2a_\beta^2 p_{UV})}{64\pi^2 a_\beta^2 p_{UV}} \\
& - \frac{\mu^2 a_1^2 a_2^2 (a_1^2 + a_2^2) p_c^2}{64\pi^2 a_\beta^2} \left(\frac{\cos[2p_{UV} \Delta\tau]}{p_{UV}} - \frac{\cos[2p_c \Delta\tau]}{p_c} \right) \\
& - \frac{\mu^2 a_1^2 a_2^2}{64\pi^2} \left(\frac{\sin[2p_{UV} \Delta\tau]}{\Delta\tau} - \frac{\sin[2p_c \Delta\tau]}{\Delta\tau} \right) \\
& + \frac{\mu^2}{323\pi^2} a_1^2 a_2^2 \frac{p_c^2}{a_\beta^2} \left(a_1^2 + a_2^2 - \frac{1}{H^2 \tau_1 \tau_2} \right) \Delta\tau \left(\text{Si}[2p_c \Delta\tau] - \text{Si}[2p_{UV} \Delta\tau] \right), \quad (3.31)
\end{aligned}$$

where we introduced $\Delta\tau := \tau_1 - \tau_2$.

Diagram (a + b + b'): Similarly we can compute the diagram (b) and its mirrored version, with the results

$$\begin{aligned}
A_{\text{amp, scalar}}^{(a+b+b')} = & + \frac{\mu^2}{32\pi^2} a_1^2 a_2^2 \left(\frac{\sin[2p_c \Delta\tau]}{\Delta\tau} - \frac{\sin[2p_{UV} \Delta\tau]}{\Delta\tau} \right) - \frac{\mu^2}{48\pi^2} a_1 a_2 a_\beta^2 p_c \cos \left[\frac{2p_c}{H a_\beta} \ln \frac{\tau_1}{\tau_2} \right] \\
& + \frac{\mu^2}{32\pi^2} a_1^2 a_2^2 (a_1^2 + a_2^2) \frac{p_c^2}{a_\beta^2} \left(\frac{\cos[2p_c \Delta\tau]}{p_c} - \frac{\cos[2p_{UV} \Delta\tau]}{p_{UV}} \right) \\
& + \frac{\mu^2}{16\pi^2} a_1^2 a_2^2 \frac{p_c^2}{a_\beta^2} \left(a_1^2 + a_2^2 - \frac{1}{H^2 \tau_1 \tau_2} \right) \Delta\tau \left(\text{Si}[2p_c \Delta\tau] - \text{Si}[2p_{UV} \Delta\tau] \right). \quad (3.32)
\end{aligned}$$

Diagram (c'): The result for the integration of diagram (c') is

$$\begin{aligned}
A_{\text{amp, scalar}}^{(c')} = & 2\mu^2 a^4(\tau_1) a^4(\tau_2) \int \frac{d^3 p}{(2\pi)^3} F_\sigma(p, \tau_1, \tau_2) \left(-iG_\sigma^R(p, \tau_2, \tau_1) \right) \quad (3.33) \\
= & + \frac{i\mu^2}{8\pi^2} a_1^2 a_2^2 \theta(\Delta\tau) \left(\frac{\cos[2p_c \Delta\tau]}{\Delta\tau} - \frac{\cos[2p_{UV} \Delta\tau]}{\Delta\tau} \right) + \frac{i\mu^2}{12\pi^2} a_1 a_2 a_\beta^2 p_c \theta(\Delta\tau) \sin \left[\frac{2p_c}{H a_\beta} \ln \frac{\tau_2}{\tau_1} \right] \\
& + \frac{i\mu^2}{4\pi^2} a_1^2 a_2^2 \frac{p_c^2}{a_\beta^2} \left(a_1^2 + a_2^2 - \frac{1}{H^2 \tau_1^2 \tau_2^2} \right) \theta(\Delta\tau) \Delta\tau \left(\text{Ci}[-2p_c \Delta\tau] - \text{Ci}[-2p_{UV} \Delta\tau] \right) \\
& - \frac{i\mu^2}{8\pi^2} a_1^2 a_2^2 (a_1^2 + a_2^2) \frac{p_c^2}{a_\beta^2} \theta(\Delta\tau) \left(\frac{\sin[2p_c \Delta\tau]}{p_c} - \frac{\sin[2p_{UV} \Delta\tau]}{p_{UV}} \right), \quad (3.34)
\end{aligned}$$

and

$$A_{\text{amp, scalar}}^{(c)}(\Delta\tau) = A_{\text{amp, scalar}}^{(c')}(-\Delta\tau), \quad (3.35)$$

Diagram (d): The integration of diagram (d) does not require the split of the integration as discussed in the Minkowski case, the result is

$$A_{\text{amp, scalar}}^{(d)} = i\lambda a^4(\tau_1) \int \frac{d^3 p}{(2\pi)^3} F_\sigma(p, \tau_1, \tau_1) \quad (3.36)$$

$$= -\frac{i\lambda}{8\pi^2} a_1^2 \left(p_{UV}^2 - \frac{p_c^2}{3} - p_c^2 \ln \frac{p_{UV}}{p_c} \right). \quad (3.37)$$

We presented the same calculations both in the Minkowski spacetime and in de Sitter for the corrections to the inflaton propagator due to the interaction with a massive scalar field. We expect,

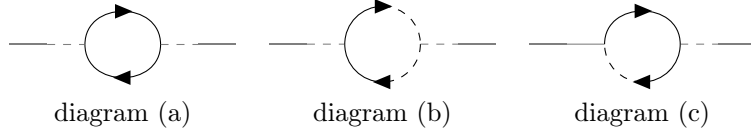


Figure 3.3: one-loop Feynman corrections to the inflaton two-point function due to the interaction with a massive scalar field.

from the results obtained in algebraic QFT, that the ultraviolet divergences are of the same order and the type and number of counterterms are the same in both spacetimes [6]. Diagram (d) shows this property clearly, we see that in both cases we have the a quadratic and logarithmic dependences on the cutoff Λ .

To understand the UV behavior of the amputated amplitude ($c + c'$), we need some further manipulations, we will present them in section 3.3 after the study of the fermionic contributions. In order to extract the singular behavior we will study the previous expressions in the language of distribution, and we will find that these divergences multiply a Dirac delta function $\delta(\Delta\tau)$, following the computation performed in [7, 52].

Note that in the de Sitter calculation when splitting the integral in small and large momentum we are keeping the next to leading order of approximation in p . This allowed us to capture the divergences more accurately. The leading order terms are easily seen, since they are in form similar to the result in Minkowski, where we kept only the leading order terms. For instance for the diagram (c), in de Sitter the first term in equation (3.34) corresponds to the second term in equation (3.21), i.e. Minkowski term.

3.2.2 One-loop corrections from a massive fermion

The discussion related to the corrections coming from the inflaton interaction with a massive fermion through an Yukawa interaction is very similar to the one we gave in the previous section. We have to keep in mind the differences from the scalar case: the factor (-1) coming from each fermionic loop and the product of the propagators in the loop is traced over [41]. The one-loop contributions to the two-point function are listed in figure 3.3; their mirror diagrams should be considered as before.

We stress again that in this section we are interested in the UV behavior and therefore we will focus on the amputated part of the diagrams.

Minkowski background

The amputated amplitude for diagram (a), neglecting the external momentum, i.e. $|\mathbf{k} + \mathbf{p}| \approx |\mathbf{p}| \equiv p$, is

$$A_{\text{amp}}^{(a)} = -\frac{V_1 V_2}{2} \int \frac{d^3 p}{(2\pi)^3} \text{Tr}[F_\psi(k + p, \tau_1, \tau_2) F_\psi(p, \tau_2, \tau_1)], \quad (3.38)$$

where the vertices are $V_1 = V_2 = -iY$, the symmetry factor is $1/2$ and we kept the same labels convention as in the previous section.

Diagram (a): Proceeding to split the integral into small and large momentum parts and using Λ has regulator we compute the integral in equation (3.38)

$$A_{\text{amp, fermion}}^{(a)} = + \frac{Y^2}{48\pi^2} \left(4M_f^3 + 6M_f \frac{\cos(2M_f\Delta\tau)}{\Delta\tau^2} - 6\Lambda \frac{\cos(2\Lambda\Delta\tau)}{\Delta\tau^3} - 3 \frac{\sin(2M_f\Delta\tau)}{\Delta\tau^3} \right. \\ \left. + 3 \frac{\sin(2\Lambda\Delta\tau)}{\Delta\tau^3} + 6M_f^2 \frac{\sin(2M_f\Delta\tau)}{\Delta\tau} - 6\Lambda^2 \frac{\sin(2\Lambda\Delta\tau)}{\Delta\tau} \right), \quad (3.39)$$

reminding that we defined $\Delta\tau = \tau_1 - \tau_2$.

Diagram (b) and (b'): Similarly to the scalar case we compute the contribution of diagram (b) and its mirrored version

$$A_{\text{amp, fermion}}^{(b)} = + \frac{Y^2}{48\pi^2} \theta(-\Delta\tau) \left(4M_f^3 + 6M_f \frac{\cos(2M_f\Delta\tau)}{\Delta\tau^2} - 6\Lambda \frac{\cos(2\Lambda\Delta\tau)}{\Delta\tau^3} - 3 \frac{\sin(2M_f\Delta\tau)}{\Delta\tau^3} \right. \\ \left. + 3 \frac{\sin(2\Lambda\Delta\tau)}{\Delta\tau^3} + 6M_f^2 \frac{\sin(2M_f\Delta\tau)}{\Delta\tau} - 6\Lambda^2 \frac{\sin(2\Lambda\Delta\tau)}{\Delta\tau} \right), \quad (3.40)$$

and

$$A_{\text{amp, fermion}}^{(b')}(\Delta\tau) = A_{\text{amp, fermion}}^{(b)}(-\Delta\tau), \quad (3.41)$$

Diagram (a + b + b'): We note that again the non-local divergence cancel when summing the three contributions

$$A_{\text{amp, fermion}}^{(a+b+b')} = + \frac{Y^2}{8\pi^2\Delta\tau^3} \left(2M_f\Delta\tau \sin(2M_f\Delta\tau) - 2\Lambda\Delta\tau \cos(2\Lambda\Delta\tau) \right. \\ \left. - (1 - 2M_f^2\Delta\tau^2) \sin(2M_f\Delta\tau) + (1 - 2\Lambda^2\Delta\tau^2) \sin(2\Lambda\Delta\tau) \right). \quad (3.42)$$

Diagram (c) and (c'): The result of the integration for diagram (c) and (c') is

$$A_{\text{amp, fermion}}^{(c)} = - \frac{iY}{4\pi^2\Delta\tau^3} \theta(-\Delta\tau) \left((1 - 2\Lambda^2\Delta\tau^2) \cos(2\Lambda\Delta\tau) - (1 - 2M_f^2\Delta\tau^2) \cos(2M_f\Delta\tau) \right. \\ \left. - 2\Delta\tau (M_f \sin(2M_f\Delta\tau) - \Lambda \sin(2\Lambda\Delta\tau)) \right) \quad (3.43)$$

and

$$A_{\text{amp, fermion}}^{(c')}(\Delta\tau) = A_{\text{amp, fermion}}^{(c)}(-\Delta\tau), \quad (3.44)$$

De Sitter background

We proceed to calculate the one-loop correction to the two-point function with the same method described in the previous sections, keeping in mind the peculiarities of working in de Sitter space-time. The WKB mode function in small and large momentum limits are

$$\eta_\sigma(p < p_c, \tau) \approx \exp\left(i \frac{M_f}{H} \log \frac{\tau}{\tau_i}\right), \quad (3.45)$$

$$\eta_\sigma(p > p_c, \tau) \approx \frac{1}{\sqrt{2}} \exp\left(-ip(\tau - \tau_i)\right), \quad (3.46)$$

$$\chi_\sigma(p < p_c, \tau) \approx 0, \quad (3.47)$$

$$\chi_\sigma(p > p_c, \tau) \approx \frac{1}{\sqrt{2}} \exp\left(-ip(\tau - \tau_i)\right), \quad (3.48)$$

from which we build the propagators using equations (2.111), (2.112), (2.113), (2.114) and (2.71).

Diagram (a + b + b'): The sum of the corrections coming from diagram (a), (b) and (b') is finite as expected from the result in the Minkowski background

$$\begin{aligned}
A_{\text{amp, fermion}}^{(a+b+b')} = & + \frac{Y^2}{8\pi^2} a_1 a_2 \left(2p_c^2 \frac{\sin[2p_c \Delta\tau]}{\Delta\tau} - 2p_{UV}^2 \frac{\sin[2p_{UV} \Delta\tau]}{\Delta\tau} \right. \\
& + 2p_c \frac{\cos[2p_c \Delta\tau]}{\Delta\tau^2} - 2p_{UV} \frac{\cos[2p_{UV} \Delta\tau]}{\Delta\tau^2} - \frac{\sin[2p_c \Delta\tau]}{\Delta\tau^3} + \frac{\sin[2p_{UV} \Delta\tau]}{\Delta\tau^3} \left. \right) \\
& + \frac{Y^2}{4\pi^2 H^2 \tau_1 \tau_2} a_1 a_2 \frac{p_c^2}{a_\beta^2} \left(p_c \cos[2p_c \Delta\tau] - p_{UV} \cos[2p_{UV} \Delta\tau] \right) \\
& - \frac{Y^2}{8\pi^2} a_1 a_2 \frac{p_c^2}{a_\beta^2} \left(a_1^2 + a_2^2 + \frac{1}{H^2 \tau_1 \tau_2} \right) \left(\frac{\sin[2p_c \Delta\tau]}{\Delta\tau} - \frac{\sin[2p_{UV} \Delta\tau]}{\Delta\tau} \right) \quad (3.49)
\end{aligned}$$

Diagram (c) and (c'): The results of the integrations of diagram (c) and (c') are

$$\begin{aligned}
A_{\text{amp, fermion}}^{(c')} = & - iY^2 \int \frac{d^3 p}{(2\pi)^3} \text{Tr} [F_\psi(p, \tau_1, \tau_2) G_\psi^R(p, \tau_2, \tau_1)] \quad (3.50) \\
= & - \frac{iY^2}{4\pi^2} a_1 a_2 \theta(\Delta\tau) \left(2p_c^2 \frac{\cos[2p_c \Delta\tau]}{\Delta\tau} - 2p_{UV}^2 \frac{\cos[2p_{UV} \Delta\tau]}{\Delta\tau} \right. \\
& - 2p_c \frac{\sin[2p_c \Delta\tau]}{\Delta\tau^2} + 2p_{UV} \frac{\sin[2p_{UV} \Delta\tau]}{\Delta\tau^2} - \frac{\cos[2p_c \Delta\tau]}{\Delta\tau^3} + \frac{\cos[2p_{UV} \Delta\tau]}{\Delta\tau^3} \left. \right) \\
& - \frac{iY^2}{2\pi^2 H^2 \tau_1 \tau_2} a_1 a_2 \frac{p_c^2}{a_\beta^2} \theta(\Delta\tau) \left(p_c \sin[2p_c \Delta\tau] - p_{UV} \sin[2p_{UV} \Delta\tau] \right) \\
& - \frac{iY^2}{4\pi^2} a_1 a_2 \frac{p_c^2}{a_\beta^2} \theta(\Delta\tau) \left(a_1^2 + a_2^2 + \frac{1}{H^2 \tau_1 \tau_2} \right) \left(\frac{\cos[2p_c \Delta\tau]}{\Delta\tau} - \frac{\cos[2p_{UV} \Delta\tau]}{\Delta\tau} \right), \quad (3.51)
\end{aligned}$$

and

$$A_{\text{amp, fermion}}^{(c')}(\Delta\tau) = A_{\text{amp, scalar}}^{(c)}(-\Delta\tau). \quad (3.52)$$

We presented the computation of the one-loop corrections to the two-point inflaton function due to the interaction with a massive fermion field in the Minkowski and de Sitter spacetime. Similarly to the scalar case, the non-local divergences in the diagrams (a), (b) and (b') cancel each other leaving with a finite amplitude. To understand the UV behavior of the fermionic corrections we will need to study the contributions coming from diagrams (c) and (c').

3.2.3 Numerical calculation

In this section we proceed to perform the full computation numerically and compare with the approximated analytical results of the amputated amplitudes for both scalar and fermion contributions. We concentrate on diagrams (c) and (d), as they are the ones containing UV divergences, as we will show in the next sections. We first check the integrands of the amputated amplitudes, that consist of propagators and vertices. Performing the numerical analysis we also neglect the external momenta in the same approximation discussed in the last sections.

In figure 3.4 we have the comparison between the analytical and numerical results for diagram (c). The integrand is expressed in equation (3.33) for the bosonic and (3.50) for the fermionic case. The red line is the analytical expression obtained using the propagators constructed from the WKB approximated mode functions in equations (2.137) and (2.138) as explained in chapter 2. The black cross points are the numerical computations where the propagators are constructed from the *full*

mode functions in equations (2.99), scalar, (2.128) and (2.129), fermion. Figure 3.4 shows that the analytical results well describe the numerical computation. This can be considered a further check of the consistency of describing the massive propagators with a WKB approximation as discussed in chapter 2.

We then performed the momentum integration in equations (3.33) and (3.50) numerically and compared with the analytical result given respectively by equation (3.34) and (3.51). Using the same convention of above in figure 3.4 we show the agreement of the two calculations. This result can be considered as a check of the goodness of the approximation given in equation (3.30) where we described the splitting of the momentum integration.

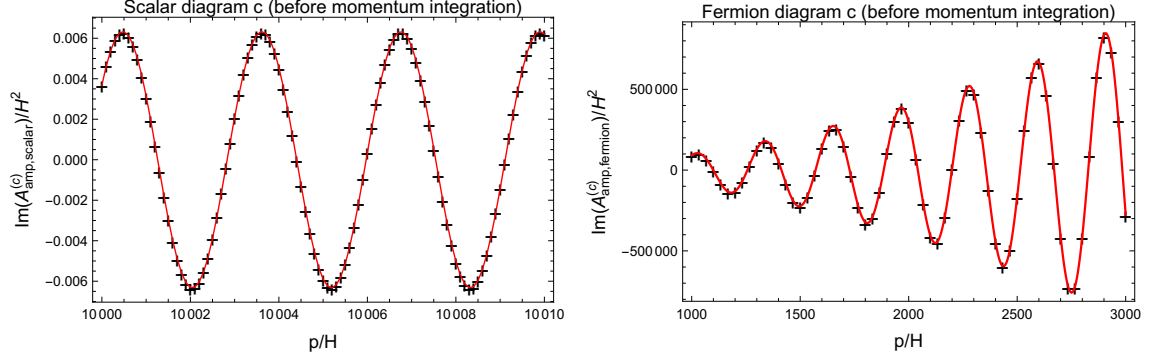


Figure 3.4: Amputated amplitudes before the momentum integration for the diagram (c) as a function of the momentum. Both the contributions from the massive scalar and fermion fields are calculated and shown on the left and the right panel, respectively. The solid red line is the analytical estimate and the black cross (+) points are the numerical computation. For the scalar case, we chose $\tau_1 = -2/H$, $\tau_2 = -1/H$, $M_s = 10H$, and $\mu = H$. For the fermion case, we chose $\tau_1 = -1.01/H$, $\tau_2 = -1/H$, $M_f = 10H$, and $Y = H$. Note that the exact values of μ and Y are irrelevant as they are an overall factor.

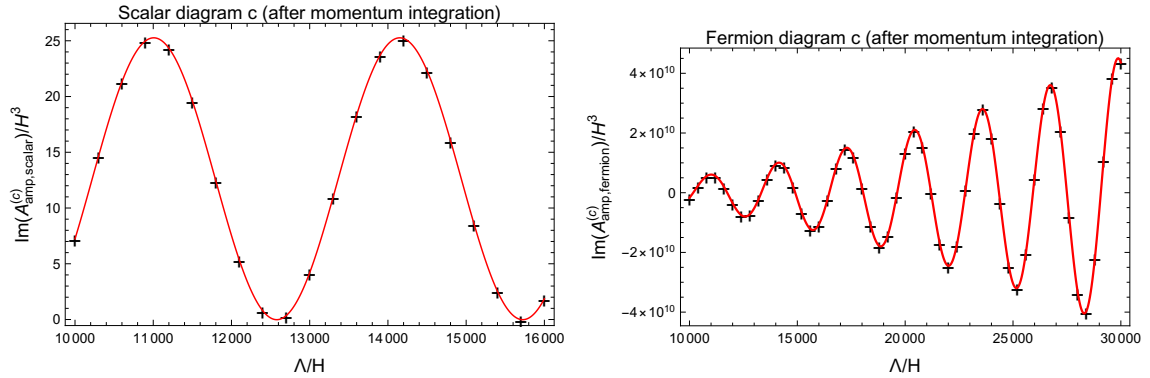


Figure 3.5: Amputated amplitudes after the momentum integration for the diagram (c) as a function of the momentum cutoff Λ . Both the contributions from the massive scalar and fermion fields are calculated and shown on the left and the right panel, respectively. The solid red line is the analytical estimate and the black cross (+) points are the numerical computation. For both scalar and fermion cases we chose $\tau_1 = -1.001/H$, $\tau_2 = -1/H$, $M_s = 10H$, $M_f = 10H$, $Y = H$, and $\mu = H$. Note that the exact values of μ and Y are irrelevant as they are an overall factor.

The same analysis was done for diagram (d) where in figure 3.6 we have on the left the comparison for the integrand in equation (3.36). In the analytical computation the propagator is build

from the WKB approximated mode function (2.136) while in the numerical computation from the complete one (2.99). We then performed the integral in equation (3.36) numerically. Figure 3.6, on the right, shows the comparison with the analytical result in equation (3.37).

We can conclude that in both diagrams the WKB approximation and the split of the momentum integrations are good approximations of the *full* result.

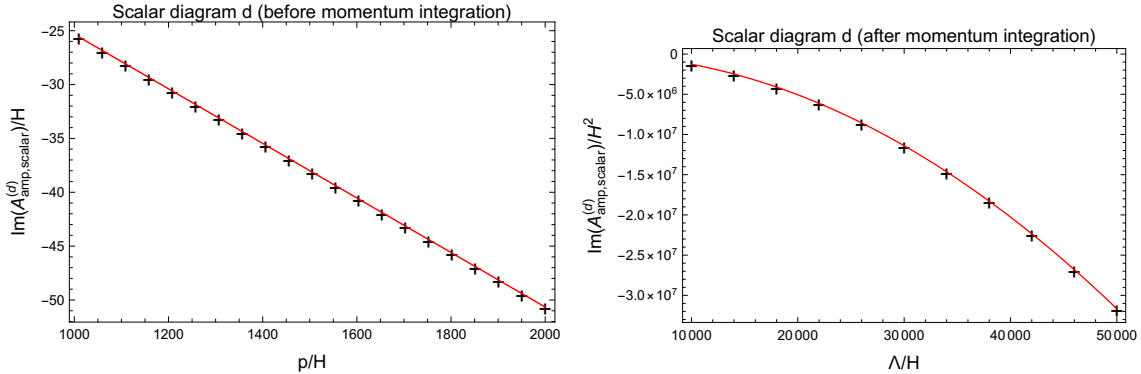


Figure 3.6: *Left panel:* Amputated amplitudes before the momentum integration for the diagram (d) as a function of the momentum. *Right panel:* Amputated amplitudes after the momentum integration for the diagram (d) as a function of the momentum cutoff Λ . The solid red line is the analytical estimate and the black cross (+) points are the numerical computation. We chose $\tau_1 = -1/H$, $M_s = 10H$, and $\lambda = 1$. Note that the exact value of λ is irrelevant as it is an overall factor. As is expected, we observe the quadratic divergence in diagram (d). See text for more details.

3.3 Ultraviolet Behavior

The main objective of this chapter is to understand the ultraviolet behavior of the one-loop correction to the two-point function of the inflaton. In the previous sections we explicitly calculated the amplitudes but we understood the need for further manipulations to extract their UV dependence on the cutoff. The idea is that the divergence is to be found in the part of the amplitude where the two times τ_1 and τ_2 coincide so we should search for a way to re-express the amplitude factorizing the equal time contribution.

These divergent terms are proportional to $\delta(\Delta\tau)$ and are the usual local divergences that can be canceled by counterterms. As we can see explicitly from the scalar result of diagram (a), (3.17), and (b), (3.18), non-local divergences can also be present but they will cancel summing the contribution coming from different diagrams. In our case the linear divergence in diagram (a) cancels the one in diagram (b). The presence of these divergences is due to the split in multiple contributions (diagrams) of the total corrections. The non-local divergences always cancel between each other.

Following [52] let us consider as an example the term present in diagram (c) for the scalar case, equation (3.34)

$$\theta(\Delta\tau) \frac{\cos[2p_{UV}\Delta\tau]}{\Delta\tau} \quad (3.53)$$

it turns out that this term is logarithmically divergent as $\Lambda \rightarrow \infty$. In order to see this consider the integral

$$\int_{-\infty}^{\infty} d\Delta\tau f(\Delta\tau) \theta(\Delta\tau) \frac{\cos[2p_{UV}\Delta\tau]}{\Delta\tau} = \int_0^{\infty} d\Delta\tau f(\Delta\tau) \frac{\cos[2p_{UV}\Delta\tau]}{\Delta\tau}, \quad (3.54)$$

where $f(\Delta\tau)$ is a test function. The integral in equation (3.54) is the prototype of the time integration of an amputated amplitude containing the term in equation (3.53), extended to $\pm\infty$, that we will perform after attaching the external legs.

We first split the time integration into two pieces,

$$\int_0^\infty d\Delta\tau = \lim_{\epsilon \rightarrow 0} \int_\epsilon^\eta d\Delta\tau + \int_\eta^\infty d\Delta\tau, \quad (3.55)$$

where η is the time regulator which will be sent to zero at the end of the calculation, after sending $\Lambda \rightarrow \infty$. In the first integral we can approximate

$$f(\Delta t) \approx f(0) \quad \& \quad \frac{\Delta\tau}{\tau_1 - \Delta\tau} \approx \frac{\Delta\tau}{t_1}, \quad (3.56)$$

and we remind $p_{UV} = \Lambda a(\tau_\beta) - \Lambda/H\tau_\beta$ and τ_β is the earliest time occurring in the loop, for instance for the diagram (c'): $\beta = 2$, for the diagram (c): $\beta = 1$. Thus we have,

$$\begin{aligned} \int_0^\infty d\Delta\tau f(\Delta\tau) \frac{\cos[2p_{UV}\Delta\tau]}{\Delta\tau} \\ = \lim_{\epsilon \rightarrow 0} \int_\epsilon^\eta d\Delta\tau f(0) \frac{1}{\Delta\tau} \cos\left[-\frac{2\Lambda\Delta\tau}{H\tau_1}\right] + \int_\eta^\infty d\Delta\tau f(\Delta\tau) \frac{1}{\Delta\tau} \cos\left[-\frac{2\Lambda\Delta\tau}{H\tau_1}\right], \end{aligned} \quad (3.57)$$

where we used $\tau_\beta = \tau_1$. The first term gives

$$\begin{aligned} \int_\epsilon^\eta d\Delta\tau f(0) \frac{1}{\Delta\tau} \cos\left[-\frac{2\Lambda\Delta\tau}{H\tau_1}\right] &= -f(0) \left[\gamma + \ln\left(-\frac{2\Lambda}{H\tau_1}\epsilon\right) \right] \\ &= -\int_{-\infty}^\infty d\Delta\tau f(\Delta\tau) \left[\gamma + \ln\left(-\frac{2\Lambda}{H\tau_1}\epsilon\right) \right] \delta(\Delta\tau), \end{aligned} \quad (3.58)$$

where the limit $\epsilon \rightarrow 0$ is to be understood and the second term vanishes, provided that $f(\Delta\tau)$ is a good test function, meaning it vanishes fast enough as $\Delta\tau \rightarrow \infty$. Therefore, we obtain

$$\theta(\Delta\tau) \frac{\cos[2p_{UV}\Delta\tau]}{\Delta\tau} = -\left[\gamma + \ln\left(-\frac{2\Lambda}{H\tau_1}\epsilon\right) \right] \delta(\Delta\tau) \quad (3.59)$$

where γ is the Euler-Mascheroni constant.

Similarly let us consider

$$\theta(\Delta\tau) \frac{\cos[2p_c\Delta\tau]}{\Delta\tau} \quad (3.60)$$

We proceed in a similar way and we have the integral

$$\begin{aligned} \int_{-\infty}^\infty d\Delta\tau f(\Delta\tau) \theta(\Delta\tau) \frac{\cos[2p_c\Delta\tau]}{\Delta\tau} &= \int_0^\infty d\Delta\tau f(\Delta\tau) \frac{\cos[2p_c\Delta\tau]}{\Delta\tau} \\ &= \int_\epsilon^\eta d\Delta\tau f(0) \frac{1}{\Delta\tau} \cos\left[-\frac{2M_s\Delta\tau}{H\tau_1}\right] + \int_\eta^\infty d\Delta\tau f(\Delta\tau) \frac{1}{\Delta\tau} \cos\left[-\frac{2M_s\Delta\tau}{H\tau_2}\right] \\ &= \int_{-\infty}^\infty d\Delta\tau f(\Delta\tau) \left(\delta(\Delta\tau) \ln\frac{\eta}{\epsilon} + \theta(\Delta\tau - \eta) \frac{1}{\Delta\tau} \cos\left[-\frac{2M_s}{H\tau_2}\Delta\tau\right] \right). \end{aligned} \quad (3.61)$$

Therefore, from equation (3.59) and equation (3.61), we find

$$\begin{aligned} \theta(\Delta\tau) \left(\frac{\cos[2p_c\Delta\tau]}{\Delta\tau} - \frac{\cos[2p_{UV}\Delta\tau]}{\Delta\tau} \right) \\ = \delta(\Delta\tau) \left[\gamma + \ln\left(-\frac{2\Lambda}{H\tau_1}\eta\right) \right] + \theta(\Delta\tau - \eta) \frac{1}{\Delta\tau} \cos\left[-\frac{2M_s}{H\tau_2}\Delta\tau\right] \end{aligned} \quad (3.62)$$

The same reasoning is applied to the similar terms we found in the amputated amplitudes previously computed, e.g. $\theta(\Delta\tau)f(\Delta\tau)\sin[2p_{UV}]/\Delta\tau^n$, where n is some exponent power. Repeating the same procedure for all the terms in the amputated amplitudes, we obtain similar expression used to derive equations (3.63), (3.64), (3.65), and (3.66).

3.3.1 Numerical calculation

From the previous discussion we understand that numerically the ultraviolet divergences become visible after performing a time integration. For instance the $\delta(\tau_1 - \tau_2)$ term in the amplitude of diagram (c) is used upon the first time integration and it is possible to appreciate the divergence behavior as function of Λ ; in this case we see the logarithmic dependence (see e.g., equation (3.59)). In the case of diagram (d), on the other hand, we have only one vertex and thus the UV behaviour is manifest and there is no need for the time integration to see the Λ dependence.

We shall present only the numerical results of diagrams that contain a divergence. In figure 3.7, we performed τ_2 -integration in an interval $(\tau_{in}, \tau_1 - \delta)$ where we chose τ_{in} close to τ_1 since the aim was only to check the UV behaviour predicted by the analytical computation for diagram (c). The black cross (+) points are the results of the full numerical computation and the red line the analytical expression.

As we expected from the analytical results, equations (3.64) and (3.66), we see a logarithmic divergence for the scalar contribution and a quadratic divergence for the fermion contribution. In the fermion diagram (c), the logarithmic divergence is expected to be present. But in order

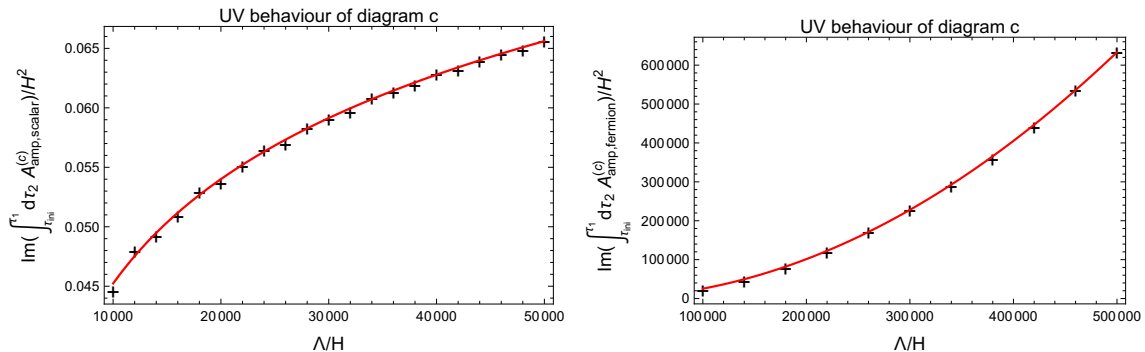


Figure 3.7: Amputated amplitudes for the scalar (left) and fermion (right) contributions after performing the τ_1 integration near τ_2 . The full numerical computation is depicted by black cross (+) points. The solid red line represents the analytical expression. In the left panel, we observe the logarithmic divergence as we expected from the analytical expression. In the right panel, we see the quadratic divergence. In order to see the logarithmic divergence, we need to subtract the quadratic divergence. See text for more details. We chose $M_s = 10H$ and $M_f = 5H$.

to see it, we need to subtract the quadratic divergence. Unfortunately, however, it is difficult to numerically subtract the quadratic divergence by using the analytical expression because of the numerical errors; due to the quadratic nature, a small difference in the coefficient makes a huge difference for the quadratic term.

Therefore we took the following approach. Since we confirmed that the quadratic divergence is in good agreement with our analytical expression, we fitted the full numerical results by fixing the coefficient of the quadratic term. We then subtracted the quadratic term from both the numerical results and the analytical expression. The comparison between the final results are shown in figure 3.8. We followed the same procedure for the diagram (d). In figure 3.6 we already saw the quadratic divergence. The logarithmic divergence is seen after subtracting the quadratic divergence as shown in figure 3.8.

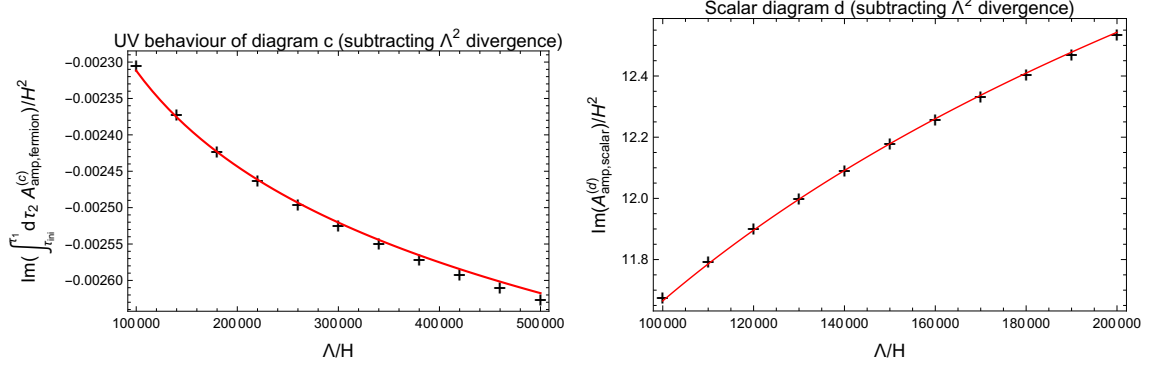


Figure 3.8: *Left panel:* Amputated amplitude of the fermion diagram c with the Λ^2 divergence subtracted. *Right panel:* Amputated amplitude of the scalar diagram d with the Λ^2 divergence subtracted. The solid red line is the analytical estimate and the black cross (+) points are the numerical computations. Subtracting the quadratic divergence we see the expected logarithmic divergence.

In this section and in section 3.2.3 we performed the numerical calculations without resorting to the adiabatic expansion approximation. We computed propagators, amputated amplitudes and UV behaviours fully numerically and compared with the analytical expressions. It shows that the use of the WKB approximation is perfectly sufficient to reproduce the behaviour of the exact numerical amplitude, both regarding the leading and sub-leading UV behaviour.

3.4 Analytical Results

In the previous sections we introduced the tools to understand the ultraviolet divergent behavior of the amplitudes and we anticipated, through the numerical computation, the type of divergences we expect. In this section we will present the complete analytical results of the calculation of the amputated amplitudes and we will then concentrate on the UV behavior studying the relevant terms. We will compare it with the singular part of the amplitudes having Minkowski as background spacetime. Finally we will discuss the implication of the result in de Sitter spacetime.

Starting from the results in (3.32) and (3.34) and applying the formalism developed in section 3.3 we obtain the amputated amplitudes for the scalar contributions to the inflaton two-point function

$$\begin{aligned}
A_{\text{scalar}}^{(a+b+b')} &= -\frac{\mu^2}{32\pi H^4 \tau_1^4} \delta(\tau_1 - \tau_2) \\
&+ \frac{\mu^2}{16\pi^2 H^4 \tau_1^2 \tau_2^2 (\tau_1 - \tau_2)} \sin\left(-\frac{2M_s}{H\tau_2}(\tau_1 - \tau_2)\right) \theta(\tau_1 - \tau_2 - \eta) \\
&- \frac{\mu^2 M_s (\tau_1^2 + \tau_2^2)}{16\pi^2 H^5 \tau_1^4 \tau_2^3} \cos\left(-\frac{2M_s}{H\tau_2}(\tau_1 - \tau_2)\right) \theta(\tau_1 - \tau_2) \\
&+ \frac{\mu^2 M_s^2 (\tau_1^2 + \tau_2^2) (\tau_1 - \tau_2)}{8\pi^2 H^6 \tau_1^4 \tau_2^4} \left[\text{Si}\left(-\frac{2M_s}{H\tau_2}(\tau_1 - \tau_2)\right) - \frac{\pi}{2} \right] \theta(\tau_1 - \tau_2) \\
&- \frac{\mu^2 M_s^2 (\tau_1 - \tau_2)}{8\pi^2 H^6 \tau_1^3 \tau_2^3} \left[\text{Si}\left(-\frac{2M_s}{H\tau_2}(\tau_1 - \tau_2)\right) - \frac{\pi}{2} \right] \theta(\tau_1 - \tau_2) \\
&+ \frac{\mu^2 M_s}{24\pi^2 H^5 \tau_1 \tau_2^4} \cos\left(\frac{2M_s}{H} \ln \frac{\tau_1}{\tau_2}\right) \theta(\tau_1 - \tau_2), \tag{3.63}
\end{aligned}$$

and

$$\begin{aligned}
A_{\text{scalar}}^{(c+c'+d+d')} = & + \frac{i\mu^2}{4\pi^2 H^4 \tau_1^4} \left[\gamma + \ln \frac{\Lambda}{M_s} + \ln \left(-\frac{2M_s}{H\tau_1} \eta \right) \right] \delta(\tau_1 - \tau_2) \\
& - \frac{i\lambda}{4\pi^2 H^4 \tau_1^4} \left[\Lambda^2 - \frac{M_s^2}{3} - M_s^2 \ln \frac{\Lambda}{M_s} \right] \delta(\tau_1 - \tau_2) \\
& + \frac{i\mu^2}{4\pi^2 H^4 \tau_1^2 \tau_2^2 (\tau_1 - \tau_2)} \cos \left(-\frac{2M_s}{H\tau_2} (\tau_1 - \tau_2) \right) \theta(\tau_1 - \tau_2 - \eta) \\
& + \frac{i\mu^2 M_s (\tau_1^2 + \tau_2^2)}{4\pi^2 H^5 \tau_1^4 \tau_2^3} \sin \left(-\frac{2M_s}{H\tau_2} (\tau_1 - \tau_2) \right) \theta(\tau_1 - \tau_2) \\
& + \frac{i\mu^2 M_s^2 (\tau_1^2 + \tau_2^2) (\tau_1 - \tau_2)}{2\pi^2 H^6 \tau_1^4 \tau_2^4} \text{Ci} \left(-\frac{2M_s}{H\tau_2} (\tau_1 - \tau_2) \right) \theta(\tau_1 - \tau_2) \\
& - \frac{i\mu^2 M_s^2 (\tau_1 - \tau_2)}{2\pi^2 H^6 \tau_1^3 \tau_2^3} \text{Ci} \left(-\frac{2M_s}{H\tau_2} (\tau_1 - \tau_2) \right) \theta(\tau_1 - \tau_2) \\
& - \frac{i\mu^2 M_s}{6\pi^2 H^5 \tau_1 \tau_2^4} \sin \left(\frac{2M_s}{H} \ln \frac{\tau_2}{\tau_1} \right) \theta(\tau_1 - \tau_2), \tag{3.64}
\end{aligned}$$

where Ci and Si are the sine and cosine integral functions. We separated the finite contributions of diagrams $(a + b + b')$ and the divergent one coming from the diagrams $(c + c' + d + d')$.

In a similar fashion from the results in equations (3.49) and (3.51) we single-out the fermionic divergent contribution in the amputated amplitudes coming from diagram $(c + c')$ and we show, once again, that the sum of diagrams $(a + b + b')$ do not present divergences.

$$\begin{aligned}
A_{\text{fermion}}^{(a+b+b')} = & + \frac{3Y^2 M_f^2}{8\pi H^4 \tau_1^4} \delta(\tau_1 - \tau_2) \\
& + \frac{Y^2 M_f^2}{2\pi^2 H^4 \tau_1 \tau_2^3 (\tau_1 - \tau_2)} \sin \left(-\frac{2M_f}{H\tau_2} (\tau_1 - \tau_2) \right) \theta(\tau_1 - \tau_2 - \eta) \\
& - \frac{Y^2 M_f}{2\pi^2 H^3 \tau_1 \tau_2^2 (\tau_1 - \tau_2)^2} \cos \left(-\frac{2M_f}{H\tau_2} (\tau_1 - \tau_2) \right) \theta(\tau_1 - \tau_2 - \eta) \\
& - \frac{Y^2}{4\pi^2 H^2 \tau_1 \tau_2 (\tau_1 - \tau_2)^3} \sin \left(-\frac{2M_f}{H\tau_2} (\tau_1 - \tau_2) \right) \theta(\tau_1 - \tau_2 - \eta) \\
& - \frac{Y^2 M_f^2 (\tau_1^2 + \tau_2^2)}{4\pi^2 H^4 \tau_1^3 \tau_2^3 (\tau_1 - \tau_2)} \sin \left(-\frac{2M_f}{H\tau_2} (\tau_1 - \tau_2) \right) \theta(\tau_1 - \tau_2 - \eta) \\
& - \frac{Y^2 M_f^2}{4\pi^2 H^4 \tau_1^2 \tau_2^2 (\tau_1 - \tau_2)} \sin \left(-\frac{2M_f}{H\tau_2} (\tau_1 - \tau_2) \right) \theta(\tau_1 - \tau_2 - \eta) \\
& - \frac{Y^2 M_f^3}{2\pi^2 H^5 \tau_1^2 \tau_2^3} \cos \left(-\frac{2M_f}{H\tau_2} (\tau_1 - \tau_2) \right) \theta(\tau_1 - \tau_2), \tag{3.65}
\end{aligned}$$

and

$$\begin{aligned}
A_{\text{fermion}}^{(c+c')} = & + \frac{iY^2}{2\pi^2 H^4 \tau_1^4} \left[\Lambda^2 - 3\gamma M_f^2 - 3M_f^2 \ln \frac{\Lambda}{M_f} - 3M_f^2 \ln \left(-\frac{2M_f}{H\tau_1} \eta \right) \right] \delta(\tau_1 - \tau_2) \\
& - \frac{iY^2 M_f^2 (\tau_1^2 + \tau_2^2)}{2\pi^2 H^4 \tau_1^3 \tau_2^3 (\tau_1 - \tau_2)} \cos \left(-\frac{2M_f}{H\tau_2} (\tau_1 - \tau_2) \right) \theta(\tau_1 - \tau_2 - \eta) \\
& - \frac{iY^2 M_f^2}{2\pi^2 H^4 \tau_1^2 \tau_2^2 (\tau_1 - \tau_2)} \cos \left(-\frac{2M_f}{H\tau_2} (\tau_1 - \tau_2) \right) \theta(\tau_1 - \tau_2 - \eta) \\
& + \frac{iY^2 M_f^3}{\pi^2 H^5 \tau_1^2 \tau_2^3} \sin \left(-\frac{2M_f}{H\tau_2} (\tau_1 - \tau_2) \right) \theta(\tau_1 - \tau_2) \\
& + \frac{iY^2}{4\pi^2 H^2 \tau_1^2 \eta^2} \delta(\tau_1 - \tau_2) \\
& + \frac{iY^2 M_f^2}{\pi^2 H^4 \tau_1 \tau_2^3 (\tau_1 - \tau_2)} \cos \left(-\frac{2M_f}{H\tau_2} (\tau_1 - \tau_2) \right) \theta(\tau_1 - \tau_2 - \eta) \\
& + \frac{iY^2 M_f}{\pi^2 H^3 \tau_1 \tau_2^2 (\tau_1 - \tau_2)^2} \sin \left(-\frac{2M_f}{H\tau_2} (\tau_1 - \tau_2) \right) \theta(\tau_1 - \tau_2 - \eta) \\
& - \frac{iY^2}{2\pi^2 H^2 \tau_1 \tau_2 (\tau_1 - \tau_2)^3} \cos \left(-\frac{2M_f}{H\tau_2} (\tau_1 - \tau_2) \right) \theta(\tau_1 - \tau_2 - \eta). \tag{3.66}
\end{aligned}$$

Note that $M_s/H \gg 1$ and $M_f/H \gg 1$, and thus the sinusoidal terms are sub-dominant. Moreover, in context of the derivation of section 3.3, as long as the test function $f(\Delta\tau)$ vanishes fast enough for large $\Delta\tau$, the cosine term can further be approximated as

$$\frac{1}{\Delta\tau} \cos \left[-\frac{2M_s}{H\tau_2} \Delta\tau \right] \approx \frac{1}{\Delta\tau}. \tag{3.67}$$

We stress that the terms dependent on η need to be treated carefully. In fact only after the integration over τ_2 we can send $\eta \rightarrow 0$. Using the above approximation the limit $\eta \rightarrow 0$ leads to a final amplitude η -independent. The dominant terms are then given below in equations (3.69) and (3.70).

As we anticipated previously the amplitude of fermion and scalar ($a + b + b'$) diagrams are finite. Note that the separation of the diagrams into two groups ($a + b + b'$) and ($c + c' + d + d'$) is natural. In fact the former group has the retarded propagator G_φ^R in both external legs while the latter has the Hadamard F_φ and the retarded G_φ^R propagators, as shown in figures 3.2 and 3.3. Therefore collecting the amplitudes in these two groups based on their external legs, that we call A_{GG} and A_{GF} , the total one-loop amplitude is

$$\begin{aligned}
A^{1\text{-loop}}(k) = & \int_{\tau_i}^\tau d\tau_1 \int_{\tau_i}^\tau d\tau_2 [-iG_\varphi^R(k, \tau, \tau_1)] [-iG_\varphi^R(k, \tau, \tau_2)] A_{GG} \\
& + \int_{\tau_i}^\tau d\tau_1 \int_{\tau_i}^\tau d\tau_2 [-iG_\varphi^R(k, \tau, \tau_1)] [F_\varphi(k, \tau, \tau_2)] A_{GF}, \tag{3.68}
\end{aligned}$$

where τ_i is the initial time and τ the horizon crossing time; the time integration will be discussed in the next chapter. Considering only the terms which dominantly contribute to the one-loop corrected amplitude we have

$$A_{GG} \approx -\frac{1}{8\pi H^4 \tau_1^4} \left(\frac{\mu^2}{4} - 3Y^2 M_f^2 \right) \delta(\tau_1 - \tau_2), \tag{3.69}$$

and

$$\begin{aligned}
A_{GF} \approx & + \frac{i}{2\pi^2 H^4 \tau_1^4} \left[\left(Y^2 - \frac{\lambda}{2} \right) \Lambda^2 + \frac{\mu^2 + \lambda M_s^2}{2} \ln \frac{\Lambda}{M_s} - 3Y^2 M_f^2 \ln \frac{\Lambda}{M_f} \right] \delta(\tau_1 - \tau_2) \\
& + \frac{i}{2\pi^2 H^4 \tau_1^4} \left(\frac{\gamma \mu^2}{2} + \frac{\lambda M_s^2}{6} - 3\gamma Y^2 M_f^2 \right) \delta(\tau_1 - \tau_2) \\
& + \frac{i\mu^2}{4\pi^2 H^4 \tau_1^4} \left[\ln \left(-\frac{2M_s}{H\tau_1} \eta \right) \delta(\tau_1 - \tau_2) + \frac{\tau_1^2}{\tau_2^2 (\tau_1 - \tau_2)} \theta(\tau_1 - \tau_2 - \eta) \right] \\
& - \frac{3iY^2 M_f^2}{2\pi^2 H^4 \tau_1^4} \left[\ln \left(-\frac{2M_f}{H\tau_1} \eta \right) \delta(\tau_1 - \tau_2) + \frac{(\tau_1^3 + \tau_1 \tau_2^2 + \tau_1^2 \tau_2)}{3\tau_2^3 (\tau_1 - \tau_2)} \theta(\tau_1 - \tau_2 - \eta) \right], \quad (3.70)
\end{aligned}$$

where Λ is the UV cutoff and η is the time-regulator which will be sent to zero after sending $\Lambda \rightarrow \infty$ (see section 3.3 for details on the role of η).

Note that the η dependence in the terms (3.63) and (3.65), that contribute to A_{GG} , is only through the step function and it does not appear together with the cut-off regulator Λ . Therefore after the integration over τ_2 we can safely send $\eta \rightarrow 0$. These are sub-leading terms and they do not contribute to the dominant part of the amplitude in equation (3.69).

Instead the third and the fourth lines of the dominant contribution to A_{GF} , (3.70), would contain the time regulator η together with Λ . We split the logarithm in two parts, isolating the η contribution

$$\ln \left(-\frac{2\Lambda}{H\tau} \eta \right) = \ln \left(\frac{\Lambda}{M} \right) + \ln \left(-\frac{2M}{H\tau} \eta \right). \quad (3.71)$$

After the integration over τ_2 , we may send $\eta \rightarrow 0$ and hence no dependence on η remains. Upon the first integration in τ_2 we also use the delta functional in the first two terms of A_{GF} .

The UV divergences of the one-loop amplitude are contained in A_{GF} and are

$$\boxed{A_{UV} = \frac{1}{2\pi^2 H^4 \tau_1^4} \left[\left(Y^2 - \frac{\lambda}{2} \right) \Lambda^2 + \left(\frac{\mu^2}{2} + \frac{\lambda M_s^2}{2} \right) \ln \frac{\Lambda}{M_s} - 3Y^2 M_f^2 \ln \frac{\Lambda}{M_f} \right]}. \quad (3.72)$$

As expected the scalar and the fermion contributions have the same dependence on the cutoff Λ but carry opposite sign. Hence let us consider a theory in which there are d_s scalar and d_f fermion degrees of freedom, which independently contribute to the one-loop diagrams. Then we may multiply our results by the corresponding degrees of freedom, resulting in the following UV structure

$$A_{UV} = \frac{1}{2\pi^2 H^4 \tau_1^4} \left[\left(Y^2 d_f - \frac{\lambda}{2} d_s \right) \Lambda^2 + d_s \left(\frac{\mu^2}{2} + \frac{\lambda M_s^2}{2} \right) \ln \frac{\Lambda}{M_s} - 3Y^2 M_f^2 d_f \ln \frac{\Lambda}{M_f} \right]. \quad (3.73)$$

As we will see in the next chapter, the supersymmetric hybrid inflation model we will consider contains one massive Dirac fermion, $d_f = 1$, and four massive real scalars, $d_s = 4$. Moreover we know that in the supersymmetric case the coefficients in the potential are not independent, they are related by $\lambda = Y^2/2$, obtained from the superpotential.

Therefore, $Y^2 d_f - \lambda d_s / 2 = 0$ and the quadratic divergence vanishes analytically. Furthermore, if the supersymmetry is unbroken, $M_s = M_f$, the logarithmic divergences also vanish. The important result is that at one-loop order the divergences cancel analytically and we do not need to require any renormalization if supersymmetry is unbroken. And if supersymmetry is broken, the resulting divergence is mild since the quadratic parts still cancel in this case and it depends on the fermion and scalar mass difference.

To conclude the chapter we show the UV divergence behavior in Minkowski. It confirms what we anticipated: the order of the UV divergences and the type and number of counterterm needed in a curved spacetime is the same as in the flat Minkowski spacetime

$$A_{UV,M} = \frac{1}{4\pi^2} \left[\left(Y^2 - \frac{\lambda}{2} \right) \Lambda^2 + \frac{1}{2} (\mu^2 + \lambda M_s^2) \ln \frac{\Lambda}{M_s} - 3Y^2 M_f^2 \ln \frac{\Lambda}{M_f} \right]. \quad (3.74)$$

In this chapter we will apply the previous general results to a specific model of inflation. The main goal is to observe the effects of loops corrections on cosmological observables such as the power spectrum of primordial curvature perturbations. We shall understand the relative importance of the radiative corrections with respect to the tree level result in the primordial Universe physics.

In section 4.1 we will present the time integration procedure we followed to calculate the full Feynman amplitudes. In particular we will address the oscillating features of the Feynman amplitudes that arise after attaching the external legs and performing the time integrations. In section 4.2 we will discuss the classical dynamics of hybrid inflation models and their supersymmetric versions that will be used to address the calculation of the one-loop corrections to the primordial power spectrum in section 4.3. These results are obtained using perturbation theory in the framework, previously discussed, of the *in-in* formalism. We will present our final results from a numerical evaluation of the primordial curvature power spectrum.

4.1 Time Integration

In the previous chapter we concentrated on the computation of the amputated amplitude to extract the ultraviolet behavior of the one-loop corrections to the two-point inflaton function. To conclude the calculation of the Feynman amplitudes we have to attach the external propagators to the amputated amplitude and integrate over τ_1 and τ_2

$$A^{1\text{-loop}}(k) = \int_{\tau_i}^{\tau} d\tau_1 \int_{\tau_i}^{\tau} d\tau_2 [-iG_{\varphi}^R(k, \tau, \tau_1)] [-iG_{\varphi}^R(k, \tau, \tau_2)] A_{GG} \\ + \int_{\tau_i}^{\tau} d\tau_1 \int_{\tau_i}^{\tau} d\tau_2 [-iG_{\varphi}^R(k, \tau, \tau_1)] [F_{\varphi}(k, \tau, \tau_2)] A_{GF}, \quad (4.1)$$

obtaining the total one-loop amplitude, where we have defined

$$A_{GG} := A_{\text{scalar}}^{a+b+b'} + A_{\text{fermion}}^{a+b+b'}, \quad (4.2)$$

$$A_{GF} := A_{\text{scalar}}^{c+c'+d'} + A_{\text{fermion}}^{c+c'}. \quad (4.3)$$

The one-loop contribution to the two-point inflaton function corrects the tree level propagator reported in equation (3.8). We can have both Hadamard F_{φ} and retarded propagators G_{φ}^R as external lines, equation (4.1), as we have seen in the explicit diagrammatic representation of the

corrections. For a (nearly) massless scalar field, such as the inflaton, from equations (2.94) and (2.95), the propagators in the Keldysh basis are

$$F_\varphi(k, \tau_1, \tau_2) = \frac{H}{2k^3} \left((1 + k^2 \tau_1 \tau_2) \cos(k(\tau_1 - \tau_2)) + k(\tau_1 - \tau_2) \sin(k(\tau_1 - \tau_2)) \right), \quad (4.4)$$

$$G_\varphi^R(k, \tau_1, \tau_2) = \theta(\tau_1 - \tau_2) \frac{H}{2k^3} \left((1 + k^2 \tau_1 \tau_2) \sin(k(\tau_1 - \tau_2)) - k(\tau_1 - \tau_2) \cos(k(\tau_1 - \tau_2)) \right). \quad (4.5)$$

To perform the time integration we decided to keep the scalar and fermion contributions separated at first to analyze the individual effect.

For the A_{GF} contributions, in the presence of the δ -functional terms, the first time integration is trivially performed analytically. For the other parts of the dominant terms the approximated form in equations (3.69) is considered. After the first time integration, taking the limit $\eta \rightarrow 0$, we explicitly checked that the results are independent on the time regulator η introduced in section 3.3, as it was the case for previous similar computation [52].

Regarding the amplitudes A_{GG} instead, as stated already in equation (3.69), the leading term is only the one including the $\delta(\Delta\tau)$ factor, therefore the τ_2 time integration is performed straightforwardly. The main reason for this term to dominate is due to the fact that the factor M/H is large and that means fast oscillation of the integrand. Therefore both τ_1 and τ_2 integration can be safely done numerically setting η to be a much smaller number than the other parameters. The last time integration, over τ_1 , was only performed numerically and we will present in section 4.3 the results fixing the parameters with the choice of the inflationary model.

4.1.1 Oscillatory behavior

The complete loop corrections show a time dependent periodic behavior and this is introduced by the inclusion of the external propagators. The dependence on oscillatory functions is present in the Feynman amplitude in the *in-in* formalism also in a Minkowski spacetime with a finite initial time t_{in} . Let us take as an example a theory that produces only diagram (d) as radiative correction, the one-loop amputated amplitude is given by equation (3.23).

Introducing a mass counterterm, in the MS renormalization scheme [72],

$$\delta m^2 = \frac{\lambda}{16\pi^2} \left(\Lambda^2 - m^2 \ln \left(\frac{\Lambda}{\mu_R} \right) \right), \quad (4.6)$$

where μ_R is the arbitrary renormalization scale, the renormalized amplitude reads

$$A_{\text{amp}}^d|_{\text{ren}} = -i \frac{\lambda}{16\pi^2} m^2 \left(1 + \ln \left(\frac{m^2}{4\mu_R^2} \right) \right). \quad (4.7)$$

The renormalized amputated amplitude is time independent but the result of the full amplitude, when attaching the external propagator and integrating in time, is not

$$A^d = A_{\text{amp}}^d|_{\text{ren}} \frac{\sin^2(\sqrt{k^2 + m^2}(t - t_{\text{in}}))}{2(k^2 + m^2)^{3/2}}. \quad (4.8)$$

The time dependence in these cases can be interpreted as a consequence of the choice of switching-on the interaction at a finite time t_{in} and to fix the mode function at that time to be as in equation (2.85), therefore fixing the Minkowski vacuum state at the initial time t_{in} .

In the Minkowski spacetime we would expect naively to recover the value of the amplitudes found in the literature [71], given the *in-out* formalism, and therefore the amplitude to be independent from the initial time, in the limit $t_{\text{in}} \rightarrow -\infty$. In most cases this limit does not exist and it is therefore necessary to address the problem in the language of distribution theory.

Also in the de Sitter spacetime the periodic behavior appears in the full two-point function amplitudes. The full solution is therefore again dependent on the initial time τ_{in} and as in the previous discussion we cannot always take the limit $\tau_{\text{in}} \rightarrow -\infty$ directly because it is not well defined.

Note that in this case there could be a time dependence of a different type, due to the background. In fact it can arise directly from the amputated amplitude a logarithmic dependence on the Hubble parameter $H(\tau)$, for example in the case of the inflaton self-interaction [7, 65]. Considering loops coming from massive particles the logarithmic dependence is instead on the mass of the mentioned particles [7], as it is in our case, and the amputated amplitude has a time dependence of a different type, through the H dependence of the different terms.

It has been shown that the oscillations are dependent on the interaction profile [7]. Considering the Minkowski background, the *in-in* formalism is equivalent to a theory that evolves freely from infinite negative time up to the t_{in} where the interaction is switched-on. Then the system evolves according to the interacting theory. It can be described by a standard action with a step function $\theta(t - t_{\text{in}})$ multiplying the interacting Lagrangian

$$S = \int_{-\infty}^{+\infty} dt \int d^3x (\mathcal{L}_0 + \theta(t - t_{\text{in}})\mathcal{L}_{\text{int}}). \quad (4.9)$$

Therefore we expect the oscillatory terms to disappear in the limit in which the interaction is always active, the *in-out* limit. The result in equation (4.8) is obtained using the 'naive' interaction profile $\theta(t - t_{\text{in}})$ and presents time oscillations.

It is possible to construct a nearly adiabatic switching-on of the interaction using different interaction profiles. The longer the transition time Δt from the free to the interacting theory the smaller the amplitude of the oscillations. It was shown that the constant contribution coming from the corrections is independent on the chosen profile and it reproduces the results of the *in-out* approach for an adiabatic switch-on of the interaction [7]. As expected the Poincaré symmetry is recovered for an adiabatic activation of the interaction.

The same arguments are valid also for the de Sitter spacetime: the amplitude of the oscillations depends on the interaction profile and they are suppressed for long transition time (adiabatic switch-on). The constant contribution is instead profile independent [7].

In the next sections we proceed to use the *in-in* formalism without changing the interaction profile therefore we expect the presence of these oscillation of the two-point functions and for them to give an imprint on the primordial power spectrum.

4.2 Hybrid Inflation

The hybrid inflation scenario was introduced by Linde [73] to overcome one specific difficulty of the new [73] and the chaotic [74] scenarios: the requirement of a small and therefore 'unnatural' coupling constant in order to fit the CMB data. This hybrid inflationary paradigm was born in the context of grand unified theories (GUTs) and the main difference with the previous models is in the presence of a second scalar field Υ , the waterfall field, besides the inflaton ϕ . In this case Υ provides the vacuum energy density that drives inflation while ϕ is the slow-rolling field [75]. Since the inflaton is freed of the role of generating the non zero VEV, much larger and 'natural' couplings are allowed in order to reproduce the experimental CMB data.

The contributions of the one-loop corrections are proportional to the coupling constants of the theory and since we are interested in enhancing these effects on top of the classical dynamics we will consider this type of models. Moreover previous studies suggested the supersymmetric hybrid inflation scenario to be the most promising model in order to appreciate loop corrections similar to the one we studied [7].

The minimal version of the hybrid inflationary model is given by the potential

Figure 4.1: The two regimes of the hybrid inflation potential. Figure from [76].

$$V(\phi, \Upsilon) = \frac{m^2}{2}\phi^2 + \lambda_h\phi^2\Upsilon^2 + \frac{g}{4}(M^2 - \Upsilon^2)^2, \quad (4.10)$$

where the last term is typical of a theory that presents a spontaneous symmetry breaking (SSB). The interaction term between ϕ and Υ keeps the field Υ 'trapped' in the origin: $\Upsilon = 0$, as long as $\phi > \phi_c$. The value ϕ_c of the inflaton corresponds to point at which the auxiliary field mass changes sign. In fact we have, as starting point

$$M_\Upsilon^2|_{\Upsilon=0} = \frac{\partial^2 V(\phi, \Upsilon=0)}{\partial \Upsilon^2} = -gM^2 + \lambda_h\phi^2, \quad (4.11)$$

therefore we have

$$\phi_c := \frac{g}{\lambda_h}M^2, \quad (4.12)$$

and it is clear that we have respectively for $\phi > \phi_c$ and $\phi < \phi_c$ the mass $m_\Upsilon > 0$ and $m_\Upsilon < 0$ and this changes the shape of the potential as shown in figure 4.1.

During the first phase $\phi > \phi_c$ the minimum along the waterfall field is stable and the field ϕ is slowing rolling with the almost flat potential

$$V(\phi, \Upsilon=0) = \frac{g}{4}M^2 + \frac{1}{2}m^2\phi^2 \equiv V_0 + \frac{1}{2}m^2\phi^2 \quad (4.13)$$

when ϕ reaches the critical value ϕ_c a phase transition to the true vacuum occur and inflation rapidly ends. The mass $M_\Upsilon < 0$ is negative and the potential has the typical Mexican hat shape with $\Upsilon = 0$ that is now a local maximum with the true minima being $\Upsilon = \pm M$.

To the effective potential in equation (4.10) we add a Coleman-Weinberg type term to account for the one-loop correction to the effective potential that can modify the classical dynamics of ϕ [77]

$$\Delta V_{CW}(\phi) = (-1)^f \frac{m_{\text{eff}}^4(\phi)}{64\pi^2} \left[\ln \left(\frac{m_{\text{eff}}^2(\phi)}{\mu^2} \right) - \frac{3}{2} \right], \quad (4.14)$$

that has a positive (negative) sign for bosonic (fermionic) fields. In the case of hybrid inflation models, $\Upsilon = 0$ during the inflationary era, and its effective mass is $M_\Upsilon^2 = 2\lambda_h\phi^2 - M$. Therefore the correction is

$$\Delta V_{CW}(\phi) = \frac{(\lambda_h\phi^2 - M)^2}{64\pi^2} \left[\ln\left(\frac{\lambda_h\phi^2 - M}{\mu^2}\right) - \frac{3}{2} \right] + \frac{m^2}{64\pi^2} \left[\ln\left(\frac{m^2}{\mu^2}\right) - \frac{3}{2} \right], \quad (4.15)$$

where the second term is constant and does not contribute to the inflaton dynamics. When considering the inflaton as nearly massless field the slope necessary to provide the slow-rolling is granted by the radiative corrections that depends on the coupling λ_h .

The Coleman Weinberg term dominates for

$$\lambda_h \geq 8\pi \frac{m}{\phi}, \quad (4.16)$$

this type of models are especially interesting in supersymmetry (SUSY) and supergravity (SUGRA) [78, 79]. In this case in fact the coupling can take larger values, of the order of 10^{-4} , 10^{-3} .

Note that in this part of the discussion we are studying the classical dynamics of the field ϕ . In the following, treating the supersymmetric case, we will restore the notation $\phi_0 = \langle \phi \rangle$ and $\phi = \phi_0 + \varphi$ to make a connection with the discussion in chapter 3.

4.2.1 Supersymmetric Hybrid Model

The scalar and the fermionic one-loop corrections are proportional to the only coupling constant of the theory λ_h in the supersymmetric hybrid inflation model. To enhance the loop effects

The supersymmetric model of inflation we will use is described by the superpotential [8, 78]

$$W = \lambda_h \tilde{\phi} (M_G^2 - \Sigma \bar{\Sigma}) + M_{SB}^2 (S + \beta), \quad (4.17)$$

where $M_G \simeq 1.688 \times 10^{-3} M_P$, $M_{SB} \simeq 1.0 \times 10^{-8} M_P$ is the supersymmetry-breaking scale. The first and the second term produce respectively the inflationary potential and the SUSY breaking after inflation. The second term is negligible during inflation for λ_h sufficiently large. The real part of the superfield $\tilde{\phi}$ is the scalar component is the inflaton, while the superfields Σ and $\bar{\Sigma}$ are the waterfall fields that draw inflation to an end we they acquire a non zero VEV. During the epoch of inflation, the approximated inflaton potential in this particular scenario is [78]

$$V_{\text{inf}} \simeq \lambda_h^2 M_G^4 + \frac{\lambda_h^4 M_G^4}{64\pi^2} \left[\ln\left(\frac{\lambda_h^2 \phi_0^2}{2\mu_\Lambda^2}\right) + \mathcal{O}\left(\frac{M_G^4}{\phi_0^4}\right) \right], \quad (4.18)$$

where μ_Λ is the renormalization scale. We are neglecting the symmetry breaking during inflation due to the scale M_{SB} . Using the same notation for the fields as in chapter 3, the interaction between the inflaton and the heavy scalar and fermion fields are

$$\mathcal{L}_{\text{int}} \ni -\frac{\lambda_h^2}{4} \phi^2 \sum_{i=1}^4 \Sigma_i^2 + \frac{\lambda_h}{\sqrt{2}} \phi \bar{\chi} \chi. \quad (4.19)$$

Note that in the model there are four massive real scalars degree of freedom, Σ_i ($i = 1, 2, 3, 4$) and one massive fermion. As anticipated in this scenario the constants of the general model introduced in chapter 3 are directly connected to the single coupling λ_h

$$M_{s_{1,3}}^2 = \frac{1}{2} \lambda_h^2 (\phi_0^2 + M_G^2), \quad M_{s_{2,4}}^2 = \frac{1}{2} \lambda_h^2 (\phi_0^2 - M_G^2), \quad M_f = \frac{1}{\sqrt{2}} \lambda_h \phi_0, \quad (4.20)$$

$$\mu = \frac{1}{2} \lambda_h^2 \phi_0, \quad \lambda = \frac{1}{4} \lambda_h^2, \quad Y = \frac{1}{\sqrt{2}} \lambda_h, \quad (4.21)$$

where M_G^2 has the effect of splitting the mass eigenstate of the scalar field. The background inflaton field ϕ_0 is given in terms of the number of e-folds N , before reaching the critical value M_G [78]

$$\frac{\phi_0^2(N)}{M_{\text{P}}^2} = \frac{\lambda_h^2}{4\pi^2} N + \frac{2M_G^2}{M_{\text{P}}^2}, \quad (4.22)$$

and the slow-roll parameters ϵ are given by

$$\epsilon = \frac{\lambda_h^4 M_{\text{P}}^2}{2(32\pi^2)^2 \phi_0^2}, \quad (4.23)$$

$$\eta = -\frac{\lambda_h^2 M_{\text{P}}^2}{32\pi^2 \phi_0^2}. \quad (4.24)$$

Remind that ϕ barely varies during inflation hence we choose $\phi_0 = \phi_0(N = N_{\text{piv}})$ to fix the parameters. N_{piv} is the number of e-folds reached when the pivot scale $k_{\text{piv}} = 0.05 \text{ Mpc}^{-1}$ exits the horizon.

4.3 Radiative Corrections to the Primordial Power Spectrum

In this section we will construct the primordial power spectrum of curvature perturbations in the effort of producing a theoretical prediction to be confronted against the cosmological observations. The primordial power spectrum is a fundamental tool to discriminate between different inflationary models. The spectrum is typically characterized by an amplitude and a tilt (given by the spectral index), that depend on the shape of the inflaton potential.

In fact in the slow-roll approximation we have [25]

$$\Delta_\zeta(k) = \frac{1}{12\pi^2 M_{\text{P}}^6} \frac{V^3}{(V')^2} \Big|_{t^*}, \quad (4.25)$$

where t^* is the horizon exit time, i.e. $k = a(t^*)H$, and the primordial power spectrum in the SUSY hybrid model presented in the previous section is

$$\Delta_\zeta(k) = \frac{1}{12\pi^2 M_{\text{P}}^6} \frac{V^3}{(V')^2} \Big|_{k=aH} = \frac{16^2 \pi^2 M_G^4 \phi_0^2(k)}{3\lambda_h^2 M_{\text{P}}^6} \sim \frac{4}{3} \frac{M_G^4}{M_{\text{P}}^4} N(k) \quad (4.26)$$

and the spectral index is given by

$$n_\zeta - 1 = \frac{d\Delta_\zeta(k)}{d \ln k}. \quad (4.27)$$

The study of features of the primordial power spectrum is therefore essential to distinguish different models. One-loop corrections can be the sources of peculiar features. They can produce time dependent oscillation [55]. Periodic properties of the primordial power spectrum are also produced at tree level for extended models [80] or for non standard initial states [81].

In the first chapter we introduced the scale invariant power spectrum of the inflaton fluctuations Δ_φ and in chapter 3 we showed that in the *in-in* formalism at tree level we have

$$\Delta_\varphi^{\text{tree}}(k) = \frac{k^3}{2\pi^2} P_\varphi^{\text{tree}}(k) = \frac{k^3}{2\pi^2} F_\varphi^{\text{tree}}(k, \tau, \tau). \quad (4.28)$$

We then proceeded calculating the quantum corrections to P_φ using the *in-in* formalism in a perturbative fashion

$$P_\varphi = P_\varphi^{\text{tree}} + P_\varphi^{1\text{-loop}} + \dots \quad (4.29)$$

From equation (1.179) we can connect the power spectrum of the inflaton fluctuations to the one of the primordial curvature perturbation

$$\Delta_\zeta(k) = \left(\frac{H^2}{\dot{\phi}^2}\right) \Delta_\varphi(k) = \left(\frac{H^2}{\dot{\phi}^2}\right) \frac{k^3}{4\pi^2} P_\varphi(k) = \frac{1}{2\epsilon M_{\text{P}}^2} \frac{k^3}{4\pi^2} P_\varphi(k), \quad (4.30)$$

where the last equivalence holds in the slow-roll approximation. In the following we will compute the effects of the one-loop corrections on the curvature perturbation assuming that the equation (4.30) holds also at that order

$$\Delta_\zeta(k) = \frac{1}{2\epsilon M_{\text{P}}^2} \frac{k^3}{4\pi^2} (P_\varphi^{\text{tree}}(k) + P_\varphi^{1\text{-loop}}(k) + \dots). \quad (4.31)$$

The primordial power spectrum is an important tool to understand the quantum nature of the inflationary physics.

4.3.1 Supersymmetric Hybrid Inflation

We will now study the one-loop correction to the power spectrum of the primordial curvature perturbations in the scenario where we expect it to produce the most promising results: SUSY hybrid inflation [7, 78]. In fact as discussed above we can produce an inflationary phase with values of the coupling λ_h in equation (4.18) up to the order 10^{-3} .

The one-loop contributions are shown separately in figure 4.2. The ratio between them and the tree level is shown and it presents an oscillatory feature in the small k regime due to the radiative corrections. As discussed earlier this feature appear including the contributions from the external propagators to the two-point function. The oscillations are a consequence of the imposing the initial conditions, the Bunch-Davies vacuum, at finite time τ_{in} , at the beginning of inflation. For longer inflationary phases the oscillations are suppressed leaving only a constant contribution. The constant shift is estimate to be proportional to the square of the coupling λ_h and to the mass difference of the fields.

The radiative corrections are the results of the time integrations, as discussed in section 4.1, of the amputated amplitudes given in equations (3.69) and (3.70). Considering the supersymmetric setting we have an analytical cancellation of the divergences in equation (3.73). In fact even if the inflaton VEV break SUSY invariance we still have the cancellation of the logarithmic divergence and the final amplitude in this setting is finite

$$\begin{aligned} A_{UV} &= \frac{1}{2\pi^2 H^4 \tau_1^4} \left[\left(\frac{1}{8} \lambda_h^4 \phi_0^2 + \frac{1}{16} \lambda_h^4 (\phi_0^2 + M_G^2) \right) \ln \left(\frac{2\Lambda^2}{\lambda_h^2 (\phi_0^2 + M_G^2)} \right) \right. \\ &\quad \left. + \left(\frac{1}{8} \lambda_h^4 \phi_0^2 + \frac{1}{16} \lambda_h^4 (\phi_0^2 - M_G^2) \right) \ln \left(\frac{2\Lambda^2}{\lambda_h^2 (\phi_0^2 - M_G^2)} \right) - \frac{3}{8} \lambda_h^4 \phi_0^2 \ln \left(\frac{2\Lambda^2}{\lambda_h^2 \phi_0^2} \right) \right] \\ &= \frac{1}{2\pi^2 H^4 \tau_1^4} \left[-\frac{3}{16} \lambda_h^4 \phi_0^2 \log \left(1 - \frac{M_G^4}{\phi_0^4} \right) + \frac{1}{16} \lambda_h^4 M_G^2 \ln \left(\frac{\phi_0^2 - M_G^2}{\phi_0^2 + M_G^2} \right) \right]. \quad (4.32) \end{aligned}$$

In this particular context the one-loop correction is fully finite and independent from the renormalization procedure.

The UV Feynman amplitude add a time dependence to the final amplitude. In fact besides the time dependence due to the external propagators and the initial time τ_{in} , discussed above, the amputated amplitude introduce a time dependence due to the background, from the H and ϕ_0 that are slowly-varying.

Using equation (4.31) we obtain the radiative corrections to the curvature power spectrum. Note that during inflation the masses of the heavy fields are dependent on ϕ_0 and therefore are slowly-varying during the evolution. Since the changes are adiabatic, due to the slow-roll conditions, we used the results of the computation for constant masses. Therefore the results are not valid towards

the critical regime, when inflation is ending. The WKB approximation for the fields breaks down at this stage since the fields are going to be massless at the end of inflation.

Because the results of chapter 3 are completely general it is possible to work also outside the supersymmetric scenario. In fact we can introduce local counterterms, using the $\overline{\text{MS}}$ scheme [72],

$$\delta m^2 = \frac{\lambda}{4\pi^2} \left(\Lambda^2 - M_s^2 \ln \left(\frac{\Lambda}{\mu_R} \right) \right), \quad (4.33)$$

for the scalar contributions and

$$\delta m^2 = -\frac{Y^2}{2\pi^2} \left(\Lambda^2 - M_f^2 \ln \left(\frac{\Lambda}{\mu_R} \right) \right), \quad (4.34)$$

for the fermion contributions, where μ_R is the renormalization mass scale. The counterterms are obtained using the WKB form of the massive propagators that is a good approximation in the UV regime and thus can be used to understand the UV divergences. We can use these time independent counterterms, to have a renormalized theory that have massive fermions and scalars interacting with the inflaton according to the Lagrangian in equation (3.2). Therefore the previous results can be extended to different models of inflation in a straightforward way.

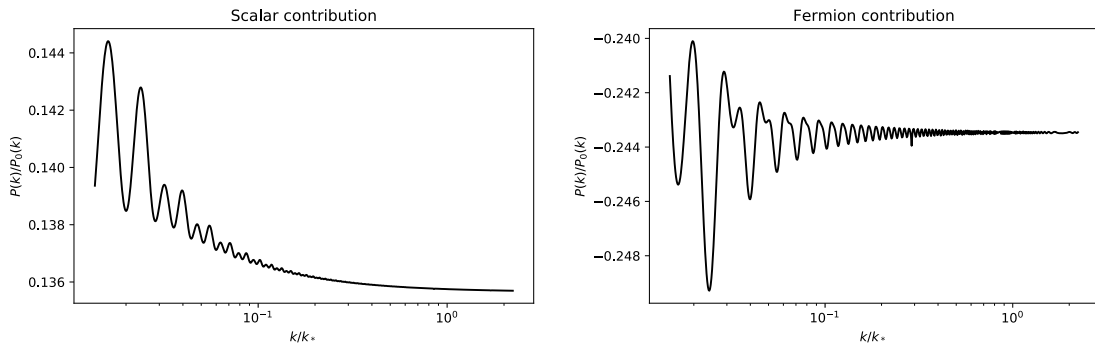


Figure 4.2: One-loop contributions to primordial power spectrum, coming from the massive scalar field (left) and the massive fermion field (right). For the parameters, we chose $\lambda_h = 1.192 \times 10^{-3}$, $M_G = 1.688 \times 10^{-3} M_{\text{P}}$, $M_{SB} \approx 1.0 \times 10^{-8} M_{\text{P}}$, and $N_{\text{piv}} = 59$. The initial time τ_i is chosen as $\tau_i = -k_{\text{piv}}^{-1} e^{N_{\text{tot}} - N_{\text{piv}}}$, with the total number of e-folds $N_{\text{tot}} = 65$. The parameters are chosen in such a way that the tree-level power spectrum gives the Planck normalization, 2.1×10^{-9} . Figure from [82].

Note that in the studied case the scalar (fermion) contribution is positive (negative) with magnitudes of $\mathcal{O}(10^{-1})$. Beside the oscillatory behavior, which does not cancel completely, the radiative corrections produce a shift of the power spectrum. This shift is non zero when summing the fermion and scalar contributions and proportional to particle mass differences squared, resulting in a relative size ~ 0.001 . We show in figure 4.3 the total power spectrum, including the contribution at one-loop order. The relative difference is proportional to the number of e-folds so a longer inflationary epoch would enhance the constant shift while, as discussed above, suppressing the oscillations.

Finally using the result for the primordial power spectrum including one-loop effects we produced a prediction for the temperature power spectrum of the CMB. In figure 4.4 we show our prediction (black curve) and the Planck best fit (green curve). Due to the smoothing around a particular angular scale, the oscillatory feature is not visible in the predicted power spectrum.

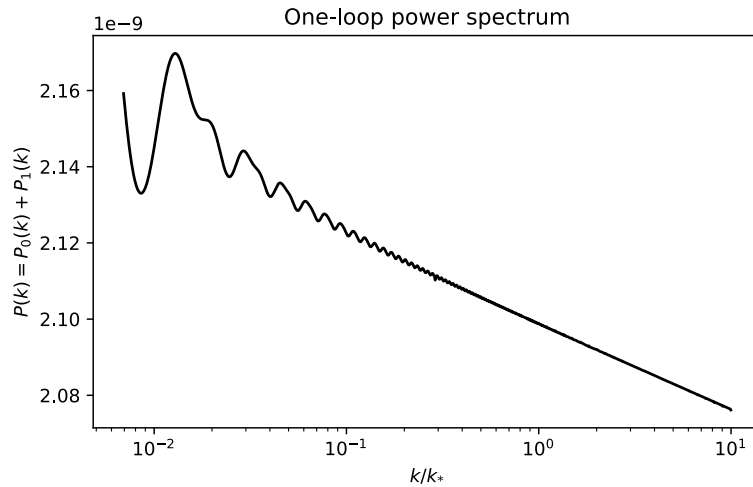


Figure 4.3: One-loop power spectrum $\Delta_\zeta(k)$. The choice of parameters is the same as in figure 4.2. Figure from [82].

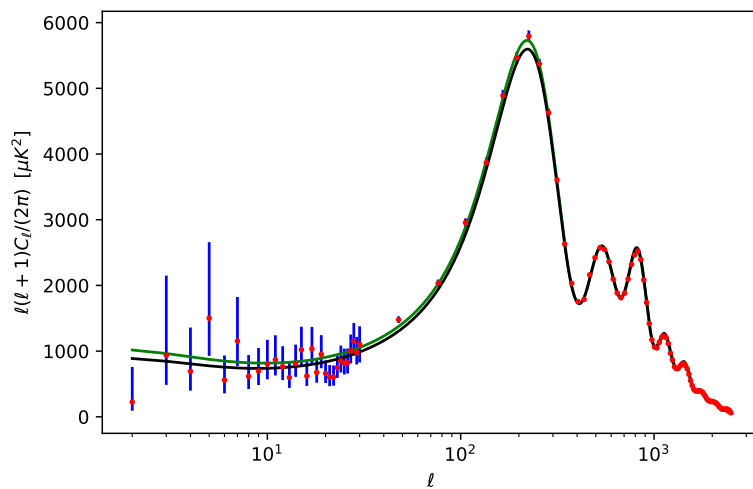


Figure 4.4: Cosmic microwave background power spectrum C_ℓ . The total e-folds number is chosen to be 70. The parameter λ_h is chosen such that the Planck normalization is met. The green curve is the Planck best-fit [3] and the black curve represents our prediction. The data is from [3]. Figure from [82].

SUMMARY AND CONCLUSION

Cosmic inflation is a widely accepted paradigm in cosmology, it describes a primordial epoch of accelerated expansion of the Universe. The CMB observations, consistent with adiabatic, scale invariant and Gaussian initial condition, are considered hints for cosmic inflation. Within this framework the problems (horizon, flatness and unwanted relic) of the Hot Big Bang model can be solved. The current observations are consistent with a nearly scale invariant primordial curvature power spectrum as the one predicted by the slow-roll scenario of a single-field inflation. Nonetheless realistic models of inflation contain multiple fields other than the inflaton. The presence of fields coupled to the inflaton may alter the predictions of the single-field inflation models.

In the past five decades different inflationary theories have been studied, focusing on the classical dynamics of the field. Less attention has been dedicated to the understanding of the quantum corrections to the power spectrum arising from the presence of other fields in the early Universe interacting with the inflaton. The radiative corrections can produce a characteristic imprint in the primordial power spectrum since they introduce a time dependence due to both the background evolution and the choice of the Bunch Davies vacuum as initial state at time τ_{in} .

In this thesis we investigated the explicit ultraviolet behavior of the inflaton two-point function and the features of the primordial power spectrum due to the radiative corrections coming from the presence of massive scalar and massive fermion fields that interact with the inflaton, respectively via the most general, Z_2 invariant, (renormalizable) interactions and a Yukawa coupling. The natural theoretical framework to use is the Schwinger and Keldysh (or *in-in*) formalism since time translation invariance is broken by the cosmological setting, i.e. the expanding Universe, and we expect a time dependence of the cosmological observables.

We computed the one-loop radiative corrections to the inflaton two-point correlation function due to the heavy fields, without specifying the inflaton potential, keeping the inflationary scenario general at first. We performed the computations in a de Sitter spacetime, choosing the initial state at some initial conformal time τ_{in} to be the Bunch-Davies vacuum. The mode functions were treated, in the analytical computation, using the WKB approximation while numerically, we used the full solution of the equations of motion in the de-Sitter spacetime. We explicitly showed that the scalar and fermion one-loop contributions contain the same quadratic and logarithmic divergences as in the case of the Minkowski spacetime background, as expected from the results in algebraic QFT. The contributions carry as usual opposite sign and they cancel exactly for the supersymmetric model considered, giving rise to a finite total result.

Time dependent features of the power spectrum arising from the one-loop corrections were expected as discussed in a previous work [55]. The time dependence is of two types. One arises from the amputated amplitude due to the evolution of the background. In fact the slow-rolling

field ϕ_0 even if varies slowly is not exactly constant and therefore neither the masses are perfectly constants. Moreover the dependence on the Hubble parameter H of the amputated amplitudes provide a second source of time dependence of this type. The other type of time dependence is on the expected oscillatory features in the power spectrum. Indeed we found that both radiative corrections coming from the fermion and the scalar produce a constant shift and this peculiar oscillatory effects on top of the tree level primordial power spectrum. The oscillatory behavior is due to the fixing of the initial conditions at finite time τ_{in} instead that at $\tau_{in} = -\infty$. It arises in the complete amplitudes when inserting the external propagators and integrating in time. When choosing the initial time large, in magnitude, we see the oscillation shifts towards lower wavenumber k , but keeping the same overall shape. In the limit $\tau_{in} \rightarrow -\infty$ the oscillations are shifted towards momenta $k \rightarrow 0$ outside of the visible range.

We can interpret the choice of the finite time in a twofold way: as the choice to set the initial conditions at the beginning of inflation, without resorting to a prolonged de Sitter phase in the far past. Then the inflation starts at τ_{in} , with all the interactions that we have considered and the correct time-evolution of the modes. Otherwise, even assuming that inflation extended to the infinite past, we can interpret τ_{in} as a starting point for the interactions between the inflaton and the other massive fields. This switching-on via a step-function is a non-adiabatic process so further analysis is needed to check if our results are reliable in this case; indeed it was shown for a self-interacting inflaton that an adiabatic switch-on of the interaction leads to no oscillations and introduces only a constant shift [7]. Further analysis is needed to understand the physical meaning of these oscillations.

Finally we applied our result in the framework of supersymmetric hybrid inflation where the coupling constant can be as large as $\mathcal{O}(10^{-3})$ and therefore the one-loop corrections are expected to be substantial. We explicitly showed that the fermion and scalar UV divergences in the inflaton two-point function corrections cancel each other analytically in this setting. The radiative corrections of both scalar and fermion fields separately are $\mathcal{O}(0.1)$.

In the various phases of the computation we performed numerical checks of the approximations used in the analytical computations using Mathematica. We computed propagators, amputated amplitudes and UV behaviors numerically starting from the *full* mode functions and compared them to the analytical results. We showed that the WKB approximation and the split of the momentum integrations are good analytical approximations for the *full* result. Moreover we argued that the WKB approximation is a good tool to capture the UV divergences of massive fields.

The final step was to make a prediction for the temperature power spectrum of the CMB including the quantum corrections. In figure 4.4 we present our prediction for the CMB power spectrum together with the best fit of the Planck data. Due to the smoothing around a particular angular scale, the oscillations are not directly visible in the predicted power spectrum. In the optimistic scenario of large coupling, we were expecting to see the imprint of the primordial power spectrum oscillations in the CMB and be able to constrain the model parameters and τ_{in} . Unfortunately at present we do not observe any features that can be traced back to the oscillations of the primordial power spectrum as a simple power-law power spectrum is a good fit of the latest Planck results without the need for any particular features.

Generically, the constraints on oscillatory features are still quite weak and surely features similar to those obtained in our model are not excluded. From future observation we can expect to improve the methods to reconstruct the primordial power spectrum from the experimental data and we can hope to detect the effect of radiative corrections, for sufficiently large couplings.

BIBLIOGRAPHY

- [1] A. H. Guth. “The Inflationary Universe: A Possible Solution to the Horizon and Flatness Problems”. In: *Phys. Rev. D* 23 (1981), pp. 347–356. DOI: 10.1103/PhysRevD.23.347.
- [2] A. Albrecht and P. J. Steinhardt. “Cosmology for Grand Unified Theories with Radiatively Induced Symmetry Breaking”. In: *Phys. Rev. Lett.* 48 (17 Apr. 1982), pp. 1220–1223. DOI: 10.1103/PhysRevLett.48.1220. URL: <https://link.aps.org/doi/10.1103/PhysRevLett.48.1220>.
- [3] N. Aghanim et al. “Planck 2018 results. VI. Cosmological parameters”. In: (2018). arXiv: 1807.06209 [astro-ph.CO].
- [4] D. H. D. H. Lyth and A. A. Riotto. “Particle physics models of inflation and the cosmological density perturbation”. In: 314.1-2 (June 1999), pp. 1–146. DOI: 10.1016/S0370-1573(98)00128-8. arXiv: hep-ph/9807278 [hep-ph].
- [5] D. Baumann. “TASI Lectures on Primordial Cosmology”. In: *arXiv e-prints*, arXiv:1807.03098 (July 2018), arXiv:1807.03098. arXiv: 1807.03098 [hep-th].
- [6] R. Brunetti and K. Fredenhagen. “Microlocal Analysis and Interacting Quantum Field Theories: Renormalization on Physical Backgrounds”. In: *Communications in Mathematical Physics* 208.3 (Jan. 2000), pp. 623–661. DOI: 10.1007/s002200050004. arXiv: math-ph/9903028 [math-ph].
- [7] S. Dresti. “Radiative Corrections in Curved Spacetime and physical implications to the Power Spectrum and Trispectrum for different Inflationary Models”. PhD Dissertation. Georg-August Göttingen University, 2018.
- [8] G. Dvali, Q. Shafi, and R. Schaefer. “Large scale structure and supersymmetric inflation without fine tuning”. In: 73.14 (Oct. 1994), pp. 1886–1889. DOI: 10.1103/PhysRevLett.73.1886. arXiv: hep-ph/9406319 [hep-ph].
- [9] S. Dodelson. *Modern Cosmology*. Amsterdam: Academic Press, 2003. ISBN: 9780122191411.
- [10] A. R. Liddle. *An introduction to modern cosmology*. Chichester, UK: Wiley, 1998.
- [11] E. W. Kolb and M. S. Turner. *The early universe*. Frontiers in Physics. Boulder, CO: Westview Press, 1990. DOI: 10.1201/9780429492860.
- [12] S. Weinberg. *Gravitation and Cosmology*. New York: John Wiley and Sons, 1972. ISBN: 0471925675, 9780471925675.
- [13] E. Hubble. “A relation between distance and radial velocity among extra-galactic nebulae”. In: *Proc. Nat. Acad. Sci.* 15 (1929), pp. 168–173. DOI: 10.1073/pnas.15.3.168.
- [14] A. A. Penzias and R. W. Wilson. “A Measurement of excess antenna temperature at 4080-Mc/s”. In: *Astrophys. J.* 142 (1965), pp. 419–421. DOI: 10.1086/148307.

- [15] R. H. Cyburt et al. “Big bang nucleosynthesis: Present status”. In: *Rev. Mod. Phys.* 88 (1 Feb. 2016), p. 015004. DOI: 10.1103/RevModPhys.88.015004.
- [16] A. D. Linde. “A New Inflationary Universe Scenario: A Possible Solution of the Horizon, Flatness, Homogeneity, Isotropy and Primordial Monopole Problems”. In: *Phys. Lett.* 108B (1982), pp. 389–393. DOI: 10.1016/0370-2693(82)91219-9.
- [17] A. A. Starobinsky. “A new type of isotropic cosmological models without singularity”. In: *Physics Letters B* 91 (1980), pp. 99–102. ISSN: 0370-2693. DOI: [https://doi.org/10.1016/0370-2693\(80\)90670-X](https://doi.org/10.1016/0370-2693(80)90670-X).
- [18] M. Marinucci. “Inflationary Tensor Fossils and their implications”. Master Thesis. University of Padua, 2018.
- [19] S. Alam et al. “The clustering of galaxies in the completed SDSS-III Baryon Oscillation Spectroscopic Survey: cosmological analysis of the DR12 galaxy sample”. In: *Mon. Not. Roy. Astron. Soc.* 470.3 (2017), pp. 2617–2652. DOI: 10.1093/mnras/stx721. arXiv: 1607.03155 [astro-ph.CO].
- [20] M. Colless et al. “The 2dF Galaxy Redshift Survey: Final data release”. In: (2003). arXiv: astro-ph/0306581 [astro-ph].
- [21] A. Einstein. “The Field Equations of Gravitation”. In: *Sitzungsber. Preuss. Akad. Wiss. Berlin (Math. Phys.)* 1915 (1915), pp. 844–847.
- [22] A. Einstein. “Hamilton’s Principle and the General Theory of Relativity”. In: *Sitzungsber. Preuss. Akad. Wiss. Berlin (Math. Phys.)* 1916 (1916), pp. 1111–1116.
- [23] S. M. Carroll. *Spacetime and Geometry*. San Francisco, USA: Cambridge University Press, 2019. ISBN: 0805387323, 9780805387322, 9781108488396, 9781108775557.
- [24] P. Coles and F. Lucchin. *Cosmology: The Origin and evolution of cosmic structure*. Chichester, UK: Wiley, 1995.
- [25] D. Baumann. “Inflation”. In: *Physics of the large and the small, TASI 09, proceedings of the Theoretical Advanced Study Institute in Elementary Particle Physics, Boulder, Colorado, USA, 1-26 June 2009*. 2011, pp. 523–686. DOI: 10.1142/9789814327183_0010. arXiv: 0907.5424 [hep-th].
- [26] D. H. Lyth and A. R. Liddle. *The primordial density perturbation: Cosmology, inflation and the origin of structure*. 2009.
- [27] Y. Fujii. “Some aspects of the scalar-tensor theory”. In: *Proceedings, 2nd Advanced Research Workshop on Gravity, Astrophysics and Strings at the Black Sea (GAS@BS 2004): Kiten, Bulgaria, June 10-16, 2004*. 2004. arXiv: gr-qc/0410097 [gr-qc].
- [28] C. Brans and R. H. Dicke. “Mach’s Principle and a Relativistic Theory of Gravitation”. In: *Phys. Rev.* 124 (3 Nov. 1961), pp. 925–935. DOI: 10.1103/PhysRev.124.925. URL: <https://link.aps.org/doi/10.1103/PhysRev.124.925>.
- [29] A. R. Liddle and D. H. Lyth. “The cold dark matter density perturbation”. In: 231.1-2 (Aug. 1993), pp. 1–105. DOI: 10.1016/0370-1573(93)90114-S. arXiv: astro-ph/9303019 [astro-ph].
- [30] V. Mukhanov. *Physical Foundations of Cosmology*. Oxford: Cambridge University Press, 2005. ISBN: 0521563984, 9780521563987.
- [31] A. Riotto. “Inflation and the theory of cosmological perturbations”. In: *ICTP Lect. Notes Ser.* 14 (2003), pp. 317–413. arXiv: hep-ph/0210162 [hep-ph].
- [32] T. S. Bunch and P. C. W. Davies. “Quantum Field Theory in de Sitter Space: Renormalization by Point Splitting”. In: *Proc. Roy. Soc. Lond.* A360 (1978), pp. 117–134. DOI: 10.1098/rspa.1978.0060.

- [33] K. A. Malik and D. R. Matravers. “TOPICAL REVIEW: A concise introduction to perturbation theory in cosmology”. In: *Classical and Quantum Gravity* 25.19, 193001 (Oct. 2008), p. 193001. DOI: 10.1088/0264-9381/25/19/193001. arXiv: 0804.3276 [astro-ph].
- [34] M. C. Guzzetti et al. “Gravitational waves from inflation”. In: *Riv. Nuovo Cim.* 39.9 (2016), pp. 399–495. DOI: 10.1393/ncr/i2016-10127-1. arXiv: 1605.01615 [astro-ph.CO].
- [35] N. D. Birrell and P. C. W. Davies. *Quantum Fields in Curved Space*. Cambridge Monographs on Mathematical Physics. Cambridge, UK: Cambridge Univ. Press, 1984. ISBN: 0521278589, 9780521278584, 9780521278584. DOI: 10.1017/CB09780511622632.
- [36] N. Bartolo et al. “Non-Gaussianity from inflation: Theory and observations”. In: *Phys. Rept.* 402 (2004), pp. 103–266. DOI: 10.1016/j.physrep.2004.08.022. arXiv: astro-ph/0406398 [astro-ph].
- [37] M. Sasaki. “Large Scale Quantum Fluctuations in the Inflationary Universe”. In: *Prog. Theor. Phys.* 76 (1986), p. 1036. DOI: 10.1143/PTP.76.1036.
- [38] A. A. Starobinsky. “Spectrum of relict gravitational radiation and the early state of the universe”. In: *JETP Lett.* 30 (1979). [767(1979)], pp. 682–685.
- [39] J. Yepez. “Einstein’s vierbein field theory of curved space”. In: (2011). arXiv: 1106.2037 [gr-qc].
- [40] A. Einstein. “A Generalized Theory of Gravitation”. In: *Rev. Mod. Phys.* 20 (1 Jan. 1948), pp. 35–39. DOI: 10.1103/RevModPhys.20.35. URL: <https://link.aps.org/doi/10.1103/RevModPhys.20.35>.
- [41] M. E. Peskin and D. V. Schroeder. *An Introduction to quantum field theory*. Reading, USA: Addison-Wesley, 1995. ISBN: 9780201503975, 0201503972.
- [42] H. Collins, R. Holman, and A. Ross. “Effective field theory in time-dependent settings”. In: *Journal of High Energy Physics* 2013, 108 (Feb. 2013), p. 108. DOI: 10.1007/JHEP02(2013)108. arXiv: 1208.3255 [hep-th].
- [43] J. S. Schwinger. “On gauge invariance and vacuum polarization”. In: *Phys. Rev.* 82 (1951). [116(1951)], pp. 664–679. DOI: 10.1103/PhysRev.82.664.
- [44] L. V. Keldysh. “Diagram technique for nonequilibrium processes”. In: *Zh. Eksp. Teor. Fiz.* 47 (1964). [Sov. Phys. JETP20,1018(1965)], pp. 1515–1527.
- [45] K.-c. Chou et al. “Equilibrium and nonequilibrium formalisms made unified”. In: *Physics Reports* 118.1 (1985), pp. 1–131. ISSN: 0370-1573. DOI: [https://doi.org/10.1016/0370-1573\(85\)90136-X](https://doi.org/10.1016/0370-1573(85)90136-X). URL: <http://www.sciencedirect.com/science/article/pii/037015738590136X>.
- [46] R. D. Jordan. “Effective Field Equations for Expectation Values”. In: *Phys. Rev.* D33 (1986), pp. 444–454. DOI: 10.1103/PhysRevD.33.444.
- [47] S. Weinberg. “Quantum contributions to cosmological correlations”. In: 72.4, 043514 (Aug. 2005), p. 043514. DOI: 10.1103/PhysRevD.72.043514. arXiv: hep-th/0506236 [astro-ph].
- [48] E. Calzetta and B. L. Hu. “Closed Time Path Functional Formalism in Curved Space-Time: Application to Cosmological Back Reaction Problems”. In: *Phys. Rev.* D35 (1987), p. 495. DOI: 10.1103/PhysRevD.35.495.
- [49] A. Bilandžić and T. Prokopec. “Quantum radiative corrections to slow-roll inflation”. In: 76.10, 103507 (Nov. 2007), p. 103507. DOI: 10.1103/PhysRevD.76.103507. arXiv: 0704.1905 [astro-ph].
- [50] C. Kiefer, D. Polarski, and A. A. Starobinsky. “Quantum-To Transition for Fluctuations in the Early Universe”. In: *International Journal of Modern Physics D* 7.3 (Jan. 1998), pp. 455–462. DOI: 10.1142/S0218271898000292. arXiv: gr-qc/9802003 [gr-qc].

- [51] D. Boyanovsky et al. “Scalar field dynamics in Friedmann-Robertson-Walker spacetimes”. In: 56.4 (Aug. 1997), pp. 1939–1957. DOI: 10.1103/PhysRevD.56.1939. arXiv: hep-ph/9703327 [hep-ph].
- [52] M. van der Meulen and J. Smit. “Classical approximation to quantum cosmological correlations”. In: 2007.11, 023 (Nov. 2007), p. 023. DOI: 10.1088/1475-7516/2007/11/023. arXiv: 0707.0842 [hep-th].
- [53] S. J. N. Mooij. “Effective Theories in Cosmology”. PhD Dissertation. University of Amsterdam, 2013.
- [54] E. A. Calzetta and B.-L. B. Hu. *Nonequilibrium Quantum Field Theory*. Cambridge Monographs on Mathematical Physics. Cambridge University Press, 2008. ISBN: 9780511421471, 9780521641685. DOI: 10.1017/CB09780511535123. URL: <http://www.cambridge.org/mw/academic/subjects/physics/theoretical-physics-and-mathematical-physics/nonequilibrium-quantum-field-theory?format=AR>.
- [55] L. Covi and S. Dresti. “Time-dependent Features in the Primordial Spectrum”. In: (2018). arXiv: 1803.02351 [gr-qc].
- [56] A. Varna Iyer et al. “Strongly coupled quasi-single field inflation”. In: 2018.1, 041 (Jan. 2018), p. 041. DOI: 10.1088/1475-7516/2018/01/041. arXiv: 1710.03054 [hep-th].
- [57] Wolfram Research, Inc. *Mathematica, Version 11.0*. URL: <https://www.wolfram.com/mathematica>.
- [58] S. P. Martin. “TASI 2011 Lectures Notes:. Two-Component Fermion Notation and Supersymmetry”. In: *The Dark Secrets of the Terascale (TASI 2011) - Proceedings of the 2011 Theoretical Advanced Study Institute in Elementary Particle Physics. Edited by Matchev Konstantin et al. Published by World Scientific Publishing Co. Pte. Ltd.* Dec. 2013, pp. 199–258. DOI: 10.1142/9789814390163_0005. arXiv: 1205.4076 [hep-ph].
- [59] A. Landete, J. Navarro-Salas, and F. Torrenti. “Adiabatic regularization and particle creation for spin one-half fields”. In: 89.4, 044030 (Feb. 2014), p. 044030. DOI: 10.1103/PhysRevD.89.044030. arXiv: 1311.4958 [gr-qc].
- [60] L. Parker. “Particle creation and particle number in an expanding universe”. In: *Journal of Physics A Mathematical General* 45.37, 374023 (Sept. 2012), p. 374023. DOI: 10.1088/1751-8113/45/37/374023. arXiv: 1205.5616 [astro-ph.CO].
- [61] M. G. Jackson and K. Schalm. “Model Independent Signatures of New Physics in the Inflationary Power Spectrum”. In: 108.11, 111301 (Mar. 2012), p. 111301. DOI: 10.1103/PhysRevLett.108.111301. arXiv: 1007.0185 [hep-th].
- [62] X. Chen, Y. Wang, and Z.-Z. Xianyu. “Loop Corrections to Standard Model Fields in Inflation”. In: *JHEP* 08 (2016), p. 051. DOI: 10.1007/JHEP08(2016)051. arXiv: 1604.07841 [hep-th].
- [63] D. Boyanovsky. “Fermionic influence on inflationary fluctuations”. In: *Phys. Rev. D* 93.8 (2016), p. 083507. DOI: 10.1103/PhysRevD.93.083507. arXiv: 1602.05609 [gr-qc].
- [64] H. Collins. “Fermionic alpha-vacua”. In: *Phys. Rev. D* 71 (2005), p. 024002. DOI: 10.1103/PhysRevD.71.024002. arXiv: hep-th/0410229.
- [65] L. Senatore and M. Zaldarriaga. “On loops in inflation”. In: *Journal of High Energy Physics* 2010, 8 (Dec. 2010), p. 8. DOI: 10.1007/JHEP12(2010)008. arXiv: 0912.2734 [hep-th].
- [66] L. Senatore. “Lectures on Inflation”. In: *Theoretical Advanced Study Institute in Elementary Particle Physics: New Frontiers in Fields and Strings*. 2017, pp. 447–543. DOI: 10.1142/9789813149441_0008. arXiv: 1609.00716 [hep-th].
- [67] A. Achucarro et al. “Effective theories of single field inflation when heavy fields matter”. In: *JHEP* 05 (2012), p. 066. DOI: 10.1007/JHEP05(2012)066. arXiv: 1201.6342 [hep-th].

- [68] M. G. Jackson and K. Schalm. “Model-Independent Signatures of New Physics in non-Gaussianity”. In: *arXiv e-prints*, arXiv:1202.0604 (Feb. 2012), arXiv:1202.0604. arXiv: 1202.0604 [hep-th].
- [69] M. G. Jackson and K. Schalm. “Model Independent Signatures of New Physics in the Inflationary Power Spectrum”. In: 108.11, 111301 (Mar. 2012), p. 111301. DOI: 10.1103/PhysRevLett.108.111301. arXiv: 1007.0185 [hep-th].
- [70] A. Zee. *Quantum field theory in a nutshell*. Nov. 2003. ISBN: 978-0-691-14034-6.
- [71] P. Ramond. “Field Theory: A modern primer”. In: *Front. Phys.* 51 (1981). [Front. Phys.74,1(1989)], pp. 1–397.
- [72] G. 't Hooft. “Dimensional regularization and the renormalization group”. In: *Nucl. Phys. B* 61 (1973), pp. 455–468. DOI: 10.1016/0550-3213(73)90376-3.
- [73] A. Linde. “Hybrid inflation”. In: *Phys. Rev. D* 49 (2 Jan. 1994), pp. 748–754. DOI: 10.1103/PhysRevD.49.748. URL: <https://link.aps.org/doi/10.1103/PhysRevD.49.748>.
- [74] A. D. Linde. “Chaotic Inflation”. In: *Phys. Lett. B* 129 (1983), pp. 177–181. DOI: 10.1016/0370-2693(83)90837-7.
- [75] G. Lazarides. “Supersymmetric Hybrid Inflation”. In: (2001). arXiv: hep-ph/0011130 [hep-ph].
- [76] M. Sakellariadou. “Production of Topological Defects at the End of Inflation”. In: *Lect. Notes Phys.* 738 (2008), pp. 359–392. DOI: 10.1007/978-3-540-74353-8_10. arXiv: hep-th/0702003.
- [77] S. Coleman and E. Weinberg. “Radiative Corrections as the Origin of Spontaneous Symmetry Breaking”. In: *Phys. Rev. D* 7 (6 Mar. 1973), pp. 1888–1910. DOI: 10.1103/PhysRevD.7.1888. URL: <https://link.aps.org/doi/10.1103/PhysRevD.7.1888>.
- [78] W. Buchmüller, L. Covi, and D. Delépine. “Inflation and supersymmetry breaking”. In: *Physics Letters B* 491.1-2 (Oct. 2000), pp. 183–189. DOI: 10.1016/S0370-2693(00)01005-4. arXiv: hep-ph/0006168 [hep-ph].
- [79] G. Dvali, Q. Shafi, and R. K. Schaefer. “Large scale structure and supersymmetric inflation without fine tuning”. In: *Phys. Rev. Lett.* 73 (1994), pp. 1886–1889. DOI: 10.1103/PhysRevLett.73.1886. arXiv: hep-ph/9406319.
- [80] J. Chluba, J. Hamann, and S. P. Patil. “Features and new physical scales in primordial observables: Theory and observation”. In: *International Journal of Modern Physics D* 24.10, 1530023 (June 2015), p. 1530023. DOI: 10.1142/S0218271815300232. arXiv: 1505.01834 [astro-ph.CO].
- [81] R. H. Brandenberger and J. Martin. “Trans-Planckian issues for inflationary cosmology”. In: *Classical and Quantum Gravity* 30.11, 113001 (June 2013), p. 113001. DOI: 10.1088/0264-9381/30/11/113001. arXiv: 1211.6753 [astro-ph.CO].
- [82] L. Covi, F. Costa, and J. Kim. *in preparation*. (2020).

ACKNOWLEDGMENTS

The work and the results obtained in the thesis were done with a close collaboration between myself and Dr. Jinsu Kim. Regarding the analytical computation I first performed the analysis in the Minkowski spacetime while Dr. Kim carried out the one in de Sitter. Then we switch to cross-check the computations. The numerical analysis and the relative results, discussed in chapter 3, were produced *in toto* by myself. While the code for the numerical integration needed to produce the plots in figures in section 4.3 was done entirely by Dr. Kim. I underlined that by explicitly citing in the thesis the article that myself and Dr. Kim are going to publish soon, together with prof. Covi.